



TAMPEREEN TEKNILLINEN YLIOPISTO  
TAMPERE UNIVERSITY OF TECHNOLOGY

DAMIANO MESCHINI  
CORROSION PROPERTIES OF THERMALLY SPRAYED BOND COATINGS

Master of Science thesis

Examiners: prof. Petri Vuoristo and  
M.Sc. (Eng.) Tommi Varis  
Examiners and topic approved by the  
Faculty of Engineering sciences  
on 28<sup>th</sup> November 2018

## ABSTRACT

**MESCHINI DAMIANO:** Corrosion Properties of Thermally Sprayed Bond Coatings

Tampere University of Technology

Master of Sciences thesis, 103 pages

November 2018

Examiners: prof. Petri Vuoristo and M.Sc.(Eng.) Tommi Varis

Keywords: Thermal spray, plasma spray, HVOF, corrosion behavior, sulphuric acid

Plasma sprayed chromia coatings are known to have excellent wear and corrosion properties in acidic conditions at ambient and elevated temperatures. Thermally sprayed metallic bond coatings are often between the ceramic top coating and the metallic base material in order to guarantee good adhesion of the ceramic coating to the substrate, however corrosion environments can be extremely damaging to such bond coatings due to absence of dissolved oxygen, high concentration of the corrosive electrolyte under the top coating, crevice corrosion mechanisms inside the coating and galvanic coupling between the coatings and even with the corrosion-resistant substrate material. When bond coatings are used, it is therefore of high importance to select the bond layer chemistry and method of manufacturing so that the bond coating can survive in such harsh conditions. In the present study, HVOF sprayed Ni-20Cr, Hastelloy C-276 and Ultimet alloy coatings, and plasma sprayed tantalum coating were studied.

The substrate material was solid Hastelloy C-276 while the top coating was plasma sprayed  $\text{Cr}_2\text{O}_3$ . Corrosion properties were studied in sulphuric acid solutions of various concentrations (0.1M, 0.5M, 1M) at room temperature and at the temperature of 60°C.

The corrosion measurements used in this study were electrochemical polarization, Electrochemical Impedance Spectroscopy measurements, and immersion tests. The coating microstructures were studied before and after the immersion test.

At room temperature, the results showed that between all the bond coatings the plasma sprayed tantalum performed significantly better, in fact it had very good response either in the electrochemical measurements and in the immersion test. The Ultimet alloy had the lowest corrosion resistance according to the tests performed.

The HVOF sprayed Ni-20Cr and HVOF sprayed Hastelloy C-276 showed an intermediate corrosion resistance between the tantalum bond coating and the Ultimet alloy bond coating.

At the temperature of 60°C the corrosion resistance of the different bond coatings changed especially for the Ni-20Cr; in fact the immersion test caused the complete dissolution of HVOF sprayed Ni-20Cr and the considerable attack of Ultimet alloy while the plasma sprayed tantalum and HVOF sprayed Hastelloy C-276Ni-20 Cr resisted to such corrosion conditions fairly well.

## **PREFACE**

The present research work has been realized during the academic year 2017-2018 in Tampere University of Technology, Laboratory of Materials Science, Thermal Spray Center Finland Department of Materials Engineering and in the University of Modena and Reggio Emilia, Department of Engineering “Enzo Ferrari”.

First of all, I would like to thank my supervisors prof. Luca Lusvarghi and prof. Petri Vuoristo who allowed this research work. With their supervision and technical support they were essential for this research work.

I also would like to thank my co-supervisors M.Sc. (Eng.) Tommi Varis and Dr. Giovanni Bolelli who guided me in every activity in the laboratory of TUT and Unimore and gave me always valuable advice.

Finally, I would like to thank my family, with their constant support they helped me to complete this experience.

Tampere, 19.11.2018

# CONTENTS

1. INTRODUCTION.....	12
2. STATE OF ART.....	14
2.1. Surface engineering.....	14
2.1.1. Integral coatings.....	14
2.1.2. Discrete coatings.....	15
2.2 Thermal spray.....	18
2.2.1. Markets and applications for thermal spray coatings.....	18
2.2.2. Description and classification of thermal spray process.....	19
2.2.2.1. Cold spray.....	20
2.2.2.2. Combustion spraying.....	21
2.2.2.3. Electrical discharge plasma spraying.....	24
2.3 Corrosion.....	29
2.3.1. Principles of aqueous corrosion.....	30
2.3.2. Forms of corrosion.....	38
2.3.3. Corrosion test methods.....	44
2.3.4. Corrosion performance of thermal sprayed two-layer coatings.....	51
3. MATERIALS AND METHOD.....	53
3.1 Coating manufacturing.....	53
3.2 HVOF deposition.....	54
3.3 Plasma spraying.....	55
3.4 Metallographic specimen preparation.....	57
3.5 Polarization curve measurements.....	57
3.6 Electrochemical impedance spectroscopy measurements.....	58
3.7 Open circuit potential measurements.....	59
3.8 Immersion testing.....	59
4. RESULTS.....	61
4.1 Corrosion resistance behavior extracted from the polarization test.....	61

4.2 Corrosion behavior extracted from the electrochemical impedance spectroscopy test .....	68
4.3 Open circuit potential as a function of time .....	74
4.4 Corrosion behavior in the immersion test .....	75
5. CONCLUSION.....	101

REFERENCES

## LIST OF FIGURES

<b><u>Figure 1.</u></b>	<i>Different elements involved in a thermal spray process.....</i>	<i>18</i>
<b><u>Figure 2.</u></b>	<i>Industrial application of thermal spray technology in Europe in 2001....</i>	<i>19</i>
<b><u>Figure 3.</u></b>	<i>Classification of thermal spray processes.....</i>	<i>20</i>
<b><u>Figure 4.</u></b>	<i>Gas temperatures and velocities obtained with different thermal spray processes.....</i>	<i>20</i>
<b><u>Figure 5.</u></b>	<i>Equipment required for cold spray process.....</i>	<i>21</i>
<b><u>Figure 6.</u></b>	<i>Flame spray system with powder as feedstock material.....</i>	<i>22</i>
<b><u>Figure 7.</u></b>	<i>Representation of a HVOF system.....</i>	<i>23</i>
<b><u>Figure 8.</u></b>	<i>Detonation gun process cycle usin nitrogen as a buffer gas: (a) injection of fuel and oxygen into the combustion chamber, (b) injection of powder and nitrogen gas, (c) gas detonation and powder acceleration, (d) chamber exhausting.....</i>	<i>23</i>
<b><u>Figure 9.</u></b>	<i>Configuration of electric arc spray process.....</i>	<i>24</i>
<b><u>Figure 10.</u></b>	<i>Relation between enthalpy and temperature for different gases.....</i>	<i>26</i>
<b><u>Figure 11.</u></b>	<i>Typical configuration for direct current plasma spraying.....</i>	<i>26</i>
<b><u>Figure 12.</u></b>	<i>Schematic of the commercial plasma torch SG100 from Praxair-TAFA.....</i>	<i>27</i>
<b><u>Figure 13.</u></b>	<i>System configuration for d.c. plasma spraying and r.f induction plasma spraying.....</i>	<i>29</i>
<b><u>Figure 14.</u></b>	<i>Typical configuration for plasma transferred arc process.....</i>	<i>29</i>
<b><u>Figure 15.</u></b>	<i>Corrosion cost in United states.....</i>	<i>30</i>
<b><u>Figure 16.</u></b>	<i>Representation of an electrochemical cell constituted during the corrosion process.....</i>	<i>31</i>
<b><u>Figure 17.</u></b>	<i>Representation of the electric double layer.....</i>	<i>32</i>
<b><u>Figure 18.</u></b>	<i>Electrochemical shell for different chemical species.....</i>	<i>33</i>
<b><u>Figure 19.</u></b>	<i>Pourbaix diagram for Iron.....</i>	<i>35</i>
<b><u>Figure 20.</u></b>	<i>Representation of Buttle-Volmer's equation.....</i>	<i>36</i>
<b><u>Figure 21.</u></b>	<i>Approximation of Buttle-Volmer's equation using tafel's equation.....</i>	<i>37</i>
<b><u>Figure 22.</u></b>	<i>Identification of corrosion point in aqueous corrosion when there isn't electrical resistance.....</i>	<i>37</i>
<b><u>Figure 23.</u></b>	<i>Anodic polarization of iron in sulfuric acid 1M.....</i>	<i>38</i>
<b><u>Figure 24.</u></b>	<i>Representation of the different forms of corrosion.....</i>	<i>38</i>

<b><u>Figure 25.</u></b>	<i>Effect of electrolyte's conductivity on galvanic corrosion: (a) low conductivity and (b) high conductivity.....</i>	<i>39</i>
<b><u>Figure 26.</u></b>	<i>Pitting propagation method in NaCl solution.....</i>	<i>40</i>
<b><u>Figure 27.</u></b>	<i>Representation of different aeration cell.....</i>	<i>41</i>
<b><u>Figure 28.</u></b>	<i>Representation of metal-ion cell.....</i>	<i>41</i>
<b><u>Figure 29.</u></b>	<i>Analysis of crevice corrosion for materials that don't have passivation behavior.....</i>	<i>42</i>
<b><u>Figure 30.</u></b>	<i>Analysis of crevice corrosion for materials that don't have passivation behavior.....</i>	<i>42</i>
<b><u>Figure 31.</u></b>	<i>Typical aspect of erosion-corrosion.....</i>	<i>43</i>
<b><u>Figure 32.</u></b>	<i>Representation of fretting corrosion process.....</i>	<i>43</i>
<b><u>Figure 33.</u></b>	<i>Representation of stress corrosion cracking.....</i>	<i>44</i>
<b><u>Figure 34.</u></b>	<i>Wohler diagrams for a part that is submitted to pure fatigue and for a part that is submitted to corrosion-fatigue.....</i>	<i>44</i>
<b><u>Figure 35.</u></b>	<i>Tafel's analysis for the polaritazion curve.....</i>	<i>46</i>
<b><u>Figure 36.</u></b>	<i>Representation of the equipment used for the polarization test.....</i>	<i>47</i>
<b><u>Figure 37.</u></b>	<i>Randles cell configuration.....</i>	<i>48</i>
<b><u>Figure 38.</u></b>	<i>Nyquist plot for the Randles cell configuration.....</i>	<i>48</i>
<b><u>Figure 39.</u></b>	<i>Bode plot for the Randles cell configuration.....</i>	<i>49</i>
<b><u>Figure 40.</u></b>	<i>Two-time constant electrical equivalent circuit.....</i>	<i>49</i>
<b><u>Figure 41.</u></b>	<i>OCP graph for mild steel exposed to artificial seawater with or without bacteria.....</i>	<i>50</i>
<b><u>Figure 42.</u></b>	<i>Vessel used for the autoclave test.....</i>	<i>50</i>
<b><u>Figure 43.</u></b>	<i>Polarization curve for sample D1.1 (HVOF sprayed Hastelloy C-276 as bond coating) at three different corrosively levels (0.1M, 0.5M, 1M)...</i>	<i>61</i>
<b><u>Figure 44.</u></b>	<i>Polarization curve for sample D2.1 (HVOF sprayed Ni-20Cr as bond coating) at three different corrosively levels (0.1M, 0.5M, 1M).....</i>	<i>61</i>
<b><u>Figure 45.</u></b>	<i>Polarization curve for sample D3.1 (APS sprayed tantalum as bond coating) at three different corrosively levels (0.1M, 0.5M, 1M).....</i>	<i>62</i>
<b><u>Figure 46.</u></b>	<i>Polarization curve for sample D4.1 (HVOF sprayed cobalt based alloy as bond coating) at three different corrosively levels (0.1M, 0.5M, 1M)...</i>	<i>62</i>
<b><u>Figure 47.</u></b>	<i>Polarization curve for sample DITC (only APS sprayed Cr<sub>2</sub>O<sub>3</sub>) at three different corrosively levels (0.1M, 0.5M, 1M).....</i>	<i>62</i>

<b><u>Figure 48.</u></b>	<i>Polarization curves for samples D1.1 (Hastelloy C-276 as bond coating), D2.1 (Ni-20Cr as bond coating), D3.1 (tantalum as bond coating), D4.1 (cobalt alloy as bond coating) and DITC (with only Cr<sub>2</sub>O<sub>3</sub> top coating) at 0.1M.....</i>	<i>63</i>
<b><u>Figure 49.</u></b>	<i>Polarization curves for samples D1.1 (Hastelloy C-276 as bond coating), D2.1 (Ni-20Cr as bond coating), D3.1 (tantalum as bond coating), D4.1 (cobalt alloy as bond coating) and DITC (with only Cr<sub>2</sub>O<sub>3</sub> top coating) at 0.5M.....</i>	<i>64</i>
<b><u>Figure 50.</u></b>	<i>Polarization curves for samples D1.1 (Hastelloy C-276 as bond coating), D2.1 (Ni-20Cr as bond coating), D3.1 (tantalum as bond coating), D4.1 (cobalt alloy as bond coating) and DITC (with only Cr<sub>2</sub>O<sub>3</sub> top coating) at 1M.....</i>	<i>64</i>
<b><u>Figure 51.</u></b>	<i>Polarization curves for samples D1.1 (Hastelloy C-276 as bond coating), D1 (no Cr<sub>2</sub>O<sub>3</sub> top coating on Hastelloy C-276 bond coating), D2.1 (Ni-20Cr as bond coating), D2 (no Cr<sub>2</sub>O<sub>3</sub> top coating on Ni-20Cr bond coating).....</i>	<i>65</i>
<b><u>Figure 52.</u></b>	<i>Polarization curves for samples D3.1 (tantalum as bond coating), D3 (no Cr<sub>2</sub>O<sub>3</sub> top coating on tantalum bond coating), D4.1 (cobalt based alloy as bond coating), D4 (no Cr<sub>2</sub>O<sub>3</sub> top coating on cobalt based alloy bond coating).....</i>	<i>65</i>
<b><u>Figure 53.</u></b>	<i>Tafel analysis for the sample D1.1 (Hastelloy C-276 as bond coating) at H<sub>2</sub>SO<sub>4</sub> 0.5M.....</i>	<i>66</i>
<b><u>Figure 54.</u></b>	<i>Tafel analysis for the sample D2.1 (Ni-20Cr as bond coating) at H<sub>2</sub>SO<sub>4</sub> 1M.....</i>	<i>66</i>
<b><u>Figure 55.</u></b>	<i>EIS test for sample D1.1 (HVOF sprayed Hastelloy C-276) after 1, 4, 7, 25 hours of immersion in 0.5M H<sub>2</sub>SO<sub>4</sub>.....</i>	<i>68</i>
<b><u>Figure 56.</u></b>	<i>EIS test for sample (HVOF sprayed Ni-20Cr) D2.1 after 1, 4, 7, 25 hours of immersion in 0.5M H<sub>2</sub>SO<sub>4</sub>.....</i>	<i>69</i>
<b><u>Figure 57.</u></b>	<i>EIS test for sample D3.1 (APS sprayed tantalum) after 1, 4, 7, 25 hours of immersion in 0.5M H<sub>2</sub>SO<sub>4</sub>.....</i>	<i>69</i>
<b><u>Figure 58.</u></b>	<i>EIS test for sample D4.1 (HVOF sprayed cobalt based alloy) after 1, 4, 7, 25 hours of immersion in 0.5M H<sub>2</sub>SO<sub>4</sub>.....</i>	<i>69</i>
<b><u>Figure 59.</u></b>	<i>Fit for the Nyquist plot obtained from sample D1.1 (Hastelloy C-276 as bond coating) after 4 hours of immersion.....</i>	<i>70</i>
<b><u>Figure 60.</u></b>	<i>Fit for the Nyquist plot obtained from sample D2.1 (Ni-20Cr as bond coating) after 4 hours of immersion.....</i>	<i>70</i>
<b><u>Figure 61.</u></b>	<i>Fit for the Nyquist plot obtained from sample D3.1 (tantalum as bond coating) after 1 hour of immersion.....</i>	<i>71</i>
<b><u>Figure 62.</u></b>	<i>Fit for the Nyquist plot obtained from sample D4.1 (cobalt based alloy as bond coating) after 1 hour of immersion.....</i>	<i>71</i>



<b><u>Figure 63.</u></b>	<i>Electrochemical potential value measured along time with the OCP test.....</i>	<i>74</i>
<b><u>Figure 64.</u></b>	<i>SEM cross section for sample D1.1 (Hastelloy C-276 as bond coating) at 100X before and after the immersion test at different temperature.....</i>	<i>76</i>
<b><u>Figure 65.</u></b>	<i>SEM cross section for sample D1.1 (Hastelloy C-276 as bond coating) at 500X before and after the immersion test at different temperature.....</i>	<i>78</i>
<b><u>Figure 66.</u></b>	<i>SEM cross section for sample D1.1 (Hastelloy C-276 as bond coating) at 2000X before and after the immersion test at different temperature.....</i>	<i>79</i>
<b><u>Figure 67.</u></b>	<i>SEM cross section for sample D2.1 (Ni-20Cr as bond coating) at 100X before and after the immersion test at different temperature.....</i>	<i>81</i>
<b><u>Figure 68.</u></b>	<i>SEM cross section for sample D2.1 (Ni-20Cr as bond coating) at 500X before and after the immersion test at different temperature.....</i>	<i>83</i>
<b><u>Figure 69.</u></b>	<i>SEM cross section for sample D2.1 (Ni-20Cr as bond coating) at 2000X before and after the immersion test at different temperature.....</i>	<i>84</i>
<b><u>Figure 70.</u></b>	<i>SEM cross section for sample D3.1 (tantalum as bond coating) at 100X before and after the immersion test at different temperature.....</i>	<i>86</i>
<b><u>Figure 71.</u></b>	<i>SEM cross section for sample D3.1 (tantalum as bond coating) at 500X before and after the immersion test at different temperature.....</i>	<i>88</i>
<b><u>Figure 72.</u></b>	<i>SEM cross section for sample D3.1 (tantalum as bond coating) at 2000X before and after the immersion test at different temperature.....</i>	<i>89</i>
<b><u>Figure 73.</u></b>	<i>SEM cross section for sample D4.1 (cobalt based alloy as bond coating) at 100X before and after the immersion test at different temperature... </i>	<i>91</i>
<b><u>Figure 74.</u></b>	<i>SEM cross section for sample D4.1 (cobalt based alloy as bond coating) at 500X before and after the immersion test at different temperature... </i>	<i>93</i>
<b><u>Figure 75.</u></b>	<i>SEM cross section for sample D4.1 (cobalt based alloy as bond coating) at 2000X before and after the immersion test at different temperature.. </i>	<i>94</i>
<b><u>Figure 76.</u></b>	<i>SEM cross section for sample D1TC (no bond coating) at 100X before and after the immersion test at different temperature.....</i>	<i>96</i>
<b><u>Figure 77.</u></b>	<i>SEM cross section for sample D1TC (no bond coating) at 500X before and after the immersion test at different temperature.....</i>	<i>98</i>
<b><u>Figure 78.</u></b>	<i>SEM cross section for sample D1TC (no bond coating) at 2000X before and after the immersion test at different temperature.....</i>	<i>99</i>

## LIST OF SYMBOLS AND ABBREVIATION

Ag	argentum
Al	aluminum
Al <sub>2</sub> O <sub>3</sub>	aluminum oxide
Ar	argon
APS	Atmospheric Plasma Spray
C <sub>2</sub> H <sub>2</sub>	acetylene
C <sub>c</sub>	coating capacitance
C <sub>dl</sub>	double layer capacitance
C <sub>x</sub> H <sub>y</sub>	generic hydrocarbon molecule
CAPS	Controlled Atmosphere Plasma Spray
Cr <sub>2</sub> O <sub>3</sub>	chromium oxide
Cr <sub>23</sub> C <sub>6</sub>	chromium carbide
Cu	copper
CVD	Chemical Vapor Deposition
Dgun	detonation gun process
E <sub>eq</sub> or E <sub>0</sub>	equilibrium potential
E <sub>corr</sub>	corrosion potential
EIS	Electrochemical Impedance Spectroscopy
FeAl	iron-aluminum alloy
FCAW	Flux-Cored Arc Welding
H <sub>2</sub>	hydrogen
H <sub>2</sub> SO <sub>4</sub>	sulphuric acid
He	helium
HB	Hydrogen Blistering
HIC	Hydrogen Induced Cracking
HPCS	High Pressure Cold Spray
HVOF	High Velocity Oxygen Fuel
i	external current
i <sub>a</sub>	anodic current
i <sub>c</sub>	cathodic current
i <sub>corr</sub>	corrosion current
LaB <sub>6</sub>	lanthanum hexaboride
La <sub>2</sub> O <sub>3</sub>	lanthanum oxide
LPCS	Low Pressure Cold Spray
M	molar concentration
N <sub>2</sub>	Nitrogen
n	parameter of the constant phase element
NaCl	sodium chloride
Ni-20Cr	nickel-chromium alloy
NiAl	nickel-aluminum alloy
NiCr	nickel-chromium alloy
NiCrAlY	nickel-chromium-aluminum-yttrium alloy
O <sub>2</sub>	Oxygen
OCP	Open Circuit Potential
OHP	Outer-Helmholtz plane

OM	Optical Microscopy
PECVD	Plasma Enhanced Chemical Vapor Deposition
PVD	Physical Vapor Deposition
$R_s$	solution resistance
$R_c$	coating resistance
$R_{ct}$	charge-transfer resistance
SCC	Stress Corrosion Cracking
SEM	Scanning Electron Microscopy
SHE	Standard Hydrogen Electrode
SMAW	Shielded Metal Arc Welding
SOHIC	Stress Oriented Hydrogen Induced Cracking
SSC	Sulfide Stress Cracking
$T_h$	ion's temperature associated with plasma state a gas
$T_i$	electron's temperature associated with plasma state
$ThO_2$	thorium dioxide
TIG	Tungsten Inert Gas
$TiO_2$	Titanium Dioxide
VPS	Vacuum Plasma Spray
$Y_0$	parameter of the constant phase element
Zn	Zinc
$ZrO_2$	Zirconium dioxide

# 1. INTRODUCTION

Thermal sprayed coatings, especially ceramic coatings, are used in many industrial sectors thanks to their good wear resistance.

However, in the majority of the case, in such conditions, it is also required a good corrosion resistance because these environments can be extremely corrosive and it is well known that thermal spray coatings do not have excellent corrosion resistance due to the defects present in the microstructure (pinholes, pores and micro cracks) [1].

These defects in fact can provide a direct path between the external environment and the substrate leading to galvanic attacks and crevice corrosion of the base materials.

For that reason, the choice of the substrate is extremely important because it must have good corrosion resistance in order to protect itself when the electrolyte penetrates through the coating.

Another key factor concerning the ceramic coating is the adhesion with the substrate. If the thermal expansion coefficients of the ceramic and the metal are too different there could be excessive stresses at the interface and this fact could compromise the survival of the coating.

To avoid these, a metallic bond layer can be deposited between the substrate and the ceramic layer, these actions can have a good effect on the mechanical properties of the coating because the metallic bond layer adheres well to the grit blasted substrate and then the ceramic coating adheres well to the sprayed metallic bond layer [2].

Despite there are different information about the effect of the bond layer on the mechanical properties of the coating, there isn't enough knowledge about the influence of the bond layer on the electrochemical properties and the corrosion behavior of the coating.

The aim of these work is therefore to investigate the influence of the bond layer composition on the electrochemical properties and corrosion behavior of the coating using  $H_2SO_4$  as the electrolyte with different concentration (0.1M, 0.5M, 1M) in distilled water.

In order to reach this scope four categories of coating samples have been prepared. In all the categories the substrate and the top coat were constituted by Hastelloy C-276 and  $Cr_2O_3$  respectively, but the bond coating changed in all of them, in fact the bond coating used were Hastelloy C-276, Ni-20Cr, tantalum and a Cobalt based alloy (Ultimet).

Moreover, some samples with only the bond coating and with only the top coating have been produced to have a better comparison of the different results.

The research methods used to characterize the different coating were electrochemical polarization test, electrochemical impedance spectroscopy, immersion testing and open circuit potential measurements.

The electrochemical test (polarization, OCP, EIS) have been carried out only at room temperature while the immersion test has been carried out at room temperature and at an elevated temperature ( $T=60^\circ C$ ) in order to investigate even the role of the temperature in the corrosion phenomena.

Before and after the immersion test, SEM analyses have been carried out to evaluate visually the corrosion damage in the various bond coatings.

Sulfuric acid has been chosen because it can be easily found in different type of application such as the manufacture of dyes, drugs, rayon, cellulose products, the alkylation of petroleum product to increase octane rating, the pickling of ferrous and nonferrous alloys, the extraction of uranium from ore, the production of hydrogen fluoride from fluorospar, in process use in copper, zinc and nickel refining and the treatment of organics in the production of alcohols and detergents [3].

These type of investigations should reveal which bond coating must be used in a configuration where the substrate is constituted by Hastelloy C-276, the top coat is constituted by  $\text{Cr}_2\text{O}_3$  and there is presence of sulfuric acid in the environment.

## **2. STATE OF THE ART**

### **2.1. Surface engineering**

Surface engineering is a technology that nowadays is used in a lot of industrial sectors such as chemical, aerospace, automotive, paper making and electrical only to mention some of them.

The aim of this technology is to improve the surface's properties in order to achieve the characteristics required in a given application.

For example, with the different treatments provided by this technology is possible to increase the wear resistance, reduce the friction coefficient, increase the surface's hardness or modify the electrical conductivity.

Moreover, in a lot of application a product should provide different kind of properties together (high temperature resistance in a corrosive environment with abrasive wear condition) and the difficulties in machining some of the specialty alloys, as well their cost, has led to an increase of the coating demand [4].

Sometimes the modification of the surface is required not for technical purposes but for extending the product's life cycle; in fact during its life a product can be exposed to several different type of environment and can face different kind of degradation conditions.

Since the surface is the interface between the component and the environment, its properties and structure are really important and have a strong influence on the survival of the component in such condition.

In these case, where it's important to control the product's cycle life, the treatment applied to the surface should avoid component's failure in fact it should lead to a degradation that can be controlled and calculated in order to plan the maintenance if the component's properties will be lower than a critical level.

The coatings obtained with the different treatments provided by surface engineering can be divided in two main categories: integral coatings and discrete coatings [5].

#### **2.1.1. Integral coatings**

Integral coatings are obtained without adding any type of layer on the surface, for that reason they don't have a discrete interface between the substrate and the coating.

For the fact that there isn't a discrete interface the additional properties given by the coating decreases slowly from the surface to the substrate.

The main treatments for producing integral coating are: strain hardening, surface hardening and thermochemical surface modification.

*Strain hardening* consists in a plastic deformation process realized on the component before or during the application.

For realizing the plastic deformation prior the application, it can be used a rolling or impact loading and a peening (shot or water jet).

The depth of hardening depends on the method used and can goes from less than 0.1mm to 20mm [4].

*Surface hardening* is generally used with low alloy steel and utilizes a source of heat to reach the austenite phase, after that the material is quickly cooled with a cooling rate faster than its critical value. The rapid cooling allows the material to form the martensitic structure that is characterized by an higher value of hardness than the original structure.

To relief the stress formed during the cooling, the material can be heated upon to 200°C but these process reduces a bit the values of final hardness.

Different types of surface hardening exist, some of them are flame hardening, induction hardening, high-frequency resistance heating, plasma torch heating [4] [6].

*Thermochemical surface modification* consists of introducing, by diffusion processes, chemical elements into the surface at high temperature (500-900°C).

The element that penetrate into the surface forms different kind of phases with the substrate that have a high value of hardness.

As for surface hardening these process is generally used for steel and the main type of elements used for diffusion are carbon and nitrogen but even niobium and vanadium can be chosen.

The main process used for steel are carburizing, nitriding and carbonitriding [4] [6].

### **2.1.2. Discrete coatings**

Discrete coatings are obtained by depositing different kind of layers on the surface. In this case there is a discrete interface between the coating and the substrate therefore the properties of the coating change drastically in these region.

The main advantage of those coatings is that a lot of different materials can be added in a lot of different substrate and these allows to form parts with combined properties, on the other hand materials with very different properties can bring to residual stresses at the interface and this fact could compromise the survival of the coatings [5].

The coating can be divided into thin coatings where the thickness is below a few micrometers and thick coatings where the thickness is over 50 micrometers [4].

In order to have a general views of the different technologies used for producing discrete coatings it's possible to divide them in six different categories: electrochemical treatments, chemical treatments, chemical vapor deposition (CVD), physical vapor deposition (PVD), hardfacing and thermal spray.

In *electrochemical treatments* the coating is deposited using an electrochemical cell, the substrate can work as cathode or as anode.

In the first case, that is called electroplating, the coating is formed thanks to the electrolytic reduction on the substrate of the ions contained in the solution.

In the second case, that is called anodizing, the coating is formed by the layer of oxide that grows on the surface, these technology is principally used for aluminum and its alloys.

The main advantage of electroplating is that the thickness of the coatings can be easily controlled by changing the parameters of the electrolytic cell and it can go from few

micrometers to hundreds of micrometers but anyway with these technology only metallic substrate can be coated and the deposition rate is not too high [5] [6].

*Chemical treatments* use chemical reactions that take place on the substrate's interface to deposit the desired component, the three main types of chemical treatments are electroless plating, phosphating and hot dip coatings.

In electroless process the coating is deposited by using a reducing reaction that take place thanks to a chemical reducing agent contained in the solution, in this case no electric current is needed therefore even nonconductive materials can be coated.

Phosphating is a chemical conversion process where a metal surface reacts with an aqueous solution of a heavy metal, primarily a phosphate plus free phosphoric acid, to produce an adherent layer of insoluble complex phosphates.

In the hot dip coatings is used a molted bath of the materials that constitute the coating, the part to be coated is dipped into the bath and the coating is formed thanks to chemical reaction occurred on the surface.

Generally, in these process are used materials with a low melting point, one of the most used is zinc and the process is called galvanizing [4] [6].

*Chemical Vapor Deposition (CVD)* is a technology where the coating is formed from reagents that are in their vapor phase.

Those reagents are introduced into a chamber where the pressure is below the atmospheric pressure, chemical reactions accurses in the surface and the coating grows.

The vapor or gases are made by different chemical species such as fluorides, bromides, chlorides, iodides, hydrocarbons, phosphorus and ammonia complex.

Generally, the chemical reactions are activated by the temperature of the surface but in this case not all the materials can be coated because the surface should be at 800-1100°C. Sometimes the reaction can be activated by introducing plasma inside the work chamber, in these case the process is called PECVD (plasma-enhanced chemical vapor deposition). In PECVD all type of substrate including polymers can be coated because the substrate's temperature goes from 25 to 400°C.

With CVD is even possible to reach thick coating but generally with these process the coating thickness is below 50  $\mu m$  [4] [5].

*Physical Vapor Deposition (PVD)* is a process where the coatings are formed from material in their vapor phase but in these case the vapor are obtained from a solid source called target.

Once the vapors have been extracted from the target they are guided into the substrate's surface, even in these case the pressure is below the atmospheric pressure.

To extract the vapor from the target there are different possibilities such as evaporation, sputtering, ion plating and laser ablation.

With these process the thickness of the coating is generally below a few  $\mu m$ .

*Hardfacing* is a group of processes where the material that forms the coating is melted and deposited to the surface.

In these process also the surface's substrate is melted in order to form a physical, chemical and metallurgical interface with the coating, for these reason these process is very similar to a welding process [6].

The material constitute the coating can be in form of powder, or wire form and the heat source can be a thermal source from combustion or electric-arc process.



Hardfacing is generally used for the rebuilding of worn components or applications where a large amount of wear is tolerated, some examples of hardfacing processes are oxyacetylene weld overlay, shielded metal arc welding (SMAW), tungsten inert gas (TIG) weld overlays and flux-cored arc welding (FCAW) [6].

*Thermal spray* is a group of processes where the coating is formed by applying a stream of particles (metallic or nonmetallic) on the substrate.

The principal unit of the equipment for the thermal spray process is the torch (or gun), this device is in fact responsible for feeding, accelerating, heating and directing the flow of a thermal spray material towards the substrate.

The particles forming the stream are generally fused (except for cold spray process) and reach the surface forming different platelets, the coating is then formed by adding different layers of those platelets, the thickness of the coatings is generally between 50  $\mu\text{m}$  and a few millimeters.

The feedstock material is usually introduced into the gun as powder, wire rod, cord or even suspension; then it is accelerated towards the substrate by an auxiliary gas fed into the spray gun and only the molten particles are accelerated towards the substrate.

If the feed materials are powders the process is different, in fact they are introduced into the jet of hot gases and accelerated towards the substrate but they are not necessarily melted before the impact since the melting event depends on the powder's size and trajectory.

If the cold spray process is used to form the coating, no heat source is used and the feed material is only accelerated towards the substrate, the coating is formed only if the particle's velocity is above a critical velocity.

Most of thermal spray processes are performed in air and these lead to coating oxidation which increases with the temperature of the sprayed particles.

The coating oxidation can be avoided by performing the spray process in a controlled atmosphere, in a soft vacuum or using the cold spray process [4].

Thermal spray has different advantages, the first is that a lot of different materials can be used to form the coating, in fact almost all the material that melts without decomposing can be used for these processes.

The second one is that the coating can be formed without heating the substrate and these lead to depositing materials with a high melting point without changing the properties of the part or inducing excessive thermal distortion on it.

A third advantage is that thermal spray can be used to repair worn or damaged coatings without changing part dimensions or properties.

On the other hand, this technology is a line of sight process and that means that only the area exposed to the particles stream can be coated, furthermore only the surfaces that have a 90° angle with the particle impact have coatings that are characterized by a high density and a strong bonding [6].

Thermal spray processes are generally classified by the type of energy source used to melt the feed material, the next chapter discusses more in detail those processes since this coating technology has been used to form the coating investigated in this work.

## 2.1. Thermal spray

The reference [4] defines thermal spray technology as follow: “Thermal spray comprises a group of coating process in which finely divided metallic or nonmetallic materials are deposited in a molten or semi-molten condition to form a coating. The coating material may be in the form of powder, ceramic rod, wire, or molten materials”.

In these definition the cold spray process should not be considered a thermal spray technique because the feed material is not in a melted or semi-melted state but it is however contemplated as a thermal spray process.

Figure 1 summarize the different elements involved in a thermal spray process.

Unlike others coating processes, thermal spray doesn't form the coating from ions, molecules or atoms but instead it uses massive particulates in the form of liquid, semi-molten or solid particulates to form the coating.

Thermal spray has different advantages such as a high deposition rate for the fact that it is a process with a high energy density and the capability to deposit a lot of different materials because the different parameters like temperature, velocity, atmospheric conditions can be easily changed.

On the other hand, thermal spray process has some disadvantage like the fact that only the surface exposed to the particle stream can be coated because this technology is a line of sight process and the fact that the coatings presents different kind of defects such as pores, pinholes or microcracks that compromise the mechanical and the corrosion properties of the coating [6].

In order increase the quality of the coating some post-treatment like sealing or laser surface remelting are conducted on the coating after the spray process.

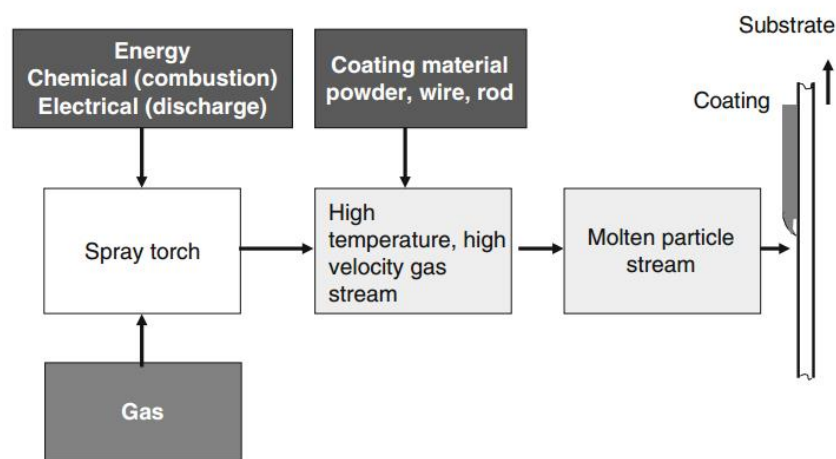


**Figure 1** - Different elements involved in a thermal spray process [4].

### 2.1.1. Markets and application for thermal spray coatings

The invention of thermal spray dates back to the first years of 1900 and is credited to M.U. Schoop who deposited different kind of patents on this coating technology.

Until 1950s thermal spray technology consisted essentially of flame spraying and its market was limited but with the introduction of plasma spray, detonation gun and HVOF the demand for thermal sprayed coating increased rapidly.

Before the 2000s, around 50% of the market for thermal sprayed coating was represented by the aerospace sector but then others markets, as shows in Figure 2, such as automotive or chemical process industry increased the need for thermal sprayed coatings and these led to a decrease demand percentage for the aerospace sector [4].

Thermal spray technology is usually chosen because it can provide coatings with a high wear resistance, in fact these coatings can be used as a substitution for hard chrome coating.

Furthermore, thermal spray can substitute steel by using a light alloy (Al, Mg) with a wear resistance coating on the top, these lead to economical advantage and weight saving [4].

Thermal sprayed coatings are also used for their thermal resistance and conductance, corrosion and oxidation resistance and electrical properties [6].

The applications for thermal sprayed application are really various because a lot of different materials can be used.

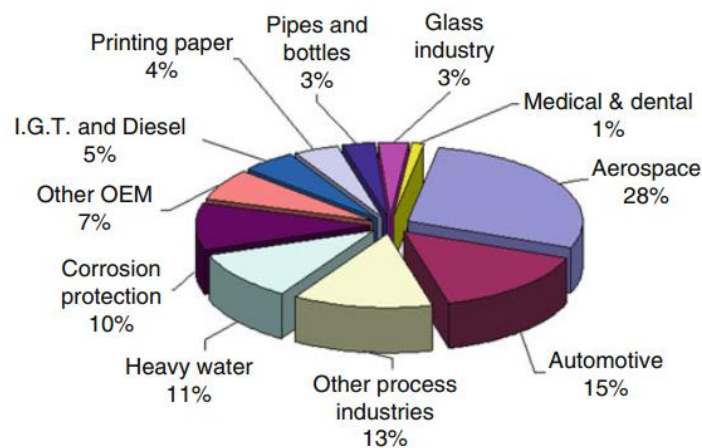


**Figure 2** – Industrial application of thermal spray technology in Europe in 2001 [4].

### 2.2.2. Description and classification of thermal spray process

There are different kind of thermal spray technology and usually they are classified, as showed by Figure 3, by the type of energy used to melt or soften the feed material [4].

Each process has its own parameters such as temperature, enthalpy, velocity and can provide different coatings in terms of porosity, bond strength, inclusions, oxides content and hardness [6].

Figure 4 shows the different gas temperature and velocities obtained in the various different thermal spray processes.

According to the classification described above, thermal spray processes can be divided in three categories that are cold spray where no heat source is used and the coating is formed using powder's kinetic energy; combustion spraying where the powder are melted or soften using chemical energy obtained by a combustion between a fuel, generally hydrocarbon molecules, and oxygen; electrical discharge plasma spraying where the feed material is melted by an electric arc or by creating plasma using two electrodes [4].

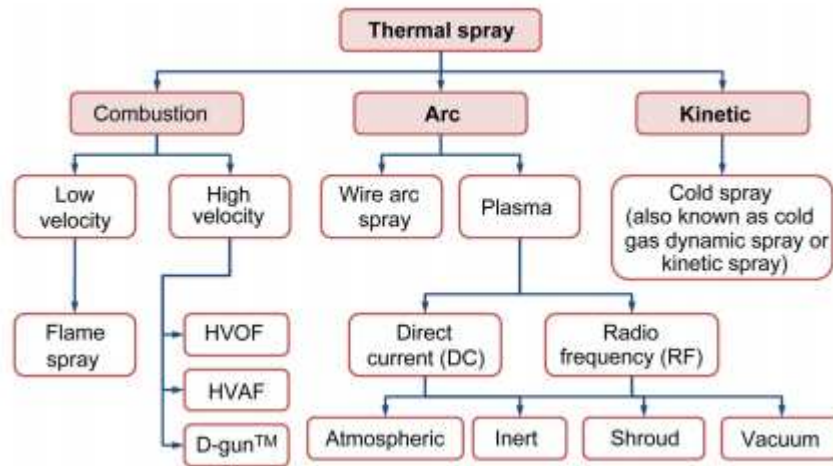


Figure 3 - Classification of thermal spray processes [7].

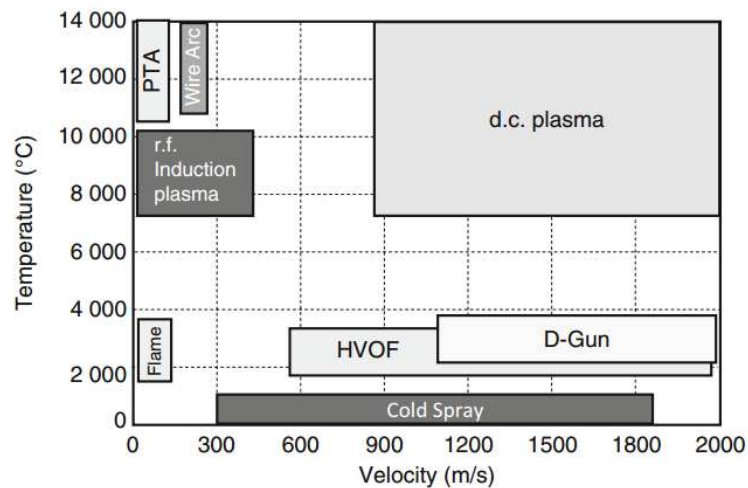


Figure 4 – Gas temperatures and velocities obtained with different thermal spray processes [4].

### 2.2.2.1. Cold spray

Compressed gas expansion or cold spray is a kinetic process that uses a high-velocity gas stream for accelerating the particles and drive them towards the substrate.

In this process the powders are not melted or heated therefore only the kinetic energy owned by the powders is responsible for the formation of the coating moreover for the fact that there isn't a heat source the coating doesn't present oxidation and other problems related to the use of a heat source.

The gas-dynamic acceleration of the particles is achieved using convergent-divergent Laval nozzle while  $N_2$   $He$ , air or their mixture are the most common gases used for this purpose. Those gases are generally heated (30-1000°C) in order to reach higher sonic flow velocities which results in higher particle impact velocities [4] [6].

The gas pressure can be used to identify different kind of cold spray process.

Low Pressure Cold Spray (LPCS) uses air or nitrogen as gas with a pressure below 1 MPa, generally 0.5 MPa.

High Pressure Cold Spray (HPCS) uses  $N_2$  or  $He$  as gas with a pressure up to 4 MPa.

Cold spray generally uses ductile materials such as metals (Zn, Ag, Cu, Al), alloys (Ni-Cr, Cu-Al, Ni alloys) and polymers because in these case the formation of the coating is more easy.

It can be demonstrated that in this process the coating is formed only if the velocity of the particles is above a critical value called critical velocity.

The velocity of the particle is generally included between 300 and 1500 m/sec and it depends on the particle material, size and morphology [4].

The coatings obtained with cold spray process present the following advantage: low level of oxide content, high density and microstructure identical to those of the feedstock materials, generation of compressive stresses during spray process that allow to deposit thick coating without adhesion failure and high deposition rate.

For the previous advantage, cold spray technology has a lot of different applications like refurbishment of aircraft parts, production of sputter targets and electronic industry[4].

Figure 5 shows the equipment required for cold spray process.

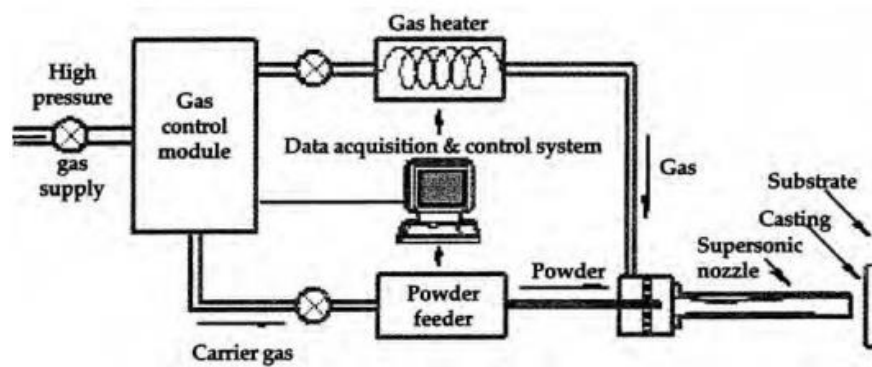


Figure 5 - Equipment required for cold spray process [6].

## 2.2.2.2. Combustion spraying

The technologies that use chemical energy to melt the feed material are flame spray, high velocity flame spraying (HVOF, HVOF) and detonation spray.

In all those technologies there is a gun responsible for feeding, accelerating, heating and directing the flow towards the substrate.

*Flame spraying* is one of the first combustion spraying technology, it uses the chemical energy of combusting fuel gases with oxygen to generate heat [6].

The most common gun used is the oxyacetylene type that uses acetylene as fuel and oxygen as oxidizing agent in the chemical reaction.

If the mixture of acetylene ( $C_2H_2$ )-oxygen ( $O_2$ ) is in a stoichiometric ratio, temperatures of 3410 K can be reach at atmospheric pressure [4].

The spray material is generally in the form of powder, wire or rods and they are introduced axially through the rear of the nozzle into the flame at the nozzle exit.

When the feedstock material is melted the particle or the droplets formed are accelerated towards the substrate surface by the expanding of hot gas flow and air jets.

Figure 6 shows a flame spray equipment with powder as feedstock material

One reason to use wire or rode material instead powder is that with those feed material is possible to reach a dense and smooth coating, moreover the material utilization is better

because the melting process is more efficient since only the fused particles leave the gun to reach the substrate.

The coatings obtained with flame spray technology are characterized by density ranging from 85 to 98% while the bond strength between the substrate and the coating depends mostly on particle temperatures and their velocities.

The particle velocity can reach a maximum of 80 *m/sec* because the jet velocity is usually below 100 *m/sec*, this fact lead to a high value of porosity (from 2 to 15%) and a low value of adhesion strength (below 30 MPa).

In some cases, a post process such as sintering or remelting can be used after the flame spray in order to obtain a better value of density and adhesion strength, in this case a diffusion bonding between the substrate and the coating is formed.

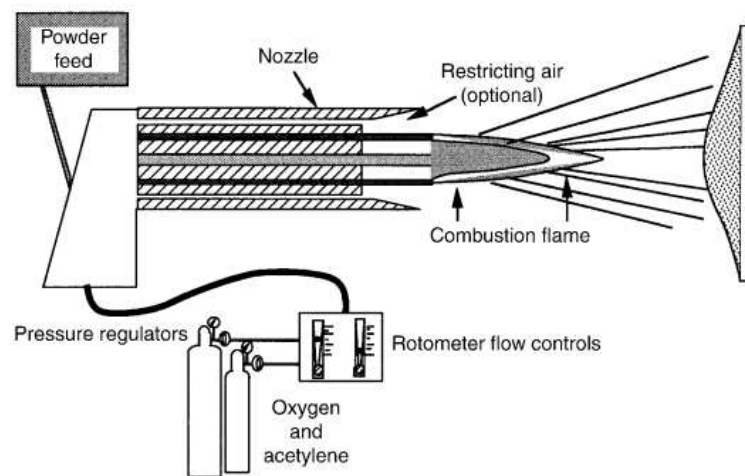


**Figure 6** – Flame spray system with powder as feedstock material [6].

*High velocity flame spraying* is a thermal spray technology where the chemical energy to produce heat is obtained by the combustion of a hydrocarbon molecule ( $C_xH_y$ ) with an oxidizer, generally oxygen or air, in a chamber with a pressure between 0.24 and 0.82 MPa and cooled with water or air.

If the oxygen is used as oxidizer the process is called High Velocity Oxy-fuel Flame (HVOF) otherwise if air is used as oxidizer the process is called High Velocity Air-fuel Flame (HVOF).

Using HVOF instead HVOF can lead to a lower operating cost, higher spray rate and to a higher density due to the higher particle velocities but on the other hand those processes can have lower deposition efficiency and can require and generate more energy that is converted into a more heating of the substrate.

In high velocity flame spraying the combustion chamber is followed by a convergent-divergent Laval nozzle in order to obtain a very high gas velocities (up to 2000 *m/sec*). However, with this technology the temperature of the particles is lower than for examples the temperatures reached with plasma spray because the dwell time in the gas stream is much lower; despite this the density value achieved with HVOF or HVOF is high because the particles have a high kinetic energy which deform particles that could not be completely melted [6].

The most common used feedstock material are powders but there are also some guns that uses wire or rod, in some case even suspension or solution can be used as feed material. Figure 7 shows a typical system configuration for HVOF.

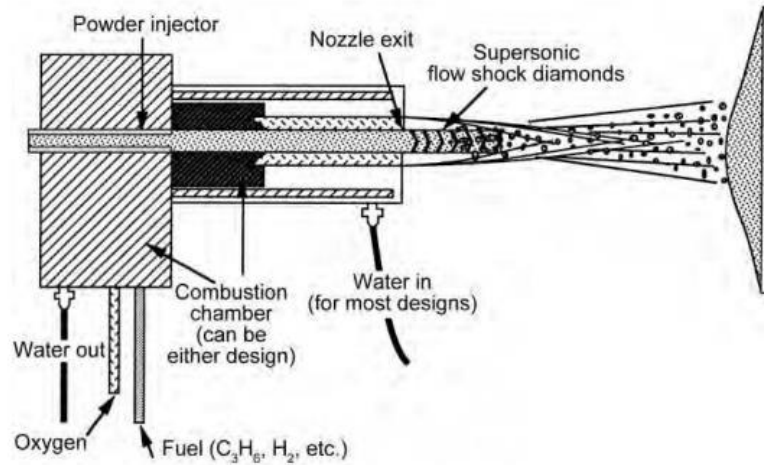


**Figure 7** – Representation of a HVOF system [6].

*Detonation gun* is another combustion spraying process but it's different from Flame Spray, HVOF and HVAF because in D-gun process instead of a flame there is a shock wave sustained by the energy of chemical reactions in the compressed explosive gas mixture.

In this process the combustion is confined within a tube (or barrel) into which the powders are introduced.

For applying coating with D-gun process is necessary to introduce an explosive mixture of fuel, oxygen and powder into the tube and then ignite them with a spark plug.

In this condition a detonation-pressure wave that heat and accelerate the powder towards the substrate is created and after that nitrogen is used to purge the barrel [6].

The different steps of D-gun process are represented in Figure 8.

D-gun process is not a continues process but it is characterized by a cycle time into which every detonation and powder spray are completed, the frequency of this cycle can goes from 3 to >10 Hz [6].

Coatings obtained with this process are characterized by a lower content of oxides because the particles are protected by the combustion gas environment of the extended barrel.

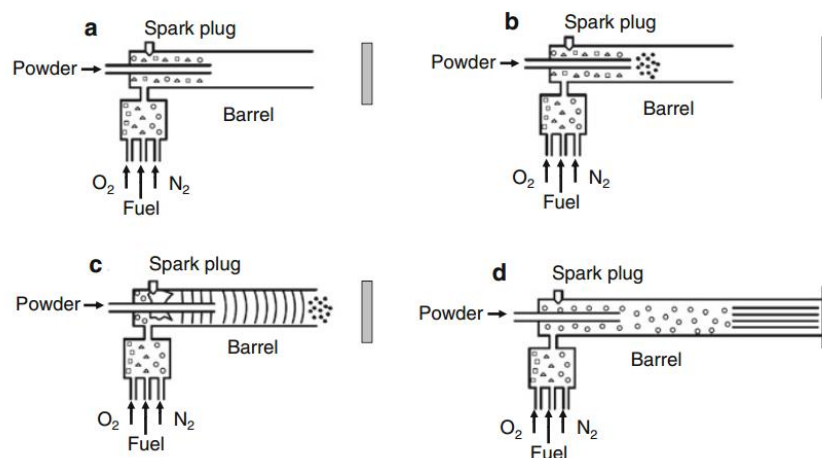


**Figure 8** – Detonation gun process cycle usin nitrogen as a buffer gas: **(a)** injection of fuel and oxygen into the combustion chamber, **(b)** injection of powder and nitrogen gas, **(c)** gas detonation and powder acceleration, **(d)** chamber exhausting [4].

### 2.2.2.3. Electrical discharge plasma spraying

In these process electrical energy is used to create an electric arc or a plasma state which are then used to melt the powders.

In this category is possible to find plasma spraying and electric arc spray.

In *electric arc spray process* an electric arc, which stakes between the wires used as feedstock material, is used to melt the feed material.

The melting process forms droplets that are accelerated towards the substrate with the assistance of a atomizing gas.

Figure 9 shows a typical configuration for electric arc spraying.

The feedstock material must allow the flow of current and must be formed into wire, therefore only conductive and ductile materials can be used in this process [6].

In this process only the melted material leaves the wire to reach the substrate therefore the cooling process begin as soon as the droplets are formed.

For that reason, to avoid a lot of oxide content in the coating the dwell time can be reduced by using short standoff distance [6].

The feed rate that can be achieved with this technology is relatively high in comparison with the feed rate of other thermal spray process.

With electric arc spray the heating of the substrate is kept very low because no flame or plasma jet is formed so this process is suitable for application where the temperature of the substrate must remain low (i.e. coating of polymers).

The coatings obtained with this process are characterized by splats that are thicker and more variable in size than those obtained with wire flame spraying and plasma spraying, the porosity value is lower than that obtained with flame spray or plasma spray for the fact that the droplet's temperature is higher and the dwell time shorter [6].

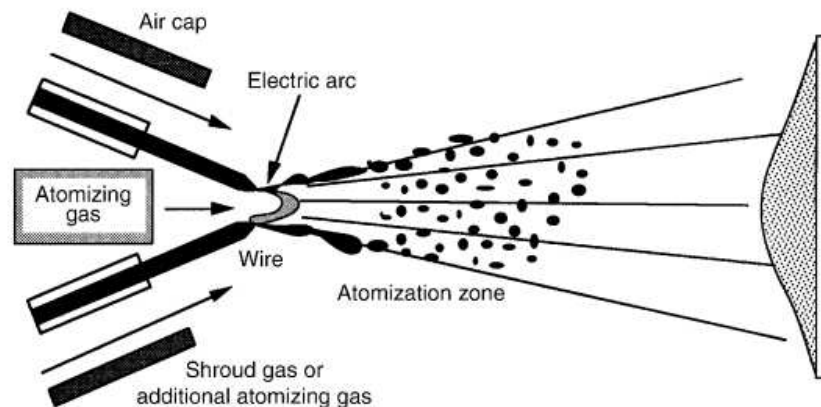


**Figure 9** – Configuration of electric arc spray process [6].

*Plasma spray* is generally used to deposit materials with a high melting point because this process allows to reach high temperatures (12 000 – 15 000 K) [4], for this reason this technology is mostly used to deposit ceramic coatings such as  $Cr_2O_3$ ,  $Al_2O_3$ ,  $TiO_2$  and their mixture.

The spray particles are heated and transported to the substrate by the plasma, when they reach the surface they form the splats and the coatings is formed by adding different layers of those particles.



The feedstock material is generally introduced radially into the plasma jet and they are in powders forms, recently different plasma spray process where the feedstock material is in form of liquid solution have been developed.

This new form of feedstock materials allows to obtain a coating with nano-sized grain and absence of lamella boundaries, cracks and porous microstructure, however this new processes are rarely used in the different industrial sectors [4].

Some process parameters for plasma spray are related to the substrate like its morphology and temperature while others parameters are related to the spray particles like their velocity, temperature, morphology and size distribution.

The spray particle's characteristics are determined by the plasma jet characteristics such as temperature and velocity distribution, thermal conductivity, viscosity.

Plasma spray process has a lot of different parameters which allow to deposit a wide range of different parameters but at the same time they can provide some process instability because it's difficult to control all of them in the same time.

The coatings obtained by plasma thermal spray are quite dense (density about 98%) thanks to the high kinetic energy of the particles and to the high melting efficiency, for these reasons also the bond strength value is quite high (34 MPa or even more than 64 MPa) [6].

Before the description of the different types of plasma spraying process is essential to describe the plasma's state.

Plasma, called also the fourth state of matter, is constituted of a mixture of ions, electrons, neutral molecules and atoms in the fundamental or excited state; in any case plasma must remain electrically neutral.

The plasma state is formed using an electric field and it is achieved when current can be sustained as the free electrons move through the ionized gas.

Two type of plasma depending on electron density can be identified: low-pressure cold plasma and high pressure thermal plasma.

The first type has an electron density typically around  $10^{-2}$  electrons per  $cm^3$  while the second one has a density of  $10^{18}$  electrons per  $cm^3$ .

The energy exchange between light, fast moving and therefore energetic electrons and heavy, slowly moving charged ions is facilitated in thermal plasma due to its high value of pressure.

This energy exchange leads to efficient transfer of energy, in fact in this type of plasma the ions temperature  $T_i$  equal the electron temperature  $T_e$  [5].

The plasma generated in plasma spraying processes is a thermal plasma because it must be capable to melt materials with a high melting point like Zirconia.

The melting efficiency depends on the plasma's enthalpy and as showed in Figure 10 hydrogen has the higher enthalpy value thanks to its small atomic dimension.

Thermal plasma should also be able to transfer the powders from the injection point to the substrate and this characteristic depends on the value of plasma's viscosity and the gases that have a high value of viscosity at the operating temperatures are Ar and He.

Therefore, in order to achieve a good value of enthalpy and viscosity a mixture of two or three gases (Ar-He, Ar- $H_2$ ,  $N_2$ - $H_2$ , Ar-He- $H_2$ ) is generally used .

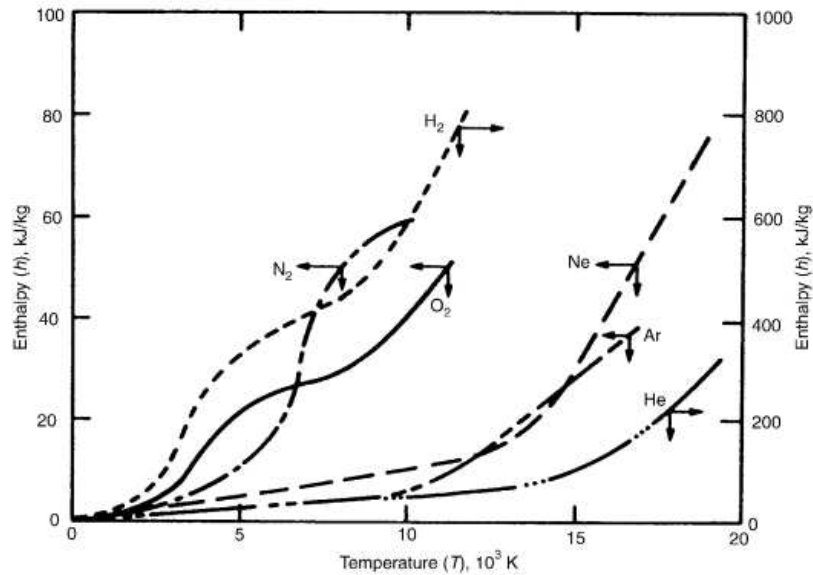


**Figure 10** – Relation between enthalpy and temperature for different gases [6].

As mentioned before there are different kind of spraying process that uses plasma gases to melt the feed material, the most relevant are direct current plasma spraying, radio frequency plasma spraying and direct current transferred arc plasma.

In *direct current plasma spraying* a plasma is generated continuously by an electric arc and it is used to melt and accelerate the feed material towards the substrate.

The arc is created between a cathode and a cylindrical anode nozzle.

The plasma gas is injected at the base of the cathode, then it's heated by the arc and exits the nozzle as a high temperature, high velocity jet [4].

At the nozzle exit can be reached temperature around 12000-15000 K and velocities ranging from 500 to 1200 *m/sec*.

The powders are usually introduced radially into the plasma jet, the point of injection can be downstream of the arc root or even inside the nozzle and sometime it can be outside the nozzle.

The point of injection can be either perpendicular or orientated in direction or against the plasma jet.

However there also some plasma torches where the injection of the powders is axially to the plasma jet.

Figure 11 shows a typical plasma spray process with radially introduction of the powders.

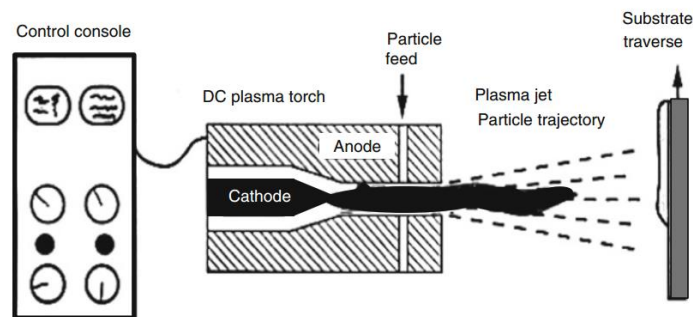


**Figure 11** – Typical configuration for direct current plasma spraying [4].

The direct current plasma spray can be divided by the type of environment in which it is utilized.

If the spraying process is realized in atmospheric environment it is called atmospheric plasma spray (APS), if it is realized in a chamber with controlled atmosphere it's called controlled atmosphere plasma spray (CAPS) and finally if it is performed in a low pressure chamber (10-30 kPa) it's called vacuum plasma spray (VPS) [4].

Spray torch is the most important part in a plasma spray system, there different type of spray torch depending on the type of anode and cathode utilized, each configuration provides optimal particle temperature and velocities for a specific configuration.

As showed from Figure 12 plasma torch can be divided into cathode region, arc column region and anode region.

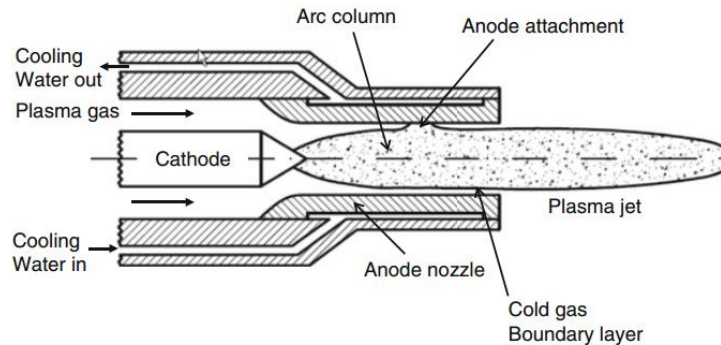


**Figure 12** – Schematic of the commercial plasma torch SG100 from Praxair-TAFA [4].

The equipment for plasma spray is constitute by a plasma torch, a process control console, plasma gas supply system, power supply system, cooling water circuit, spray powder supply system and additional ancillary equipment.

The arc cathode must supply electrons and those electrons are supplied through thermionic emission. The most common used material for cathode is tungsten with an addition of  $ThO_2$ ,  $La_2O_3$  or  $LaB_6$  in order to decrease the working temperature (with only tungsten the temperature reach 4500 K and the cathode will be molten).

However, the tungsten based cathode can't be used with oxidizing gases because it is eroded by the formation of volatile tungsten oxides.

With these gases is used the button-type electrodes, in this case the thermionic emission material is insert in form of a bottom into a water-cooled copper holder. The button is generally made with hafnium or zirconium and the surface of the material is molten [4].

The arc column presents different kind of species like molecules, atoms, ions, and electrons and it can be described by the conservation equations for mass, momentum and energy.

Its characteristics are determined by the energy dissipation per unit length for example by the arc current, the plasma gas flow and composition, and the arc channel diameter [4].

Torch anode is usually made by a water-water cooled channel and it is a passive component just, collecting electrons to allow the current to flow from the solid conductors of the electrical circuit to the plasma.

Nozzle design can emphasize high gas velocities, high gas temperature, profile temperature and different average arc lengths thus arc voltages and torch powers.

There are commercial plasma torches that use anodes with cylindrical nozzle bores but even anode with Laval-type diverging exits, this type of nozzle provides a more uniform velocity and temperature distribution at its exit and reduce turbulent cold gas entrainment resulting in a more uniform particle heating and acceleration [4].

Direct current plasma spray is generally performed in open air therefore there are always some oxides in the coating that decrease its quality.

To minimize the oxide content or even to eliminate it, it is possible to use processes like CPS or VPS where the spraying environment is controlled by introducing argon (CPS) or by achieving a low pressure value (VPS).

Table 1 compare APS and VPS process with the other thermal spray process.

**Table 1 - Main properties for different thermal spray process**

Attribute	Flame spray	High-velocity oxyfuel	Detonation gun	Wire arc	Air plasma	Vacuum plasma
<b>Jet</b>						
Jet temperature, K	3500	5500	5500	>25,000	15,000	12,000
Jet velocities, m/s (ft/s)	50-100 (160-300)	500-1200 (1600-4000)	>1000(>3300)	50-100 (160-300)	300-1000 (1000-3300)	200-600 (700-2000)
Gas flow, sLm	100-200	400-1100	N/A	500-3000	100-200	150-250
Gas types	O <sub>2</sub> , acetylene	CH <sub>4</sub> , C <sub>3</sub> H <sub>6</sub> , H <sub>2</sub> , O <sub>2</sub>	O <sub>2</sub> , acetylene	Air, N <sub>2</sub> , Ar	Ar, He, H <sub>2</sub> , N <sub>2</sub>	Ar, He, H <sub>2</sub>
Power input, kW equiv.	20	150-300	N/A	2-5	40-200	40-120
<b>Particle feed</b>						
Particle temperature (max), °C (°F)	2500 (4500)	3300 (6000)	N/A	>3800 (>6900)	>3800 (>6900)	>3800 (>6900)
Particle velocities, m/s (ft/s)	50-100 (160-300)	200-1000 (700-3300)	N/A	50-100 (160-300)	200-800 (700-2600)	200-600 (700-2000)
Material feed rate, g/min	30-50	15-50	N/A	150-2000	50-150	25-150
<b>Deposit/coating</b>						
Density range, %	85-90	>95	>95	80-95	90-95	90-99
Bond strength, MPa (ksi)	7-18 (1-3)	68 (10)	82 (12)	10-40 (1.5-6)	<68 (<10)	>68 (>10)
Oxides	High	Moderate to dispersed	Small	Moderate to high	Moderate to coarse	None

Radio frequency induction plasma spraying doesn't use electrode to generate plasma as d.c. plasma spraying, because the energy transferred into the discharge is governed by electromagnetic coupling.

Figure 13 shows d.c. plasma spray and r.f plasma spray equipment.

The process used to transfer energy in this process is similar to the induction heating of metals, the only different is that in this case is used a plasma gas instead of a metallic cylinder [4].

The first step to create plasma is to apply a high frequency voltage to a water cooled coil surrounding the discharge vessel, this step lead to a high frequency current flow in this coil which create an a predominantly axial high frequency oscillating magnetic field within the discharge cavity.

Then an electric field perpendicular to the magnetic field lines is generated by the oscillating magnetic field and this event allow the presence of an alternating current flow (induction current) that sustains the plasma thanks to joule heating.

The direction of the induction current is opposite to the direction of the current in the coil and it generates a magnetic field that has an opposite direction to the magnetic field generated by the current coil [4].

Radio frequency plasma spray is generally used where advance materials and composite forming must be processed.

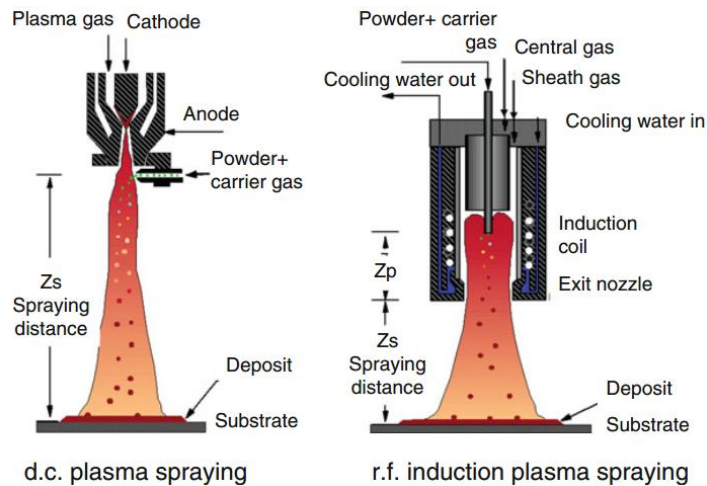


**Figure 13** – System configuration for d.c. plasma spraying and r.f. induction plasma spraying [4].

*Plasma transferred arc process* is very similar to d.c. plasma spraying with the only difference that in this case the arc is transferred between a floated electrode and the substrate that must be metallic.

The coating is formed thanks to the transferred arc that melts the substrate and the powders, this process is in fact very to a welding process.

Figure 14 shows a typical configuration for plasma transferred process.

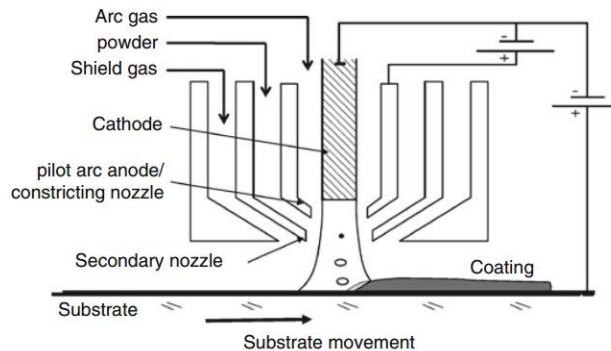


**Figure 14** – Typical configuration for plasma transferred arc process [4].

### 2.3. Corrosion

The term corrosion refers to the degradation of materials caused by chemical or electrochemical process which take places with the exposure to an aggressive environment. Corrosion is a spontaneous event because the oxidation of a metal is a process that leads to lower level of energy therefore every metallic material is affected by this phenomenon [8].

However, despite every element is effected by corrosion some of them can respond in a better way, this mean that the level of corrosion damage along time is less relevant.

A part effected by corrosion can lose its functional properties and in the worst case it can face a failure event.

Different studies have been conducted to determinate the cost of corrosion and some results are showed in Figure 15.

Corrosion phenomena represent a huge cost for industry therefore its control and prevention is extremely important, in fact it can be demonstrated that with valid prevention methods the total cost of corrosion can be reduced by 40% [10].

Corrosion event can be divided in two main categories which are aqueous corrosion and high-temperature corrosion.

The first one takes place when the part is exposed to an environment that contain a liquid electrolyte (i.e. water) while the second one takes place when the part is exposed to an environment that contains hot gases [10].

In aqueous corrosion is possible to individuate a flow of electrons from one metals to another that come from the electrochemical reactions between the metallic materials and the environment while in the high-temperature corrosion no flow of electrons can be individuate and the oxide layer is formed thanks to the reaction of metals with oxygen at high-temperatures.

The type of corrosion exanimated in this work is the aqueous therefore only this category will be studied in in the next paragraphs.

	1975 (billions of current dollars)	1995
<i>All Industries</i>		
Total	82.0	296.0
Avoidable	33.0	104.0
<i>Motor Vehicles</i>		
Total	31.4	94.0
Avoidable	23.1	65.0
<i>Aircraft</i>		
Total	3.0	13.0
Avoidable	6	3.0
<i>Other Industries</i>		
Total	47.6	189.0
Avoidable	9.3	36.0

Figure 15 – Corrosion cost in United states [9].

### 2.3.1. Principles of aqueous corrosion

As mentioned before, aqueous corrosion is characterized by a flow of current between two metal parts. This current is the result of the material's deterioration which takes place due to the exposure in an aggressive environment.

In order to have aqueous corrosion the system must present four elements which are anode component, cathode component, electrolyte solution, and electrical conductor material.

In the anode component occurs the oxidation of metals while in the cathode the reduction reaction of environment takes place, the electrolyte solution and the metallic conductor allows the flow of current between the anode and the cathode.

These four elements forms together an electrochemical cell as showed by Figure 16.

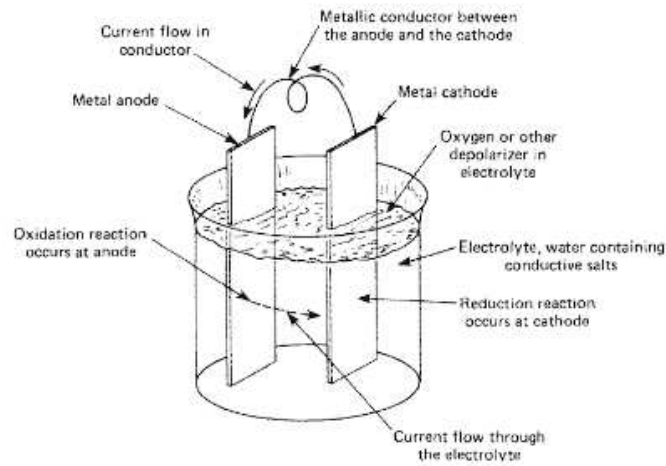


**Figure 16** – Representation of an electrochemical cell constituted during the corrosion process [10].

When corrosion takes place a current flow between anode and cathode occurs and a potential difference between anode and cathode could be measured by using a voltmeter. The metal oxidation reaction produces electrons and can be described as follow:



The reduction reaction is performed by the environment and it consumes the electrons produced by the anode.

The two chemical elements who generally takes place to the reduction reaction are hydrogen or oxygen and their reaction can be described as follow:



During aqueous corrosion an electrified interface is formed between the electrode and the electrolyte, this interface is characterized by a potential difference which leads to the definition of electrode potential that is an important parameter for evaluating corrosion phenomena [8].

The electrified interface is really complex but it can be simplified in the following way. During corrosion metal electrode lose electrode and release cations in the solution; because electrons remains in the metal, cations will be attracted by them and they will remain close to the electrode interface leading to a presence of charged interface which results in an electric field.

If the electrolyte is composed by water as primary solvent, this electric field has a consequence in the orientation of water molecules.

In fact, water is polar and it can be seen as a dipolar molecules that have a positive side (hydrogen atoms) and a negative side (oxygen atoms) therefore the dipolar will be aligned in the direction of the electric field [8].

Furthermore, the ions which are charged for the loss or gain of electrons, attract the water molecules which orientates themselves in the electric field established by the charge of the ions.

The attraction between ions and water molecules is so strong that ions can't move without taking with them the water molecules, this complex of chemical species is called hydrated ion.

For the fact that cations have smaller dimension than anions they can attract more easily water molecules.

The final configuration of metal interface is shown in Figure 17, it is composed by a first row of water molecules which limit the distance between metal surface and cations and by cations which are surrounded by the water molecules bonded with them.

As can be seen from Figure 17, the positive charge stays in a fixed distance from the metal and the plane containing the positive charge is called outer-Helmholtz plane (OHP) [8]. The region where the charges are so arranged is called electric double layer and can be seen as a charged capacitor [8].

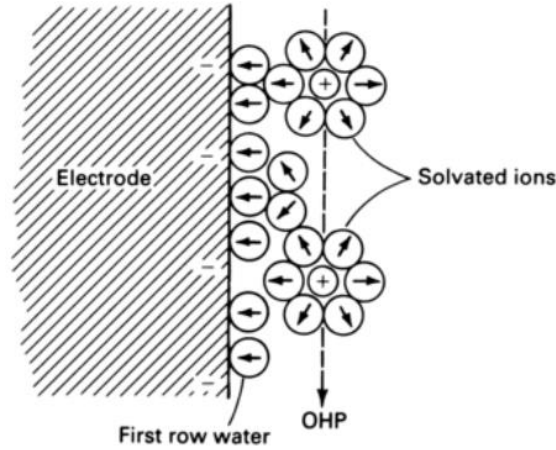


**Figure 17** – Representation of the electric double layer [8].

In this condition, if a generic chemical species is considered, in order to have an equilibrium condition the electrochemical potential in the solution and the electrochemical potential in the metal must be the same.

$$\tilde{\mu}_i^M = \tilde{\mu}_i^S \quad (\text{Eq.4})$$

This mean that the variation of electrochemical potential through the difference phases must be zero.

$${}^M\Delta^S \tilde{\mu}_i = 0 \quad (\text{Eq.5})$$

The electrochemical potential is the variation of the system's free energy after the introduction of a mol of particles  $i$  into the phase at constant temperature and pressure.

$$\tilde{\mu}_i = (\partial \tilde{G} / \partial n_i)_{T,P,j \neq i} \quad (\text{Eq.6})$$

$\tilde{G}$  indicates a free electrochemical energy which contains also the electric contributions to the energy

$$\tilde{G} = G + nF\phi \quad (\text{Eq.7})$$

Where  $F$  is the faraday's constant and  $\phi$  the Galvani potential.

These lead to the following mathematic definition of electrochemical equilibrium:

$$\begin{aligned} {}^M\Delta^S \tilde{\mu}_i &= \tilde{\mu}_i^S (\text{initial state}) - \tilde{\mu}_i^M (\text{final state}) = \\ &= (\mu_i^S + z_i F\phi_i^S) - (\mu_i^M + z_i F\phi_i^M) = \\ &= (\mu_i^S - \mu_i^M) + z_i F(\phi_i^S - \phi_i^M) = \end{aligned}$$



$$= M \Delta^S \mu_i + z_i F M \Delta^S \phi_i = 0$$

$$M \Delta^S \phi_i = - M \Delta^S \mu_i / z_i F$$

$$M \Delta^S \mu_i = - z_i F M \Delta^S \phi_i$$

$$\Delta G = -nF\Delta\phi \quad (\text{Eq.8})$$

In conclusion, when there is a condition of equilibrium there is also a free flow of species through the interface and the chemical contribute is equal to the electrical contribute.

It's not possible to measure directly the potential galvanic difference  $\Delta\phi$  because to perform the measure the electric circuit must be close and this imply that the electrode must be connected to another electrode adding to the system another interface that compromise the final measure, in fact the potential value that in general is indicated with E is not the measurement of  $\Delta\phi$ . That means that E is not the value of  $\Delta\phi$  but instead the potential difference between the electrode where the reactions occur and the electrode used to close the circuit [11].

For that reason, the hydrogen electrode (SHE electrode) has been chosen as a reference to perform all the electrochemical measures, in fact to this electrode has been assigned a value of potential equal to 0 V.

This convention allowed to define the electrochemical shell, Figure 18, which contain the electrochemical potentials of different reactions using an hydrogen electrode in standard condition (  $T= 25^\circ\text{C}$ ,  $P = 1$  atm for gases and concentration 1M for solutions).

Electrode reaction	Standard potential at 25 °C (77 °F), volts versus SHE
$\text{Au}^{3+} + 3e^- \rightarrow \text{Au}$	1.50
$\text{Pd}^{2+} + 2e^- \rightarrow \text{Pd}$	0.987
$\text{Hg}^{2+} + 2e^- \rightarrow \text{Hg}$	0.854
$\text{Ag}^+ + e^- \rightarrow \text{Ag}$	0.800
$\text{Hg}_2^{2+} + 2e^- \rightarrow 2\text{Hg}$	0.789
$\text{Cu}^+ + e^- \rightarrow \text{Cu}$	0.521
$\text{Cu}^{2+} + 2e^- \rightarrow \text{Cu}$	0.337
$2\text{H}^+ + 2e^- \rightarrow \text{H}_2$	0.000
$\text{Pb}^{2+} + 2e^- \rightarrow \text{Pb}$	-0.126
$\text{Sn}^{2+} + 2e^- \rightarrow \text{Sn}$	-0.136
$\text{Ni}^{2+} + 2e^- \rightarrow \text{Ni}$	-0.250
$\text{Co}^{2+} + 2e^- \rightarrow \text{Co}$	-0.277
$\text{Tl}^+ + e^- \rightarrow \text{Tl}$	-0.336
$\text{In}^{3+} + 3e^- \rightarrow \text{In}$	-0.342
$\text{Cd}^{2+} + 2e^- \rightarrow \text{Cd}$	-0.403
$\text{Fe}^{2+} + 2e^- \rightarrow \text{Fe}$	-0.440

Electrode reaction	Standard potential at 25 °C (77 °F), volts versus SHE
$\text{Fe}^{2+} + 2e^- \rightarrow \text{Fe}$	-0.440
$\text{Ga}^{3+} + 3e^- \rightarrow \text{Ga}$	-0.53
$\text{Cr}^{3+} + 3e^- \rightarrow \text{Cr}$	-0.74
$\text{Cr}^{2+} + 2e^- \rightarrow \text{Cr}$	-0.91
$\text{Zn}^{2+} + 2e^- \rightarrow \text{Zn}$	-0.763
$\text{Mn}^{2+} + 2e^- \rightarrow \text{Mn}$	-1.18
$\text{Zr}^{4+} + 4e^- \rightarrow \text{Zr}$	-1.53
$\text{Ti}^{2+} + 2e^- \rightarrow \text{Ti}$	-1.63
$\text{Al}^{3+} + 3e^- \rightarrow \text{Al}$	-1.66
$\text{Hf}^{4+} + 4e^- \rightarrow \text{Hf}$	-1.70
$\text{U}^{3+} + 3e^- \rightarrow \text{U}$	-1.80
$\text{Be}^{2+} + 2e^- \rightarrow \text{Be}$	-1.85
$\text{Mg}^{2+} + 2e^- \rightarrow \text{Mg}$	-2.37
$\text{Na}^+ + e^- \rightarrow \text{Na}$	-2.71
$\text{Ca}^{2+} + 2e^- \rightarrow \text{Ca}$	-2.87
$\text{K}^+ + e^- \rightarrow \text{K}$	-2.93
$\text{Li}^+ + e^- \rightarrow \text{Li}$	-3.05

**Figure 18** – Electrochemical shell for different chemical species [8].

All the reactions are written in the reduction verse therefore if the potential is positive the electrode works as cathode otherwise it works as anode and it oxides.

As can be seen, almost all the metals used generally in industry sectors (except Cu) show an anodic behavior versus hydrogen, this mean that they behave as an anode compared to this chemical agent.

Nowadays SHE electrode is rarely used because it has been substitute by other electrode which have always a fixed value of the potential (i.e. saturated calomel electrode SCE). If this a reaction doesn't take places under the standard conditions the potential value must be modified using Nernst's equation.

$$E_{eq} = E_0 + \frac{RT}{nF} \ln \frac{a_{\text{oxidized species}}}{a_{\text{reduced species}}} \quad (\text{Eq.9})$$

Written in this way the Nernst's equation is valid for the semi reaction and n are the electrons involved in the reaction.

It must be pointed out that the aqueous corrosion should be studied by a thermodynamic approach and by a kinetic approach.

When a metal component is exposed to a determinate environment it can have different behavior, in fact it can have an active behavior which means that it starts to corrode, it can have an immune behavior which mean that the component isn't affected by corrosion or it can have a passive behavior which means that corrosion takes place but the oxide layer that grows on the surface is protective for the future corrosion (i.e. stainless steel). Thermodynamic studies determinate if the material has an active, immune or passivate behavior while kinetic approach allows to determinate the corrosion rate, which is extremely important, because sometimes corrosion phenomena can be accepted if its corrosion rate is lower than a determinate value.

Thermodynamic behavior can be studied using potential-pH diagrams also called Pourbaix diagrams.

These diagrams allow in fact to determine the behavior of metal (active, immune, passivated) in a given pH and potential value.

Pourbaix diagram are therefore divided in different areas where in each of them is stable a phase of metal.

To have a complete analysis with the Pourbaix diagrams also the line corresponding to the reduction of hydrogen and oxygen must be reported.

Corrosion occurs if the work point individuated by the value of potential and pH is in a region where the metal has an active behavior and the reduction of hydrogen or oxygen take place.

Pourbaix diagram for iron is showed in Figure 19.

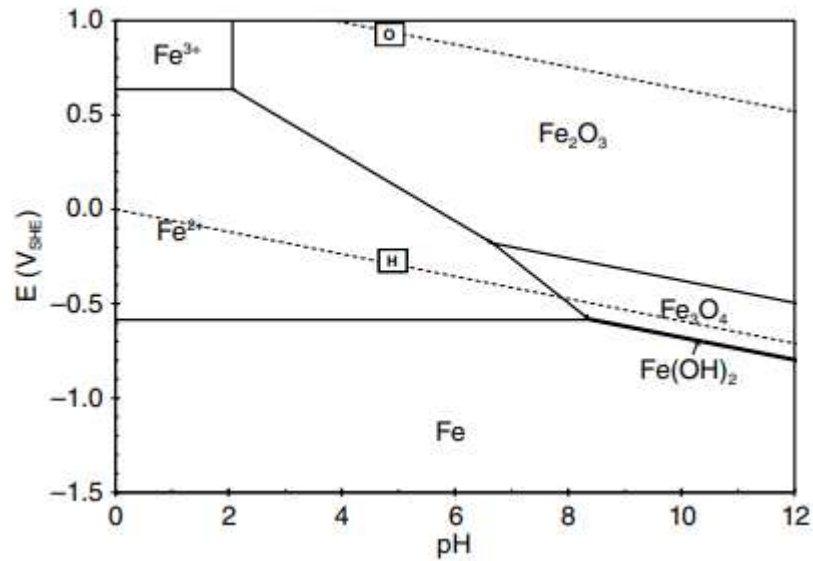


**Figure 19** – Pourbaix diagram for Iron [12].

Pourbaix diagrams are useful to have a first approach to the corrosion phenomena but they can't be sufficient to have a complete vision of corrosion because, as mentioned before, they only approach corrosion on its thermodynamic aspect without considering the kinetic aspect, moreover they consider pure metal while alloys are general used in industrial application. In that case a Pourbaix diagram must be drawn considering any single case.

Kinetic approach has as aim to individuate the corrosion current involved in a corrosion process.

During corrosion there are electrons that are relieved by the anode and electrons that are acquired by the cathode therefore it's possible to individuate an anodic current  $i_a$  (electrons relieved with time by anode) and a cathodic current  $i_c$  (electrons achieved with time by cathode).

When the system is in an equilibrium condition, in other words when the potential value is equal to  $E_0$  or  $E_{eq}$ , the anodic current is equal to the cathodic current.

To move from the equilibrium condition is must be applied a potential from outside the system  $E(i)$  which leads to the presence of an overvoltage  $\eta$ .

$$\eta = E(i) - E_{eq} \quad (\text{Eq.10})$$

For convention, if the overvoltage value is positive, the anodic reaction is favorited and the value of external current ( $i = i_a - i_c$ ) is positive otherwise the cathodic reaction is favorited and value of external current is negative.

$$\text{a) } \eta = E(i) - E_{eq} > 0$$

$$i_a > i_c$$

$$i = i_a - i_c > 0$$

$$\text{b) } \eta = E(i) - E_{eq} < 0$$

$$i_a < i_c$$

$$i = i_a - i_c < 0$$

The relation between the external current and the overvoltage can be described by the Buttle-Volmer equation:

$$i = i_0 \{ \exp[(1 - \alpha)\eta nF/RT] - \exp(-\alpha\eta nF/RT) \} \quad (\text{Eq.11})$$

Where  $\alpha$  is the charge's transfer coefficient,  $n$  the number of electrons involved in the reaction and  $F$  the Faraday's constant.

Graphically the Buttle-Volmer's equation has the form represented in Figure 20.

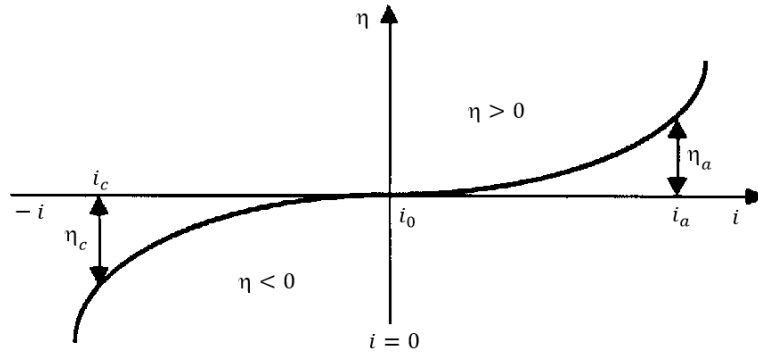


**Figure 20** – Representation of Buttle-Volmer's equation [11].

In corrosion phenomena is possible to consider  $\eta \gg 0$  or  $\eta \ll 0$ , therefore the Buttle-Volmer's equation is simplified as follow:

a)  $\eta \gg 0$

$$e^{(1-\alpha)\eta nF/RT} \gg 0 \quad e^{-\alpha\eta nF/RT} = 0$$

$$i = i_0 e^{(1-\alpha)\eta nF/RT}$$

$$\eta = - \left[ \frac{RT}{(1-\alpha)nF} \right] \ln i_0 + \left[ \frac{RT}{\alpha nF} \right] \ln i$$

$$\eta = a + b \lg i \quad (\text{Eq.12})$$

b)  $\eta \ll 0$

$$e^{(1-\alpha)\eta nF/RT} = 0 \quad e^{-\alpha\eta nF/RT} = 0$$

$$i = i_0 e^{-\alpha\eta nF/RT}$$

$$\eta = \left[ \frac{RT}{\alpha nF} \right] \ln i_0 - \left[ \frac{RT}{\alpha nF} \right] \ln i$$

$$\eta = c + d \lg i \quad (\text{Eq.13})$$

In both case is possible to see that the relation between the overvoltage and the current logarithm is linear, these equations are called Tafel's equation.

There is another case where is possible to modify the Buttle-Volmer equation and this is when the overvoltage is below 10 mV.

In this case the relation between the overvoltage and the current is described by the Stern-Geary equation, there is always a linear relation but in this case with the current and not with its logarithm:

$$\eta = \left(\frac{RT}{i_0 n F}\right) i \quad (\text{Eq.14})$$

In this work it is considered only the Tafel's Equation, with a little modify of the Buttle-Volmer graph showed before (potential value instead overvoltage and relation described in the first quarter).

From Figure 21 it's possible to see how the Tafel's equation can describe properly the Buttle-Volmer's equation in a given region of the graph.

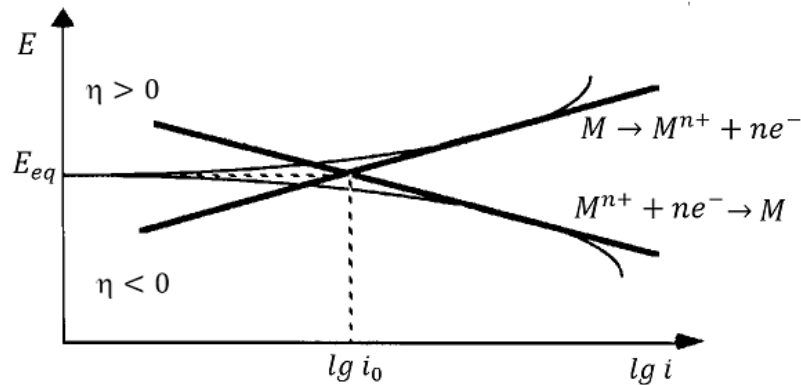


**Figure 21** – Approximation of Buttle-Volmer's equation using tafel's equation [11].

When the two Tafel straight line are individuated it's possible to calculate the current by calculating the intersection point as showed in Figure 21.

However, the corrosion phenomenon involves the oxidation reactions of anode electrode and the reduction reaction of cathode electrode therefore in order to evaluate the corrosion current value the anodic line and the cathodic line of the two electrode must be extended. In addition, for the fact that aqueous corrosion process can be described as a short circuit without electrical resistance the value of current is given by the intersection of anodic and cathodic line as showed in figure 22.

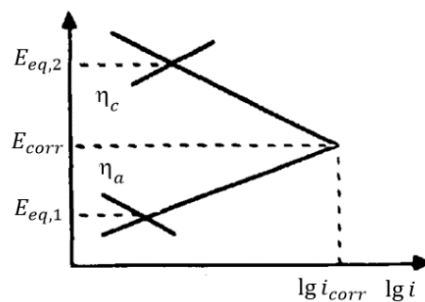


**Figure 22** – Identification of corrosion point in aqueous corrosion when there isn't electrical resistance [11].

As mentioned before, the kinetic approach to corrosion is to determinate the value of current and the potential that occur during corrosion. This goal is achieved using particular instrument called potentiometer which allow to change continuously the value of potential and to measure the flow of current at the same time.

The result of this measure is a graph called potentiodynamic curve which shows the connection between potential value and logarithm of the current.

As showed by Figure 23, with this graph is possible to calculate the value of current and potential during corrosion by fitting it with tafel straight line and calculating their intersection point.

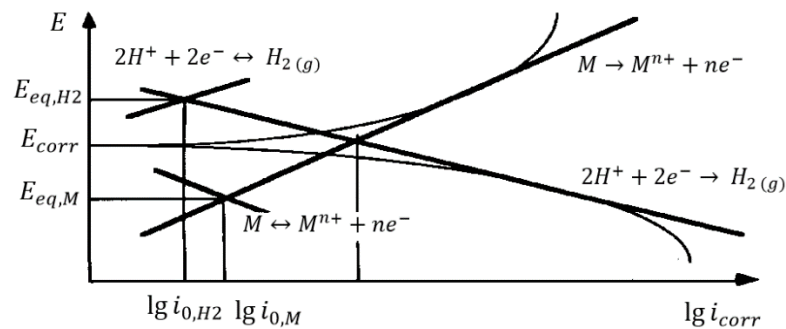


Figure 23 - Anodic polarization of iron in sulfuric acid 1M [11].

In conclusion it can be say that if corrosion phenomenon is studied using simultaneously the thermodynamic and the kinetic approach is possible to determine the behavior of a metal in a determinate type of environment.

### 2.3.2. Forms of corrosion

Corrosion is an electrochemical or chemical events that leads to the deterioration of materials. It can be divided in different forms according to the appearance of the corrosion damage or the mechanism of attack.

The main type of corrosion that can be individuated are: uniform corrosion, galvanic corrosion (dealloying corrosion), pitting corrosion, crevice corrosion, intergranular corrosion (i.e. exfoliation), erosion-corrosion (cavitation corrosion, fretting corrosion), and corrosion assisted by mechanical stress (stress corrosion cracking SCC, corrosion-fatigue, hydrogen damage) (surface engineering).

Figure 24 provide a visual classification of the different forms of corrosion.

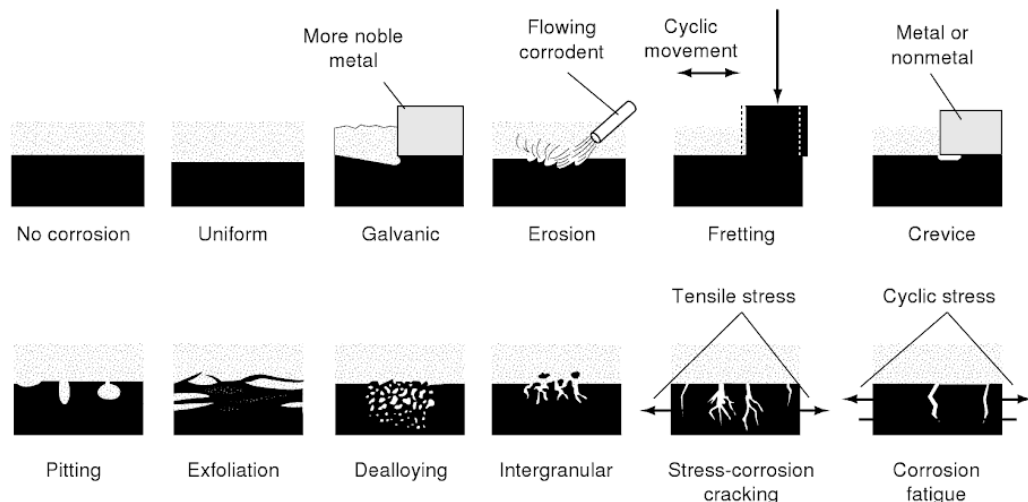


Figure 24 – Representation of the different forms of corrosion [10].

*Uniform corrosion* happens when it's not possible to distinguish the anodic area from the cathode area, in fact the negative electrode and the positive electrode change continuously with each other leading to a homogenous presence of corrosion products on the part.

This type of corrosion is the only one where it's possible to make an initial estimate of corrosion damage which is generally reported as millimeter per year (mm/year) of corroded material, for that reason uniform corrosion is not so dangerous because maintenance can be performed during the part's life time.

*Galvanic corrosion* occurs when two metals (or two different phases in the same material) with different electrochemical nobility are connected together through an electric circuit. If this condition is verified the material with the lower nobility acts as anode and starts to corrode while the other material that has a higher nobility acts as a cathode and allows the reduction on its surface of the chemical species contained in the environment.

When the galvanic takes place between two different materials a key factor is the electrical conductivity of the solution, if it is high the corrosion of the anode will be more uniform otherwise the anode corrosion will be more localized.

Figure 25 the effect of electrolyte's conductivity on galvanic corrosion.

This type of corrosion can be avoided by interrupting the electric circuit between the two metals, this can be done using insulating materials between the metals.

Sometimes galvanic corrosion can be used to protect a certain material (i.e. galvanized steel), this happens by connecting the material that must be saved with another that has lower nobility called sacrificial electrode, in this case, the sacrificial electrode starts to corrode protecting the other electrode.

An example of galvanic corrosion between different phases in the same material can be the dealloying corrosion like the brass's dezincification.

In this type of corrosion, the more active metal (i.e. Zn) is continuously removed from the alloy due to the galvanic couple with the more noble metal (i.e. Cu) which leads to a porous alloy with a higher content of the nobler material.

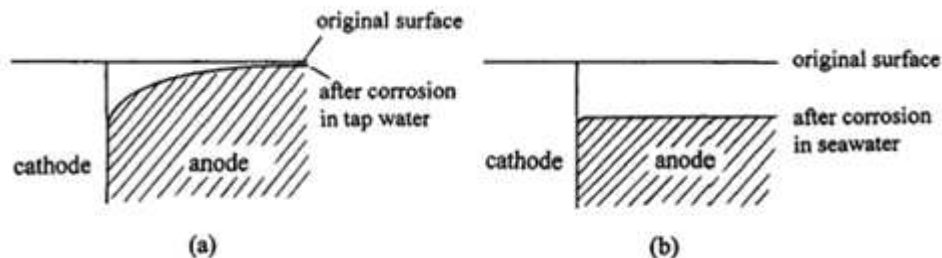


**Figure 25** - Effect of electrolyte's conductivity on galvanic corrosion: (a) low conductivity and (b) high conductivity [11].

*Pitting corrosion* is a localized form of corrosion and it's really dangerous because it can lead to a sudden failure of the part.

It's characterized by a first stage of activation and a second one of propagation.

The activation can occur for localized damage of a protective oxide or a localized damage of a nobler coating, it can also be caused by the presence of non-homogenous phases in the oxide.

If the environment doesn't allow the reformation of protective oxide (low content of oxygen, high content of chlorides) the pitting propagates through the part.

The propagation of pitting can be an autocatalytic process and the presence of chlorides is usually critical for this process.

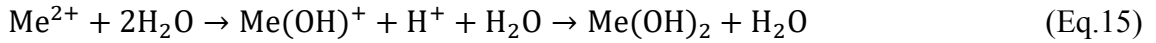
Chloride is a relatively small anion with a high diffusivity therefore it penetrates and reaches the bottom of pitting for electrostatic attraction because in this area metal cations are relieved with the corrosion process.

At this point chlorides tend to form a chemical bond with the cations, called ionic complex, which is soluble in the solution, this fact promotes the formations of new metal cations and the corrosion goes on.

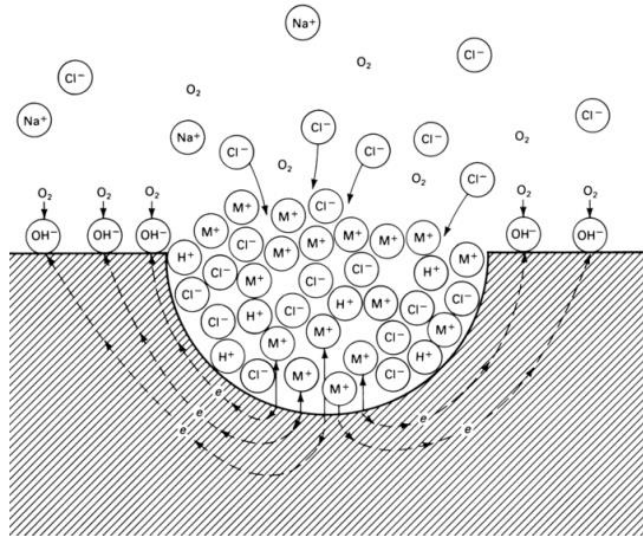
In this state of propagation, the reduction reaction is formed by oxygen.

Figure 26 shows the mechanism of pitting propagation in NaCl solution.

After that some metal cations can also react with water generating the process of water electrolysis, this process lead to the formations of ions  $H^+$  which decrease the value of pH at the bottom of pitting and become the new oxidizing agent [8].



At this point the pitting propagation is autocalytic because the acide chloride enviroment ( $pH \cong 2$ ) is aggressive for most of the metals and corrode them continuously.



**Figure 26** – Pitting propagation method in NaCl solution [8].

*Crevice corrosion* occurs when a part of the metal is isolated by the external environment and therefore the electrolyte finds more difficulties to reach this zone.

In order to evaluate the crevice corrosion, it's important to introduce two types of electrochemical cells, that are the different aeration cell and the metal-ion cell.

The first one takes place when the electrolyte has zones with different concentration of oxygen, the zone with the lower content of oxygen acts as a cathode while the zone with the higher content acts as an anode.

The reason for this behavior is connected with the value of oxygen pressure in the different zone, where the concentration of  $O_2$  is lower then pressure is lower too and according to Nerst's equation this lead to a less valued of electrochemical potential compared to the one where the concentration and pressure is higher, therefore the zone with the less value of potential starts to corrode.

This situation is showed by Figure 27.



$$E_{eq} = E_0 + \frac{RT}{4F} \ln \frac{PO_2}{[OH^-]^4} \quad (\text{Eq.17})$$



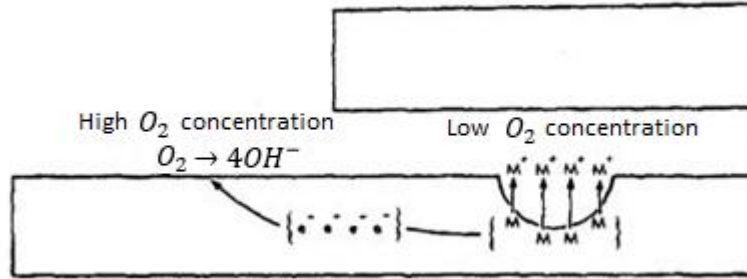


Figure 27 – Representation of different aeration cell [11].

The metal-ion cell occurs when the concentration of cations released by the corrosion process is not constant in the electrolyte.

In fact, outside the covered area is more probable that the cations are transported away from the surface.

According to the Nernst's equation this lead to a lower value of potential outside the covered area so this part acts as anode and starts to corrode as showed in Figure 28.



$$E_{eq} = E_0 + \frac{RT}{nF} \ln \frac{[M^{n+}]}{1} \quad (\text{Eq.19})$$

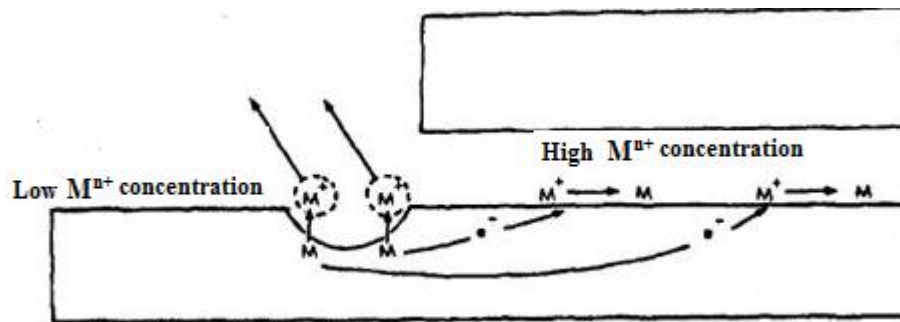


Figure 28 – Representation of metal-ion cell [11].

During crevice corrosion it's possible to have both situation and to understand better which one is prevalent it must be considered also the passivation phenomena.

Materials that doesn't show passivation behavior corrode inside the covered area because here the corrosion rate is higher as showed in Figure 29.

For materials that shows passivation behavior is possible to distinguish three situations.

Materials that have value of potential similar to the value of oxygen (i.e. Cu) corrodes outside the isolated area because the corrosion rate is higher while materials that have a bit difference in the potential value with oxygen (i.e. stainless steel) corrodes internally the covered area because in this point the oxygen content is not enough to form a passivation oxide.

Finally, the material that have a high different in potential value with oxygen (i.e. Ti) are not interested by crevice corrosion because they can form a passivation oxide inside and outside the covered area.

The three situation for materials that have passivation behavior are showed in Figure 30.

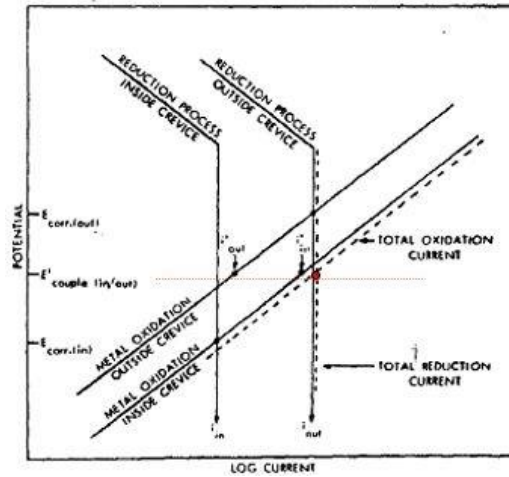


Figure 29 – Analysis of crevice corrosion for materials that don't have passivation behavior [11].

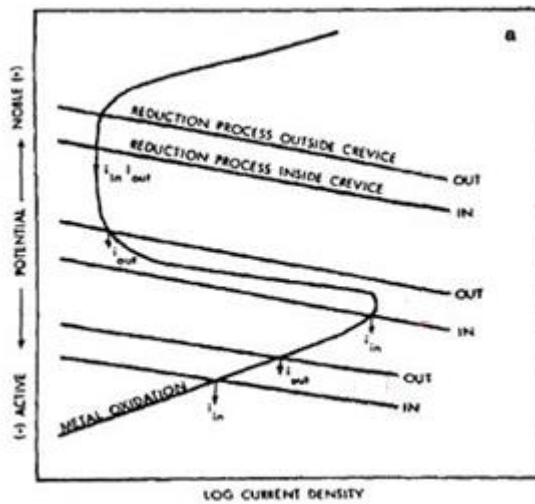


Figure 30 - Analysis of crevice corrosion for materials that don't have passivation behavior [11].

*Intergranular corrosion* takes place when the grain boundary presents different phases which can act as anode respect to the other phases contained in the microstructure. In this situation the grain boundary starts to corrode while the other part of the microstructure acts as a cathode, the results is the detachment of the different grains. Stainless steel can be affected by intergranular corrosion if they are subjected to the sensitization process.

This phenomena takes place during welding process (where temperatures of 450-800 °C are reached) and refers to the precipitations of chromium carbides ( $Cr_{23}C_6$ ).

After the precipitation of chromium carbides, the areas closed to the grain boundary starts to corrode because they are characterized by a lower content of Chromium resulting in a lower value of potential.

Sensitization can be controlled by adding some elements (Ti, Ni) that substitute chromium in the carbides bonding.

Aluminum and its alloy are also susceptible to intergranular corrosion due the aluminum precipitate that are formed after the aging process.

This precipitate acts as anode and cause the corrosion of the grain boundary.

Intergranular corrosion in aluminum is also called exfoliation due to the its aspect, in fact aluminum alloy are generally submitted to a lamination process which tend to generate bi-dimensional grain and when this grains corrode they are detachment with each other like an exfoliation process.

*Erosion-corrosion* takes place when a fluid containing or not abrasive particles impact towards the metal.

The fluid can accelerate the corrosion process in different ways.

For example it can transport away from the surface the corrosion product promoting therefore the anodic reaction or can transport to the surface an higher amount of reduction species such as  $H^+$  or  $O_2$ .

It can also destroy the protective coating with the impact between the particles and the surface.

The typical aspect of an erosion-corrosion event is showed in Figure 31 where the narrow indicates the direction of the fluid.

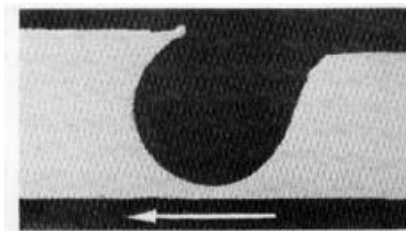


**Figure 31** – Typical aspect of erosion-corrosion [11].

Cavitation corrosion and fretting corrosion are two other forms of erosion-corrosion.

Cavitation corrosion is a different form of erosion-corrosion that is caused by the formation and collapse of vapor bubbles in a liquid against the surface [10].

The continuously collapse causes a fatigue mechanism and lead to the degradation of material's surface.

Cavitation is different from boiling because in the cavitation process the bubbles are formed due to a decrease of the dynamic pressure under a critical value called  $p_{min}$  at constant temperature while in the boiling process the bubbles are formed after a decrease of the static pressure or an increment of the temperature.

Fretting corrosion occurs when two metals surface, where at least one of them is constituted by a protective oxide or a coating, are connected together with a mutual movement between the two parts (i.e. vibrations).

The reciprocal movement of the surfaces damage the protective oxide or coating which can't be replaced, generating therefore a crevice corrosion process.

The corrosion can be increased by the presence of metal and oxide debris which can act as abrasive particles.

Figure 32 illustrates the process of fretting corrosion.

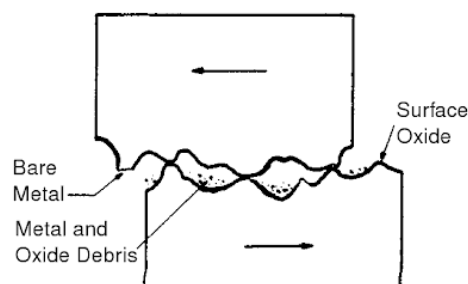


**Figure 32** – Representation of fretting corrosion process [10].

*Corrosion assisted by mechanical stress* occurs when the metal is simultaneously submitted to a mechanical stress and to corrosion phenomena.

Stress corrosion cracking (SCC), fatigue corrosion and hydrogen embrittlement are part of this category.

SCC needs a localized defect to be activated, when it's provided it penetrates through the surface due to stress which tend to open the fissure and due to the chemical reactions which tend to corrode the fissure, the process is showed in Figure 33.

The mechanical stress can be provided by an external load or by internal stressed which can be generated with the manufacturing of the part.

The mechanical stress and the corrosion event are extremely related with each other in fact to prevent stress corrosion cracking it can be blocked only one of this event (i.e. cathodic protection for corrosion or compression stress on the surface for the mechanical event).

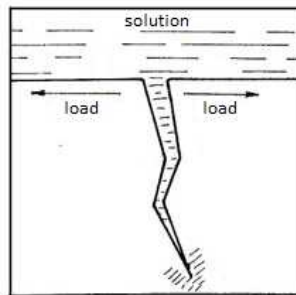


**Figure 33** – Representation of stress corrosion cracking [11].

Corrosion-fatigue occurs when the part is exposed to an aggressive environment and simultaneously it's submitted to a fluctuating or a cyclic stress.

While fatigue process presents a limit value of the stress under which the part can't be affected by fatigue failure, with corrosion-fatigue it's not possible to individuate this value as can be seen from Figure 34.

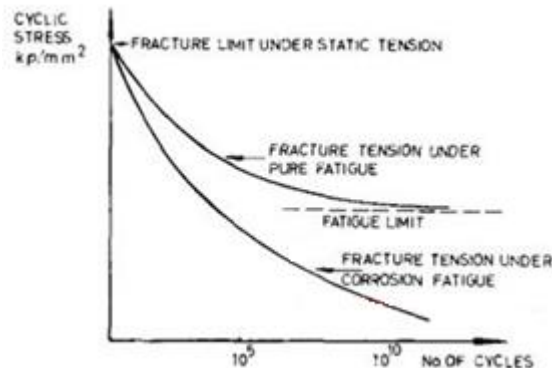


**Figure 34** – Wohler diagrams for a part that is submitted to pure fatigue and for a part that is submitted to corrosion-fatigue[11].

Hydrogen damage occurs when atomic hydrogen penetrates through the surface, this event can lead to a decrease of the plasticity because hydrogen tends to block the dislocation movement.

There are different kinds of hydrogen embrittlement like hydrogen blistering (HB), hydrogen-induced cracking (HIC), stress-oriented hydrogen-induced cracking (SOHIC) and sulfide stress cracking (SSC).

### 2.3.3. Corrosion test methods

The aim of corrosion tests is to evaluate the behavior of the tested material in a given environment and trying to evaluate the total amount of material corroded or to determinate the corrosion rate by measuring the corrosion current  $i_{corr}$ .

However, corrosion phenomenon can be influenced by a lot of factors such as temperature, pH and geometry therefore the evaluation of the exact corrosion event can be difficult to realize.

For that reason, sometimes the results of a corrosion experiment are not composed by an exactly value but instead by a general indication like poor, good or excellent corrosion resistance.

Corrosion test can be divided into three main categories: field test, simulated service test and laboratory test.

*Field tests* consist of exposing the material in the same conditions on which they will work and evaluating after a precision time the total corrosion occurred.

Despite their results are really reliable, this types of tests are rarely used because the time needed for the measurement is long, in fact some experiment can be performed for different years.

*Simulated service tests* reproduce a model of the real corrosion environment and use it to evaluate the corrosion phenomena.

*Laboratory tests* are accelerated tests where one or more corrosion's variables are accelerated in order to reduce the time test.

The results obtained with these tests must be used in a comparative way because there is no connection between the result of the tests and the real conditions in which the material works.

Some examples of accelerated test are electrochemical tests, humidity test and salt spray test.

Successively will be described more in details the polarization test, the EIS, the OCP test and the immersion test because these kind of tests have been utilized during the present work.

Polarization test consists on applying an external potential to the sample within a wide range and measuring the current generated by this external signal; it's also possible to measuring the potential value generated by an applied current but this measurement is less common [8].

The graph obtained from this measurement is built by plotting the applied potential  $E$  versus the logarithm of the measured current density  $i$  and it's called polarization curve.

A polarization curve is constituted by a cathodic part which contain information about the reduction reactions and by an anodic part which instead contain information about the oxidation reactions.

With the analysis of the anodic process it's possible to understand if the sample has been affected by a passivation phenomenon and which is the potential values for the formation of the passive oxide and for the appearance of the pitting phenomena.

It's also possible to conduct a quantitative analysis where the aim is to obtain information about the kinetic of corrosion and the corrosion rate.

This is achieved by conduction the Tafel's analysis in the region where the relation between the applied potential and the logarithm od the current density is linear (at least 50 mV higher than the equilibrium potential).

In this region in fact the relation between  $E$  and  $\log i$  for the anodic and the cathodic reaction can be written as follows:

$$E = E_{\text{corr}} + \beta_a \log\left(\frac{i}{i_{\text{corr}}}\right) \quad (\text{Eq.20})$$

$$E = E_{\text{corr}} + \beta_c \log\left(\frac{i}{i_{\text{corr}}}\right) \quad (\text{Eq.21})$$

The corrosion current is determined by the intersection point between the anodic and the cathodic straight line as shown in Figure 35.

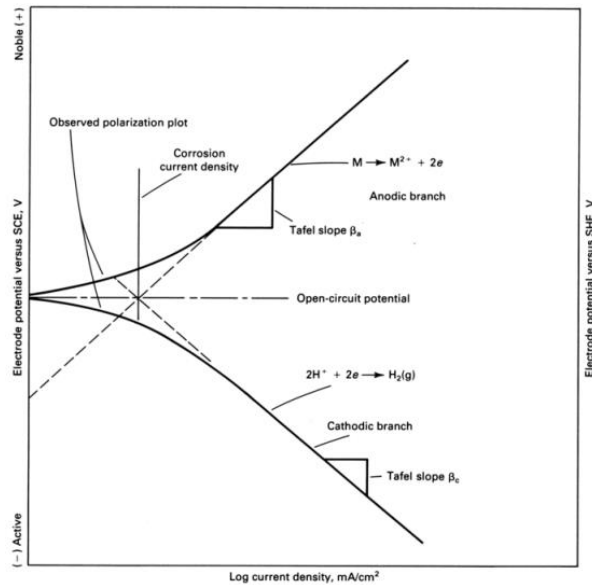


**Figure 35** – Tafel's analysis for the polarization curve [8].

The instrument used for this test, called polarization cell, is constituted by three electrodes and it is shown in Figure 36.

The first electrode is the work electrode made by the sample, the second one is a counter electrode used to close the electrical circuit and it's generally made by a grid of Platinum while the third one is a reference electrode which doesn't take part to the chemical reactions but is used only to measure the potential value of the work electrode.

In this work potentiodynamic technique was utilized to carry out the polarization test.

The first step of this technique is to evaluate the potential value of the work sample along time, when it reaches a stable value the polarization starts.

The first polarization is cathodic, that means the potential value is decreased until a specific value; after that the potential value is brought back to the initial value and then an anodic polarization of the sample until a given value is carried out.

The cathodic polarization allows to obtain information about the reduction reactions made by the environment on the sample's surface while the anodic polarization is used to have information about the oxidation process made by the sample.

In this measurement it is possible to set up the delay time, the potential values reached with the cathodic and the anodic polarization and the scan rate.

The delay time is the time in which the instrument measures the variation of the potential value along time while the scan rate is the variation velocity for the potential during the polarization period.

Polarization test is an accelerated test but if the scan rate is low the corrosion current obtained with the Tafel's plot is a current in absence of polarization, which means that this is the corrosion current that the material presents in the environment where it's tested. In any case there is an accelerated factor that is represented by that fact that during the test the surface of the sample is completely exposed to the solution while during service life only a little fraction of the surface might be exposed to the aggressive environment.

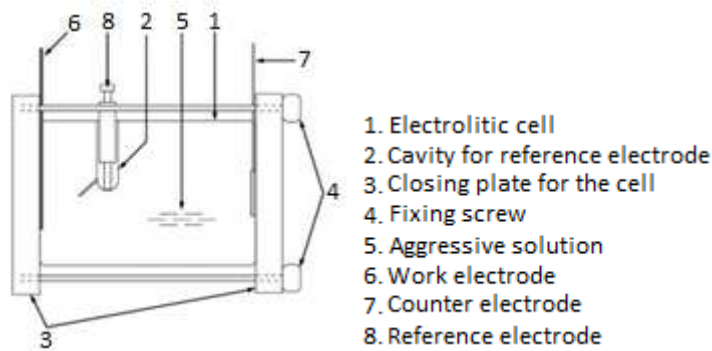


**Figure 36** – Representation of the equipment used for the polarization test [11].

Electrochemical impedance spectroscopy (EIS) is an electrochemical test which is used to obtain quantitative data related to the quality of a coating on a metal substrate.

EIS is a nondestructive measurement therefore it can be used to track the condition of a coated metal sample as it changes [18].

The test consists of applying a series of sine waves of constant amplitude potential and varying the frequency, the respond to this applied potential is an AC current signal which is of the same frequency but shifted in phase of an angle  $\phi$ , generally the frequency range extends from kHz to mHz [8].

The aim of the test is to measure the impedance of the electrochemical circuit that is formed at the interface between the solution and the sample.

Impedance is the ratio between the applied potential and the responded current, it's a measure of a circuit's tendency to resist the flow of an alternating current:

$$Z = \frac{V_{ac}}{I_{ac}} \quad (\text{Eq.22})$$

Analytically the impedance is a complex number therefore is composed by a real part  $Z'$  and by an imaginary part  $Z''$ :

$$Z = Z' + iZ'' \quad (\text{Eq.23})$$

The results obtained with EIS can be displayed in two main ways:

The first one is the Nyquist plot where the negative value of the imaginary impedance ( $Z''$ ) is plotted versus the real part ( $Z'$ ) using linear coordinates in a complex plane.

In this diagram the length of the vector that connects each point represent the modulus of the impedance  $|Z|$  while the angle between the vector and the real axes is the phase angle  $\phi$ .

The shortcoming of Nyquist plot is that it doesn't show any information about the frequency that is used to perform the experiment.

The second one is the Bode plot where the  $\log|Z|$  and the phase angle  $\phi$  are plotted versus the logarithm of the frequency ( $f$ ) of the applied signal [19].

Both plotting formats are used because each has its advantage, in fact subtle features that are difficult to identify in the Nyquist plot can be readily apparent in the Bode plot and vice versa.

The EIS measurement can be interpreted with two main approach which their aim is to determine the properties of the elements of the electrochemical interface by adjusting the parameters of the model to match the measured data [19].

The first approach consists on analyzing the respond of the system to a fluctuating potential with a mathematical or numerical model in order to produce a simulated spectrum, the parameters of the model are adjusted in order to fit the measured spectrum [19].

The second approach consists of modelling the components of the system under investigation with an electrical equivalent circuit which produce the same spectrum of the test.

This second approach is possible because, as described in section 2.3.1, the corrosion phenomenon can be described by electrochemical reaction, this mean that every part of the system can be simplified as a component of an electric circuit. A resistor can represent the solution resistance, the polarization resistance or the charge transfer resistance while a capacitor can represent the electric double layer or the coating.

To simplifier the deduction of the EIS plots some standard electric circuit have been built. The Randles cell is constituted by two resistors and a capacitor, the two resistors  $R_s$ ,  $R_p$  represent respectively the solution resistance and the polarization resistance while the capacitor represent the electric double layer.

This type of interpretation for the elements of the Randles cell is valid for a corroding metal, in fact if it's necessary to study the behavior of a coating, the system can be represented in the same way but the element changes their meaning.

$R_s$  represent always the solution resistance but the capacitor represents the capacity of the coating while the second resistor represent the coating's resistance (evaluation of organic coating part 1).

Figure 37 shows the Randles cell while Figure 38 and Figure 39 shows respectively the Nyquist plot and the Bode plot for this specific type of cell.

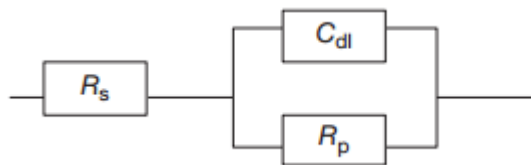


**Figure 37** – Randles cell configuration [19]..

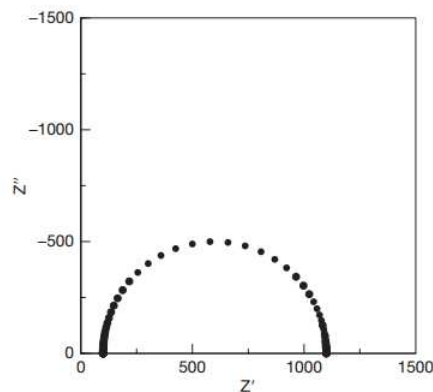


**Figure 38** – Nyquist plot for the Randles cell configuration [19].



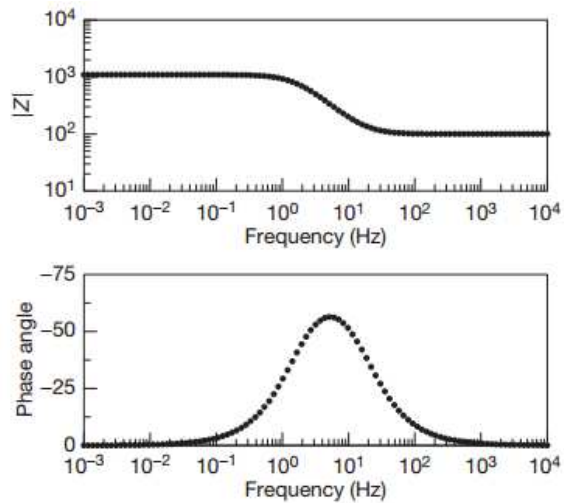


**Figure 39** – Bode plot for the Randles cell configuration [19].

It's possible to demonstrate that, concerning the Nyquist plot for the Randles cell, the interception with the real axis at high frequency (near the origin of the graph) represent the value of the solution resistance while the interception with the real axis at low frequency represent the sum of the solution resistance and the polarization resistance, for that reason the diameter of the circle represent the value of the polarization resistance. Starting from the Randles cell is possible to build more complex circuit in order to match spectrums that are more complex.

In the case of a coated substrate it is possible to use the two-time constant electrical equivalent circuit that is showed in Figure 40.

$R_s$  represents the solution resistance,  $R_c$  and  $C_c$  represent respectively the coating resistance and the coating capacity while  $R_{ct}$  and  $C_{dl}$  represent respectively the resistance to the charge transfer and the capacity of the electrical double layer.

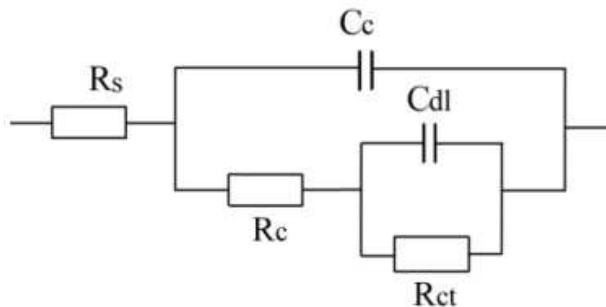


**Figure 40** – Two-time constant electrical equivalent circuit [21].

OCP test (Open Circuit Potential) is the easiest electrochemical test to perform but at the same time it provides the least amount of mechanistic information.

It consists in evaluating along time the electrochemical potential value that the surface of the sample establishes with the aggressive solution.

An example of graphs obtained by OCP measurements is given in Figure 41.

The equipment for the measure is constitute by a reference electrode and a high-impedance voltmeter which doesn't allow the flow of current between the work sample and the reference sample.

The value of electrochemical potential can have different trends along time, if it grows with the time it means that a passive and protective oxide is growing on the surface while if it decreases with the time it means that the corrosion of the sample is occurring.

In any case this kind of test doesn't give any information about the corrosion rate therefore additional test must be perform in to have a better view of the corrosion mechanism.

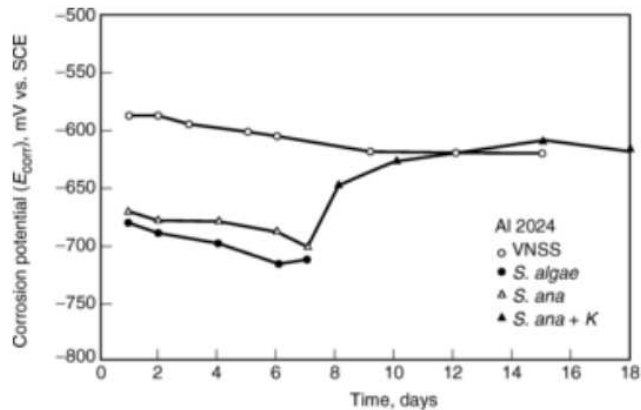


Figure 41 – OCP graph for mild steel exposed to artificial seawater with or without bacteria [8].

Immersion test is a frequently test used to evaluate the corrosion of metals in aqueous solution, in this test a sample is complete or partially immersed in a solution for a given time and then it is removed in order to evaluate the corrosion occurred to it [8].

There are different kind of immersion that can be performed such as total immersion, autoclave tests, partial immersion to vapor phase and intermitted immersion.

In this work autoclave tests have been used because they allow to performed the immersion test at high temperature.

The high temperature is used because it promotes the corrosion reactions and therefore the corrosion rate and yield are improved.

If the temperature is high inside the vessel, even the pressure can reach high value and for that reason some vessels have devices for safety and for the control of pressure and temperature.

In any case all the vessels have a limit for the temperature and the pressure at which they can be work.

Figure 42 shows the vessel used in this work for the immersion test.

For evaluating the corrosion phenomenon, it can be measured the weight lost by the sample and also an analysis of the cross section with SEM or OM can be done in order to have a visual approach to the corrosion event.

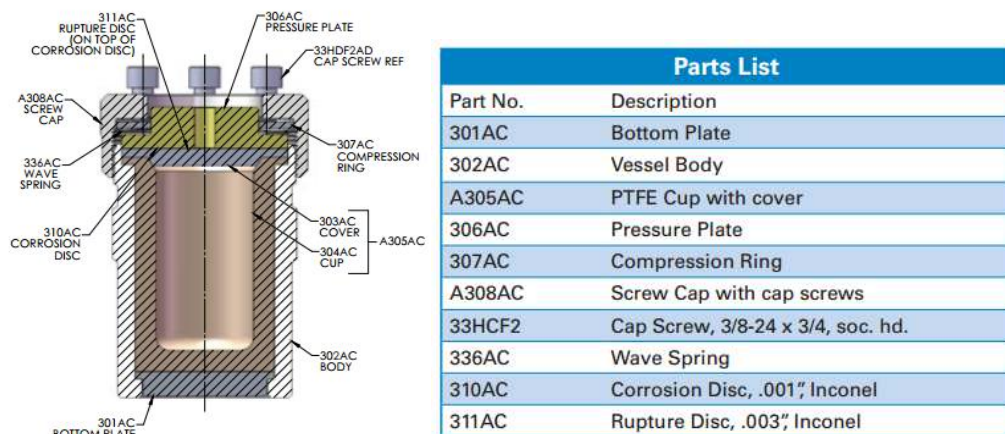


Figure 42 – Vessel used for the autoclave test [13].

### 2.3.4. Corrosion performance of thermal sprayed two-layer coatings

The performance of a thermal sprayed coating depends a lot on its microstructure type which is generally non-homogenous [8].

The microstructure is mainly characterized by the splats, which are the flattened and solidified droplets of the feedstock material that have been accelerated towards the substrate. Also others species such as unmelted particles, oxides particles, porosity and cracks can be distinguished in the microstructure and all of them influence the mechanical and electrochemical properties of the coating [8].

The main artifacts that influence the corrosion resistance of a thermal sprayed coating are the inhomogeneous micro phase and the chemical structure, porosity level and the content of micro cracks, in fact the presence of this defects in the coating can favorite the corrosion events because they constitute a direct path for the electrolyte to the substrate. For that reason, an accurate control of the porosity and micro cracks is extremely important for having a good corrosion resistance.

When an excellent corrosion resistance is required the coating can be submitted to a post-processing treatments such as sealing or laser surface remelting. These treatments close the porosity and therefore allow to densify the coating so that the electrolyte has more difficulties to reach the substrate.

J. Tuominen et al. [14] reported that laser surface remelting can improve the general and the localized corrosion resistance of high-chromium and nickel-chromium coatings made by HVOF in aqueous chloride solution.

Concerning the sealants, the most common types are vinyl, epoxies, polyurethanes, phenolic and silicones, the sealant should have a low viscosity in order to simplify their penetration through the pores [8].

In a lot of application components are exposed to wear and corrosion condition at the same time, also at high temperatures. In this cases ceramic coatings such as  $Cr_2O_3$ ,  $Al_3O_3$ ,  $ZrO_2$  or they mixture are used to ensure a long service life of the component.

When a ceramic coating is applied to a metallic substrate residual stress at the interface can occur due to the different thermal expansion coefficient, this fact leads to a poor adhesion between the coating and the substrate.

To ensure a good adhesion an intermediate layer called bond layer is sprayed between the ceramic coat and the substrate.

The bond coating is constituted generally by alloys of nickel, chromium, molybdenum and aluminum and it has an intermediate value of the thermal expansion coefficient and therefore guarantee a good bond strength between the substrate and the top coat [8].

Yilmaz et al. [14] has proved that adding a Ni-5wt. % Al bond coat on plasma sprayed  $Al_2O_3$ ,  $Al_2O_3 - 13wt\% TiO_2$  top coating increase the bonding strength and the hardness of the coatings.

Despite the bond coating influence on the mechanical properties is well described in literature [4] [8], the influence that the bond coating has on the electrochemical properties and on the corrosion resistance must be studied more deeply.

As reported in [16] the corrosion behavior of the bi-layer coatings depends on the chemical composition and the microstructure's defects of each single layer, in fact the different chemical composition can lead to galvanic couple between them while the microstructure's defects, such as porosity, can promote the contact between the different layers and the electrolyte.

Furthermore, the corrosion phenomena can be very localized due to the large ratio of cathodic surface are to that of anode as well as the high corrosion current density concentrated at the defects in the coating.

In general, the corrosion properties of a bi-layer coating are not easily to predict because they depend from different factors such as materials used for the different layers (substrate, bond coat, top coat), microstructure of the coating (porosity, cracks), corrosive media and the work temperature.

For this reasons, in order to have a good knowledge about corrosion behavior of bi-layer coatings produced by thermal spray, every single combination of coatings should be tested in the environment in which the will operate.

In order to give some examples Sadeghimeresht at [16]\_showed that the best Ni-based alloy bond coat for  $Cr_3C_2$ -*NiCr* top coat and steel substrate in terms of corrosion properties in a solution constituted by 3.5 wt.% wt NaCl is *NiCoCrAlY* or *NiCr*.

Jam et al. [17] studied the electrochemical behavior of dual-layer NiCrAlY/mullite plasma sprayed coating on high silicon cast iron alloy in 3.5 wt.% NaCl solution.

After this test, it can be said that with the bond coat made of NiCrAlY no intense corrosion occurred and that the coating exhibits more appropriate adhesion to the substrate.

Some corrosion products can be formed in the NiCrAlY coating/ substrate interface but they act as a barrier and accumulate in the defects, this fact lead to an increase of the corrosion resistance.

Liu et al. [2] investigated the effect of different bond layer (Ni60, NiAl and FeAl) on the corrosion behavior of a plasma sprayed  $Al_2O_3$  in simulated seawater.

The results show that all three metallic coatings could provide corrosion protection for the substrate and the best corrosion resistance is obtained by using Ni60 as bond coating.

The study shows that even the bond coating's thickness influences the corrosion behavior, in fact the corrosion resistance of the coating first increase and then decrease with the increase of this parameter.

### 3. MATERIALS AND METHODS

#### 3.1 Coating manufacturing

In this work four different coating structures/stacks of sample were manufactured. In all of them the substrate and the top coat were respectively constituted by Hastelloy C276 and  $Cr_2O_3$  while the bond coat material changed in each of them.

The Hastelloy C-276 has been chosen as a substrate thanks to its good corrosion resistance therefore if the electrolyte reaches it, it can resist to corrosion attack.

Chromium oxide has been chosen because it's one of the most ceramic materials used in thermal spray thanks to its wear and corrosion resistance.

The material chosen as bond coat are: Hastelloy C-276, Ni-20Cr, tantalum and a cobalt based alloy.

In order to understand better the role of each layer on the corrosion behavior even some sample constituted by only the top coat and by only the four different bond layers were manufactured.

Table 2 shows the characteristics of the powders used in this works while Table 3 shows the code used to classified every type of sample.

**Table 2** – Properties of the powders used to realize the bond layer and the top coat.

<b>Powder name</b>	<b>Type of layer</b>	<b>Composition</b>	<b>Particle size distribution [<math>\mu m</math>]</b>
Diamalloy 4276 (Hastelloy C276)	Bond layer	Ni-15-5Cr-16Mo- 4.5W-4Fe	-53+20
Amperit 251.1 (Ni20Cr)	Bond layer	Ni-20Cr	-45+22.5
Amperit 150.074 (Tantalum)	Bond layer	Ta	-45+15
Anval Ultimet (Cobalt based alloy)	Bond layer	Co-25.5Cr- 9Ni-5Mo-3Fe- 2W	-45+15
Amperit 704.001 (Chromium oxide)	Top layer	$Cr_2O_3$	-45+22

**Table 3** – Type of samples and codes associated with them.

<b>Sample</b>	<b>Code</b>
Hastelloy C276 / Hastelloy C276	D1
Hastelloy C276 / Ni20Cr	D2
Hastelloy C276 / Tantalum	D3
Hastelloy C276 / Co alloy	D4
Hastelloy C276 / Hastelloy C276 / Cr <sub>2</sub> O <sub>3</sub>	D1.1
Hastelloy C276 / Ni20Cr / Cr <sub>2</sub> O <sub>3</sub>	D2.1
Hastelloy C276 / Tantalum / Cr <sub>2</sub> O <sub>3</sub>	D3.1
Hastelloy C276 / Co alloy / Cr <sub>2</sub> O <sub>3</sub>	D4.1
Hastelloy C276 / Cr <sub>2</sub> O <sub>3</sub>	D1TC

The substrate has been realized by cutting an Hastelloy C-276 bar with a diameter of 50 mm, the thickness of each sample is about 4 mm.

To deposit the different types of coatings two thermal spray technologies were used.

The Hastelloy C-276, Ni-20Cr and the Ultimet cobalt alloy bond layers have been deposited with HVOF technology while the tantalum bond layer and the top coat have been deposited with APS technology.

Before each deposition all the samples have been sandblasted in order to achieve a proper roughness.

### 3.2 HVOF deposition

As mentioned above, the HVOF technology has been used to deposit the Hastelloy C276 (Diamalloy 4276), Ni20Cr (Amperit 251.1) and the Cobalt alloy (Anval Ultimet).

The pistol used in HVOF works with propane as fuel, oxygen and its nozzle is 2701.

The thickness reached for all the bond coat is about 100  $\mu\text{m}$ .

Table 4 shows the spray parameters for each type of bond coat while Table 5 shows the deposition data for each sample.

**Table 4** – Spray parameters for the sample manufactured with HVOF technology.

<b>Parameter</b>	<b>Diamalloy 4276</b>	<b>Amperit 251.1</b>	<b>Anval Ultimet</b>
Powder feed rate [g/min]	50	50	50
Spray distance [mm]	230	230	230
Step [mm]	4	4	4
Robot speed [mm/sec]	800	800	800
Propane flow [l/min]	64	64	70
Propane pressure [bar]	6.3	6.3	6.3
Propane flowmeter reading FMR	34	34	38

Oxygen flow [l/min]	240	240	240
Oxygen pressure [bar]	10.5	10.5	10.5
Oxygen flowmeter reading FMR	38	38	38
Air flow [l/min]	375	375	375
Air pressure [bar]	7	7	7
Air flowmeter reading FMR	48	48	48
Carrier gas flow [l/min]	20	20	20
Carrier gas pressure [bar]	8.6	8.6	8.6
Carrier gas flowmeter reading FMR	42	42	42

**Table 5** – Deposition data for the sample manufactured with HVOF.

Parameter	Diamalloy 4276	Amperit 251.1	Anval Ultimet
Number of passes	6	5	7
Thickness [ $\mu\text{m}$ ]	110	90	90
Thickness/pass [ $\mu\text{m}$ ]	18.33	18	12.86
Substrate temperature [ $^{\circ}\text{C}$ ]	140-180	100-120	100-120

### 3.3 Plasma spraying

The APS technology has been used to deposit Tantalum bond layer and  $\text{Cr}_2\text{O}_3$  top coat because it allows to reach high temperatures.

During the spray process the powders were injected radially at a distance of 7 mm with an angle of  $90^{\circ}$  with the plasma flow.

The gas used to create the plasma was a mixture of Argon and Hydrogen while the carrier gas was only Argon.

Some of the APS parameters for the top coat deposition were modified between the different spraying sessions in order to improve the quality of the coating.

The top coat has a thickness of  $300 \mu\text{m}$  while the bond coat has a thickness of  $80 \mu\text{m}$ .

Table 6 shows the spray parameters for the bond coat and the different top coats made with APS while Table 7 shows the deposition data for each sample.

**Table 6** – Spray parameter for the sample manufactured with APS technology.

Parameters	Tantalum	$Cr_2O_3$ on Hastelloy bond coat	$Cr_2O_3$ on Ni20Cr bond coat	$Cr_2O_3$ on Tantalum bond coat	$Cr_2O_3$ on Cobalt alloy bond coat
Powder feed rate [g/min]	40	40	40	40	40
Spray distance [mm]	120	120	120	120	120
Step [mm]	4	4	4	4	4
Robot speed [mm/sec]	850	500	500	850	850
Current [A]	620	650	650	650	650
Argon flow [l/min]	42	43	43	43	43
Hydrogen flow [l/min]	11	14	14	11	11
Carrier gas flow [l/min]	2.5	4.5	4.5	3.3	3.3
Voltage [V]	72	76.6	76.8	71.4	76.8
Power [kW]	44	50	50	46.5	46.5

**Table 7** – Deposition data for the sample manufactured with APS technology.

Parameter	Amperit 150.074	$Cr_2O_3$ on Hastelloy bond coat	$Cr_2O_3$ on Ni20Cr bond coat	$Cr_2O_3$ on Tantalum bond coat	$Cr_2O_3$ on Cobalt alloy bond coat
Number of passes	8	10	10	30	30
Thickness [ $\mu m$ ]	80	300	300	300	300
Thickness/pass [ $\mu m$ ]	10	30	30	10	10
Substrate temperature [ $^{\circ}C$ ]	120	300	300	160	160



### 3.4 Metallographic specimen preparation

After the coating deposition, the different samples have been cut in order to obtain specimens with a suitable dimension for each type of tests.

To cut the different specimens has been used a wheel that contains  $Al_2O_3$  particles as abrasive and Bakelite as bond material, during the cutting process a particular attention was taken to ensure that the coating was exposed to a compression load.

Some of the as sprayed samples were cut to conduct the cross section analysis with SEM in order to evaluate the quality of the coating.

To perform the cross section analysis after the cutting process, the cut samples have been embedded in a room temperature-setting epoxy resin.

When the resin solidified the samples were grounded with SiC abrasive paper (from mesh 200 to mesh 1200) and then polished with diamond paste ( $9\ \mu m$ ,  $3\ \mu m$ ,  $\frac{1}{4}\ \mu m$ ) in order to achieve a mirror-polish finish.

For the reason that the resin used is not electrically conductive, the samples have been sputtered with carbon before the SEM analysis.

The samples used for polarization test were grounded with SiC abrasive paper (from 320 mesh to 1200 mesh) in order to obtain a smooth surface which is extremely important for this type of test.

The sample preparation procedure for the EIS test is the same procedure used for the polarization test.

The samples used for immersion test were grounded on their side with a SiC abrasive paper (320 mesh), after the test the corrosion products were removed with a brush and an ultrasonic cleaner and then they have been cut, embedded and polished using the same procedure described for the cross section analysis.

For the OCP test the samples were used in their as sprayed condition.

### 3.5 Polarization curve measurements

This test allows to determinate the corrosion current and the corrosion potential by performing the Tafel's analysis.

It also allows to determinate if the sample is interested by a passivation phenomenon and in this case is possible to calculate the passivation current and the passivation potential.

This test has been performed by using a three electrode cell, the first one is constituted by the sample and is called the work electrode, the second one is a counter electrode used to close the electrical circuit and it's made by a grid of Platinum while the third one is a reference electrode which doesn't take part to the chemical reactions but is used only to measure the potential value of the work electrode.

The electrochemical cell is then filled with the electrolyte at room temperature.

To perform this type of test is really important to have a smooth surface and for that reason all the samples has been polished with SiC papers from 320 mesh to 1200 mesh.

The electrolyte used for this test is sulfuric acid with different concentration (0.1M, 0.5M, 1M).

When every part of the electrochemical cell is assembled is possible to start the test.

As first step the instrument measures the electrochemical potential without any polarization, when this value doesn't change with the time the different polarizations take place.

The time while the machine measures the electrochemical potential value  $E_{oc}$  without any polarization is called the delay time and it can be set up by the user.

The first polarization performed on the sample is a cathodic polarization, the user can decide the final value of the potential reached with the polarization.

The second polarization performed on the sample is an anodic polarization and even in this case the user can decide the final value of the potential reached with the polarization. In both polarizations the user set a value of the scan rate which is the potential variation velocity.

When the two polarization are completed is possible to build, with the different value of current and potential collected during the test, a graph that shows the trend between the logarithmic of the current and the potential value.

When the graph is completed with the Tafel's analysis is possible to individuate the electrochemical potential corrosion  $E_{corr}$  and the corrosion current density  $i_{corr}$ .

The software used to build the different graphs and to perform the Tafel's analysis was OriginPro.

Table 8 shows the different parameters used to performed the test.

**Table 8** – Table of the parameters used for polarization test.

Parameter	Value
Delay time [sec]	1800
Initial E vs $E_{oc}$ [V]	-0.8
Final E vs $E_{oc}$ [V]	1.6
Scan rate [m V/sec]	1

### 3.6 Electrochemical impedance spectroscopy measurements

The Electrochemical Impedance Spectroscopy experiment has been conducted in the laboratory of the department of engineering “Enzo Ferrari” using a three electrode cell, the solution concentration used for the test was 0.5M.

The work electrode is represented by the sample, the reference electrode is a Ag/AgCl type with KCl as solution while the counter electrode is made by a grid of Platinum.

For every sample four consequently EIS test has been conducted in order to evaluate how the corrosion evolves with the time, the different test have been performed after 1,4, 7, 25 hours of immersion of the sample.

The test starts by measuring the open circuit potential value, in the first measurement the OCP is valuated for one hour otherwise in the two remaining tests it's valuated for two minute.

When the OCP measurement it's completed, the EIS test can start.

To perform the EIS test is important to insert some parameters such as the start and the end frequency, the amplitude of the signal, the number of points, the points per decade and the data quality.

Table 9 shows the value of the different parameters used to perform the test.

**Table 9** – Parameters used to perform the EIS test.

Parameter	Value
Start frequency [Hz]	500000
End frequency [Hz]	0.005
Amplitude [mV RMS]	20
Number of points	30
Points Per Decade	8
Data quality	2

The results from EIS tests have been analyzed with the software FRA which allows to fit the registered EIS plot and to determinate the values of the different resistance and capacitors.

The equivalent electrical circuit taken as reference was the one showed in Figure 39.

### 3.7 Open circuit potential measurements

The OCP test is used to measure along the time the open circuit potential of the electrochemical double layer described in 2.4.3.

The equipment for this test is really simple, in fact it consists only of reference electrode (SCE reference electrode) used to measure the potential value and of a high-impedance voltmeter which doesn't allow the flow of current between the work sample and the reference sample.

If the potential value grows with the time it means that on the surface is growing a passivate layer that protects from further corrosion while if the potential value decrease with the time it means that the surface is interested by a corrosion phenomenon that degrade the sample.

In this test the samples have been used in their as-sprayed condition and a tube has been joined on their surface with epoxy resin in order to host the electrolyte.

When all the samples were ready the electrolyte was filled into the tube and the potential value of each sample was measured along time.

The solution concentration used for this test was 1M.

The time step for measuring the potential value was the following: 0sec, 30 sec, 1 min, 2 min, 5 min, 10 min, 20 min, 30 min, 1 h, 2 h, 4 h, 7 h, 24 h.

After that a graph that reports the trend of potential value versus time has been built for each sample.

### 3.8 Immersion testing

This test consists on immerse the sample into the electrolyte, at different temperature values.

The samples used for this test have a dimension of 20x20mm and they have been polished on their side with a SiC paper of 320 mesh.

In this test only the electrolyte with the concentration of 1M has been used because this condition has been considered the most dangerous.

When the samples are ready they are introduced into the different vessels, then if the test is performed at high temperature they are positioned into the oven where they remain for 120 hours at 60°C otherwise they are kept at room temperature.

After that time, the vessels are removed and the samples are extracted from them.

The corrosion products are then removed from the samples by brushing and by ultrasonic cleaner, after that they are cut in a suitable dimension and embedded in

a room temperature-setting epoxy resin and then, when the resin is solidified, they are polished with the same parameters illustrated on section 3.4. After the carbon sputtering, the different cross sections are analyzed with SEM.

## 4. RESULT

### 4.1 Corrosion resistance behavior extracted from the polarization test

The aim of the polarization test is to build the polarization curve and evaluate, with the Tafel, plot the corrosion current and the corrosion potential.

In order to understand clearly the role of the electrolyte corrosively and the role of the bond coat, two type of polarization curves have been built: in the first category the bond coat material is constant and the corrosively level changes while in the second category the corrosively level is constant and the bond coat materials changes.

The following Figures show the polarization curve for each samples when the corrosively levels changes.

In this case the test has been carried out even for the configuration with only the top coat.

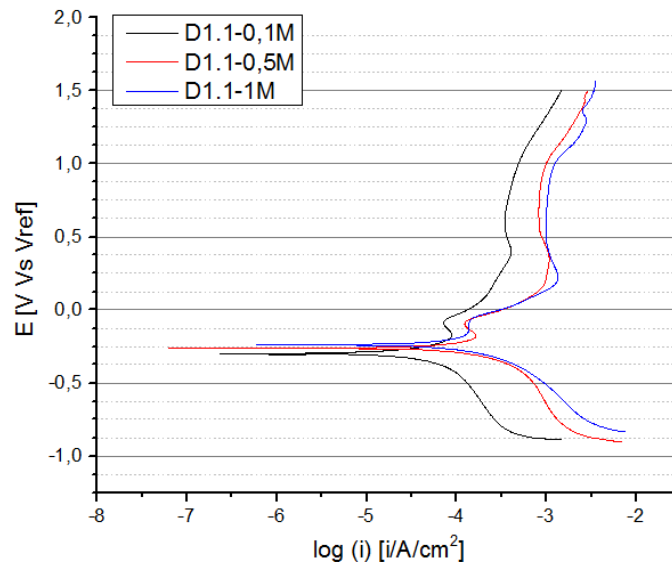


**Figure 43** – Polarization curve for sample D1.1 (HVOF sprayed Hastelloy C-276 as bond coating) at three different corrosively levels (0.1M, 0.5M, 1M)

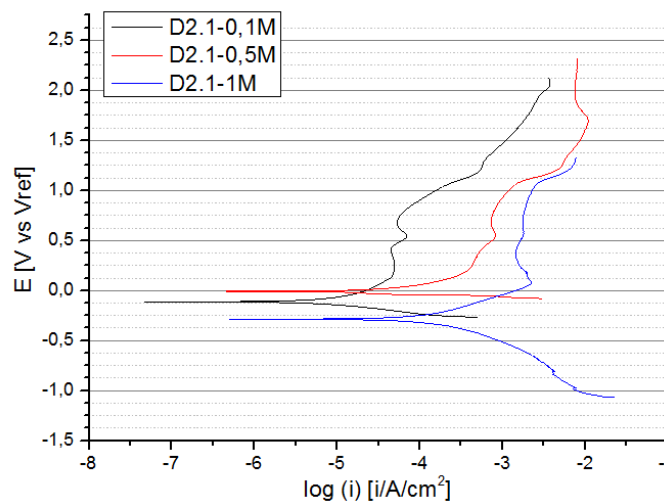


**Figure 44** - Polarization curve for sample D2.1 (HVOF sprayed Ni-20Cr as bond coating) at three different corrosively levels (0.1M, 0.5M, 1M).

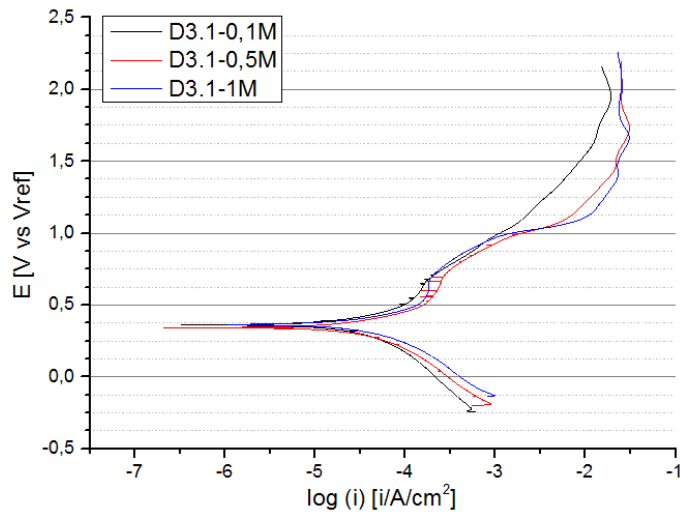


**Figure 45** - Polarization curve for sample D3.1 (APS sprayed tantalum as bond coating) at three different corrosively levels (0.1M, 0.5M, 1M).

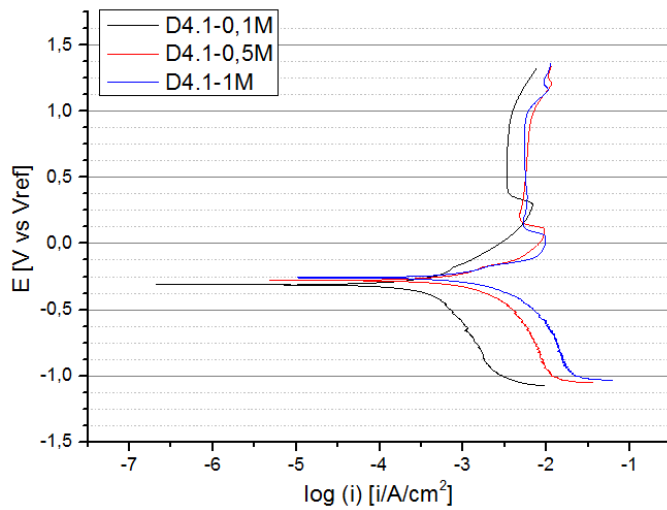


**Figure 46** – Polarization curve for sample D4.1 (HVOF sprayed cobalt based alloy as bond coating) at three different corrosively levels (0.1M, 0.5M, 1M).

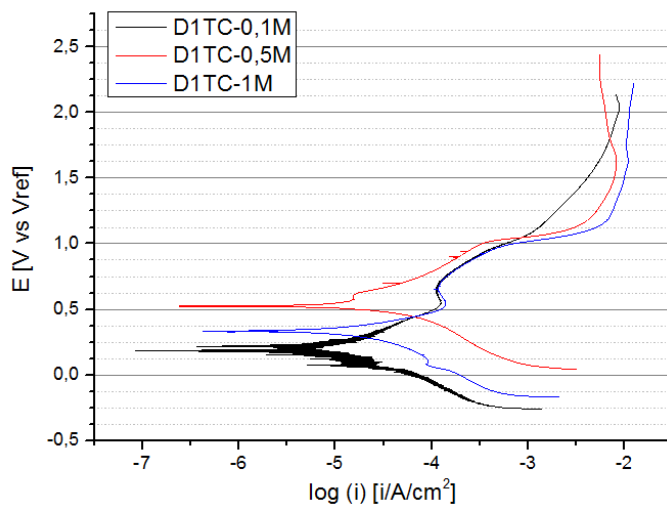


**Figure 47** - Polarization curve for sample D1TC (only APS spayed  $Cr_2O_3$ ) at three different corrosively levels (0.1M, 0.5M, 1M).

From the Figure 43 is possible to say that for the sample D1.1 (Hastelloy C-276 as bond coating) the electrochemical potential value doesn't change significantly, the curves at 0.1M and 0.5M are quite similar with each other and more shifted to the right respect to the curve at 0.1M, this fact means that the corrosion phenomenon is more intense.

It's also possible to individuate a region where the current density doesn't change with the potential but it can't be interpreted as a passivation region because the value of the at which this region appears is too high.

For the sample D2.1 (Ni-20Cr as bond coating), Figure 44, the electrochemical potential value changes with the solution concentration but it's not possible to individuate a general trend, in fact the increase of the molar value of the solution doesn't correspond to a decrease of the potential value as it should be expected.

Even in this case when the molar value increase the different polarization curve moves to the right therefore the corrosion phenomenon is more intense.

At a concentration of 1M is possible to see a passivation region but the corresponded value of the current density is too high to consider this region as a protective one.

From the Figure 45 is possible to see that for the sample with tantalum as bond coating (D3.1) the electrochemical potential values are very similar at every molar value of the solution and only the curve at 0.1M is a bit more shifted to the left, this mean that in this case the corrosion is a bit less intense.

The passivation region appears at high value of the current density so it can't be seen as a protective region.

Even for the sample the cobalt based alloy as bond coating (D4.1), Figure 46, the electrochemical potential values don't change with the molar value of the solution and the curve at 0.5M and 1M are very similar while the curve at 0.1M is a bit shifted to the left.

For the sample D1TC (with only the top coat constituted by  $\text{Cr}_2\text{O}_3$ ), Figure 47, is possible to see that the electrochemical potential value changes with the molar value but it's not possible to find a general trend, the curves doesn't move along the x-axis, it means that the increase of the molar value of the solution doesn't affect so much the corrosion phenomenon.

The next Figures show the polarization curve for the different samples in a fixed value of corrosively level.

Even in this case the polarization curve has been carried out for the sample with only the top coating, moreover for the solution 1M also the sample with only the different bond coatings has been tested in order to evaluate the role of the top coat.

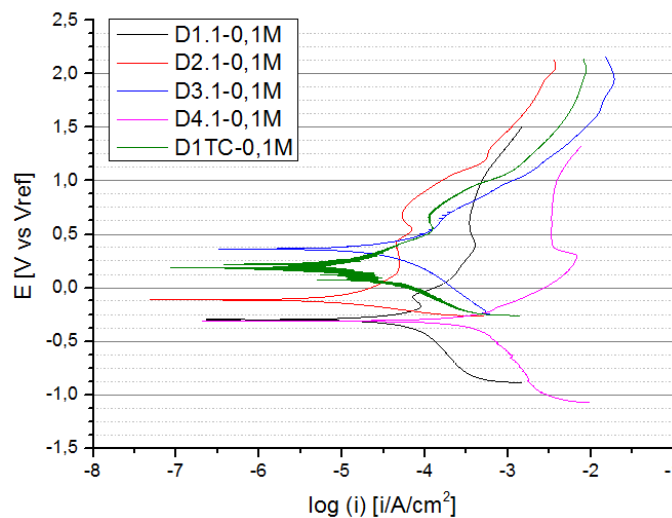


**Figure 48** – Polarization curves for samples D1.1 (Hastelloy C-276 as bond coating), D2.1 (Ni-20Cr as bond coating), D3.1 (tantalum as bond coating), D4.1 (cobalt alloy as bond coating) and D1TC (with only Cr<sub>2</sub>O<sub>3</sub> top coating) at 0.1M.

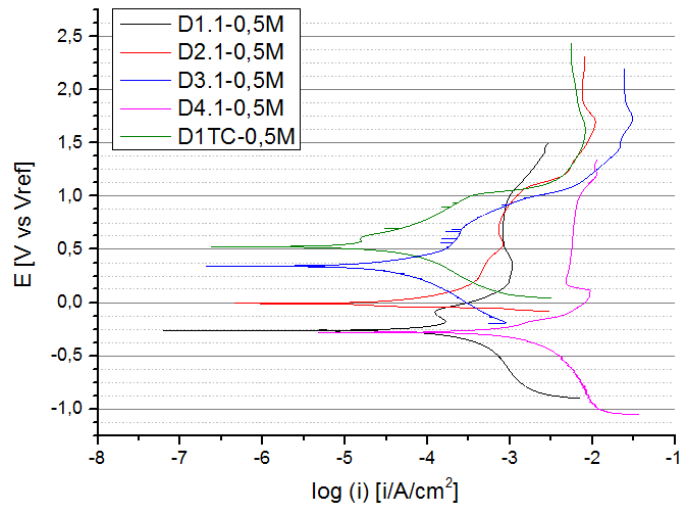


**Figure 49** – Polarization curves for samples D1.1 (Hastelloy C-276 as bond coating), D2.1 (Ni-20Cr as bond coating), D3.1 (tantalum as bond coating), D4.1 (cobalt alloy as bond coating) and D1TC (with only Cr<sub>2</sub>O<sub>3</sub> top coating) at 0.5M.

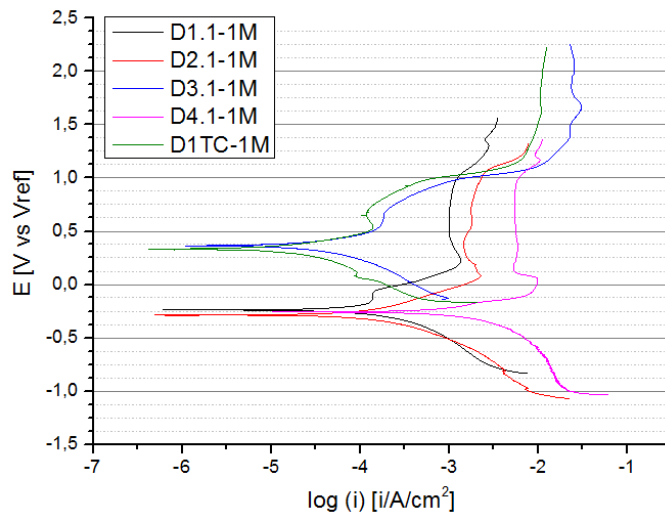


**Figure 50** – Polarization curves for samples D1.1 (Hastelloy C-276 as bond coating), D2.1 (Ni-20Cr as bond coating), D3.1 (tantalum as bond coating), D4.1 (cobalt alloy as bond coating) and D1TC (with only Cr<sub>2</sub>O<sub>3</sub> top coating) at 1M.



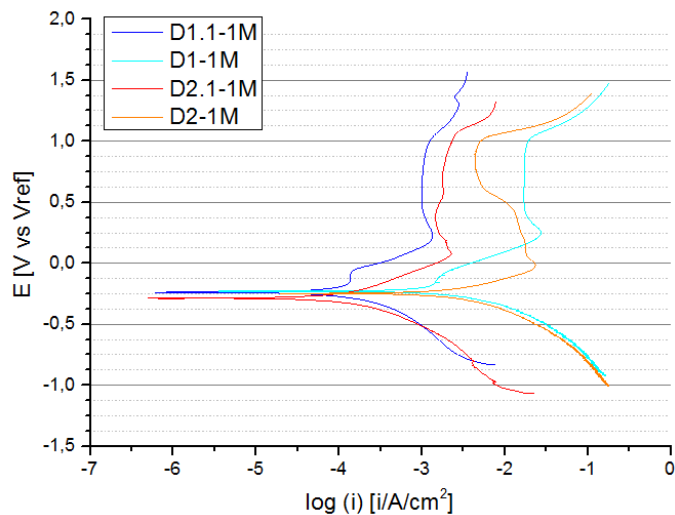


**Figure 51** – Polarization curves for samples D1.1 (Hastelloy C-276 as bond coating), D1 (no Cr<sub>2</sub>O<sub>3</sub> top coating on Hastelloy C-276 bond coating), D2.1 (Ni-20Cr as bond coating), D2 (no Cr<sub>2</sub>O<sub>3</sub> top coating on Ni-20Cr bond coating).

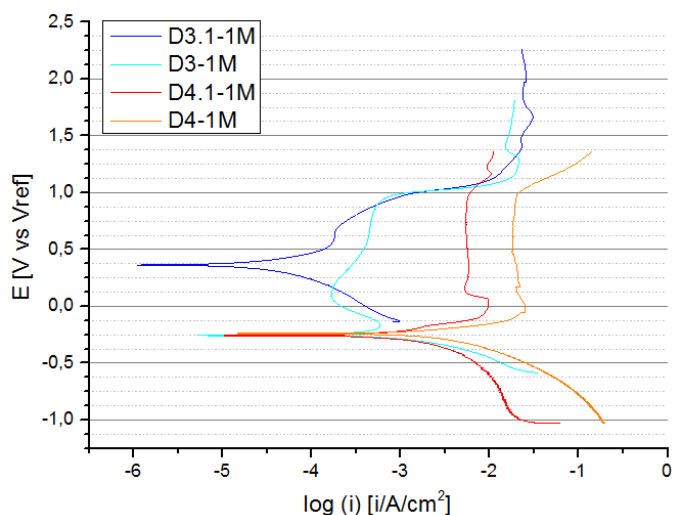


**Figure 52** – Polarization curves for samples D3.1 (tantalum as bond coating), D3 (no Cr<sub>2</sub>O<sub>3</sub> top coating on tantalum bond coating), D4.1 (cobalt based alloy as bond coating), D4 (no Cr<sub>2</sub>O<sub>3</sub> top coating on cobalt based alloy bond coating).

From the previous Figure (48, 49, 50, 51, 52) is possible to notice that between the all the samples, the one with tantalum as bond coat shows the best nobility.

In fact, its electrochemical potential value is always higher than the values of the others samples, it's also comparable at every corrosively level, with the potential value presented by the sample with only the top coat, which confirm the nobility of this type of bond coating.

The electrochemical potential value for the sample D1.1 (Hastelloy C-276 as bond coating) is similar to the one presented by the sample D4.1 (cobalt based alloy as bond coating) at every corrosively levels while the sample D2.1 (Ni-20Cr as bond coating) presents a potential value between those two values and the one of the sample D3.1, that has tantalum as bond coating (except for 1M where all those values are quite similar to each other).

Moreover, at every corrosively level, the polarization curve for the samples that have Hastelloy C-276, Ni-20Cr and the cobalt based alloy as bond coating are more shifted to

the right respect to the polarization curve for the sample that has tantalum as bond coating, this means that for those sample the corrosive phenomenon is more intense  
 Lastly, the polarization curve for the samples with only the bond coating are more shifted to the right respect to the polarization curve for the samples with the same bond coating but also the top coating.

This means that the top coating acts as a barrier respect to the bond coating therefore the bond coating is less exposed to the environment which means that the corrosion phenomenon is less significant.

To have more analytical result from the polarization test, every curve has been analyzed with the Tafel analysis.

This analysis has been carried out with the software OriginLab which allows to extract the anodic and the cathodic straight line, particular attention was taken to take the linear region in area with a potential higher at least 50 mV then the equilibrium potential.

From the intersection of these lines the values of  $i_{corr}$  and  $E_{corr}$  have been collected, Figure 53 and Figure 54 show two example of the Tafel analysis carried out with the different polarization curve while Table 10 shows the data collected from this analysis.

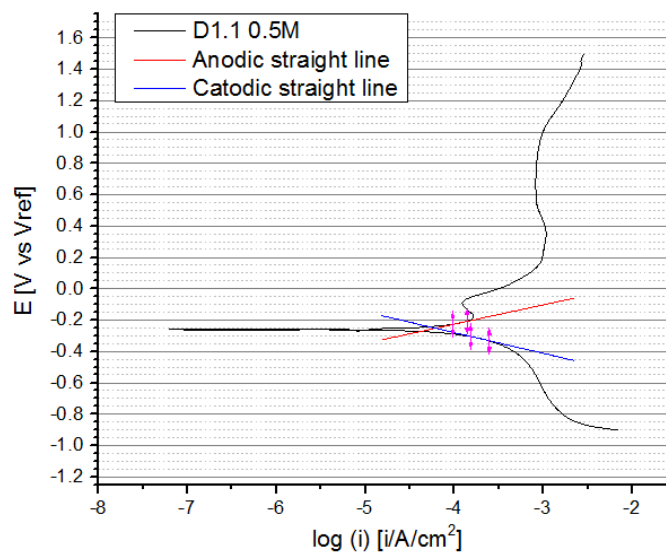


**Figure 53** – Tafel analysis for the sample D1.1 (Hastelloy C-276 as bond coating) at  $H_2SO_4$  0.5M.

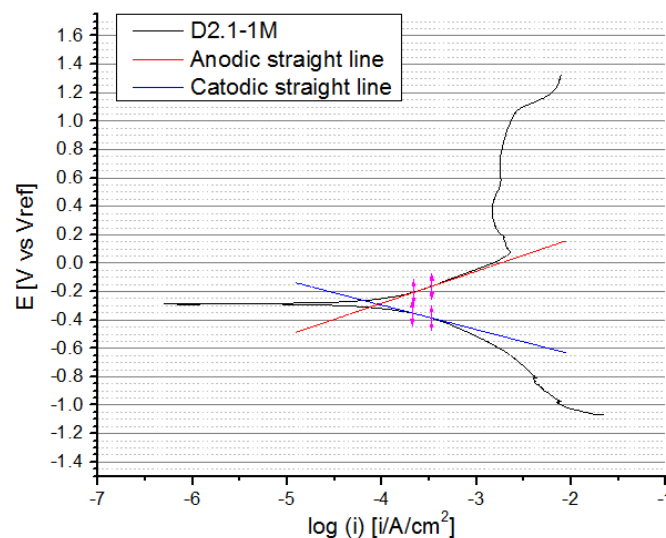


**Figure 54** – Tafel analysis for the sample D2.1 (Ni-20Cr as bond coating) at  $H_2SO_4$  1M

**Table 10** – Results of the Tafel analysis for the different samples.

Type of sample (layers)	0.1M		0.5M		1M	
	$E_{corr}$ [V vs SCE]	$i_{corr}$ [ $\mu A \cdot cm^2$ ]	$E_{corr}$ [V vs SCE]	$i_{corr}$ [ $\mu A \cdot cm^2$ ]	$E_{corr}$ [V vs SCE]	$i_{corr}$ [ $\mu A \cdot cm^2$ ]
D1.1 (Hastelloy C-276/ Cr <sub>2</sub> O <sub>3</sub> )	-0,30	23.7	-0,25	61.2	-0,25	66.1
D2.1 (Ni-20Cr/ Cr <sub>2</sub> O <sub>3</sub> )	-0,12	5,91	-0,02	25.7	-0,29	92.3
D3.1 (tantalum/ Cr <sub>2</sub> O <sub>3</sub> )	0,36	11.8	0,35	17.6	0,38	21.8
D4.1 (cobalt based alloy/ Cr <sub>2</sub> O <sub>3</sub> )	-0,31	180	-0,28	537	-0,25	615
D1TC (Cr <sub>2</sub> O <sub>3</sub> )	0,16	24.6	0,55	13	0,34	10.6
D1 (Hastelloy C-276)	-	-	-	-	-0,23	936
D2 (Ni-20Cr)	-	-	-	-	-0,25	1553
D3 (tantalum)	-	-	-	-	-0,25	439
D4 (cobalt based alloy)	-	-	-	-	-0,23	1564

The table confirms the considerations made before, in fact it's possible to see that for every sample except the one with only the top coating when the corrosively levels increase even the corrosion current increase. This fact corresponded to the right shift of the different curves.

The sample with tantalum as bond coating (D3.1) has the lowest value of the corrosion current at every corrosively level (except versus D2.1 at 0.1 M but those value are in any case comparable).

The sample D4.1 (cobalt based alloy as bond coating) behave worst at every corrosively levels, moreover its corrosion current value is one magnitude higher than the values of the others samples with the bond coat.

The sample with only Cr<sub>2</sub>O<sub>3</sub> top coating (D1TC) behaves better then the samples with the bond coating, the corrosion value is lower for every corrosively level (except versus D2.1 and D3.1 at 0.1 M but those value are in any case comparable).

The electrochemical potential values respect the trend observed before, in any case their values are comparable with each other.

The samples with only the bond coating present a corrosion current value that is one magnitude higher than the one present by the samples with the same bond coating but with the top coating.

This fact can be explained by saying that in the case with only the bond coating the exposed bond coat's area is higher than the area in the case with the bond coating and the top coating, therefore there are more material that can be affected by corrosion.

This means that the top coating acts as a barrier for the bond coating and protects it from the external environment.

Anyway it must be said that the corrosion density measure with the top coating and the bond coating refers to the total area exposed.

Even with the top coat covering the bond coating, a percentage of the external solution reaches the bond coating through the porosity and the microcracks presented in the coatings, therefore locally the value of corrosion density is much higher than the one registered by the instrument because the area exposed to corrosion is really small (the size of a pore or crack).

This fact can lead to an intense corrosion phenomenon even in the configuration with the bond coating and the top coating.

## 4.2 Corrosion behavior extracted from the electrochemical impedance spectroscopy

As mentioned in section 3.6 the EIS plot obtained with the different experiments have been analyzed with the software FRA.

This software allows to build an equivalent electric circuit that fits the experimental points of the registered plot, it's therefore possible to extract from the curve built by the software the physical value of the different elements that compose the circuit.

The experimental points obtained from the different tests have been fitted with the circuit showed in Figure 39.

For each type of sample, Figures 55, 56, 57, 58 show the plot obtained with the EIS test after 1, 4, 7, 25 hours of immersion in 0.5M  $H_2SO_4$ .

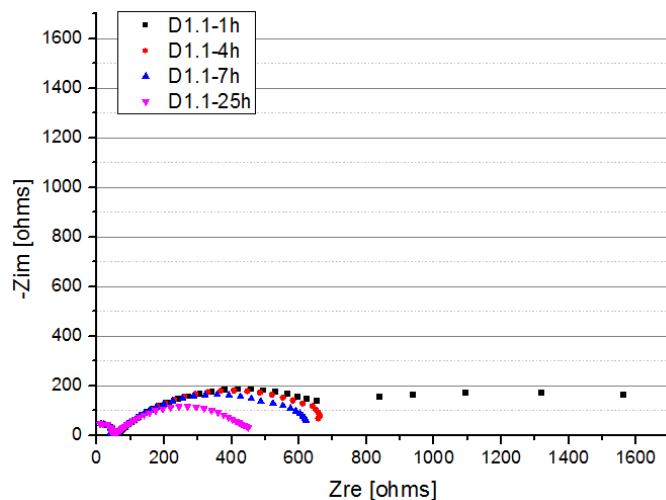


**Figure 55** – EIS test for sample D1.1 (HVOF sprayed Hastelloy C-276) after 1, 4, 7, 25 hours of immersion in 0.5M  $H_2SO_4$ .

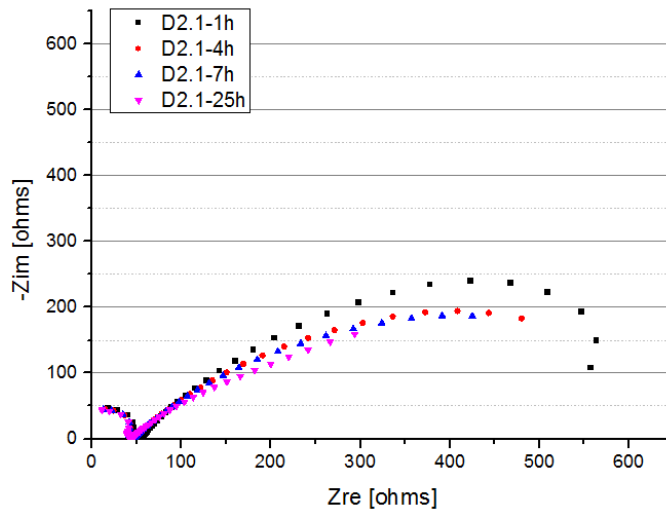


**Figure 56** – EIS test for sample D2.1 (HVOF sprayed Ni-20Cr) after 1, 4, 7, 25 hours of immersion in 0.5M H<sub>2</sub>SO<sub>4</sub>.

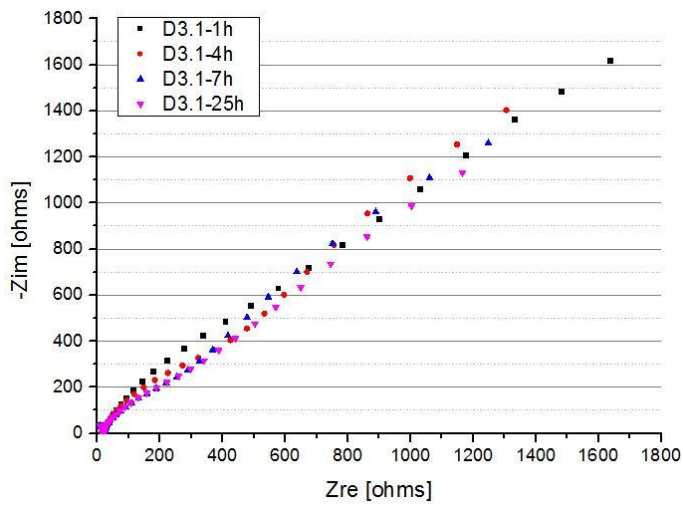


**Figure 57** – EIS test for sample D3.1 (APS sprayed tantalum) after 1, 4, 7, 25 hours of immersion in 0.5M H<sub>2</sub>SO<sub>4</sub>.

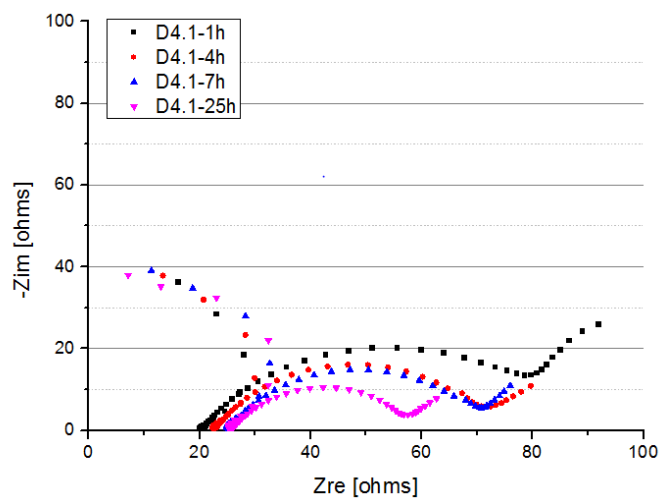


**Figure 58** – EIS test for sample D4.1 (HVOF sprayed cobalt based alloy) after 1, 4, 7, 25 hours of immersion in 0.5M H<sub>2</sub>SO<sub>4</sub>.

From the EIS results is possible to see that for every sample the two circles observed in the Nyquist plot tend to be smaller with the increase of the immersion time.

This trend can be explained by saying that with the increase of the immersion time the corrosion phenomenon is more intense and tend to damage the coating, therefore since the diameters of the two circle represent the value of the coating resistance  $R_c$  (first circle) and the value of the charge transfer resistance  $R_{ct}$  (second circle) those two circles tend to be smaller because the value of the resistance decrease.

It's also possible to deduce the qualitative behave of the different samples.

In fact, like in the polarization test, the samples with tantalum as bond coating shows the best behave to the test. The two circles have a high diameter compared to the others, this means that this type of samples present the higher value of resistances.

Even the sample the cobalt based alloy as bond coating D4.1 reflect the behave showed with the polarization test, in fact this sample seems to have the lowest value of resistance.

The sampled with Hastelloy C-276 and Ni-20Cr as bond coating seems to have an intermediate behave between the samples with tantalum and cobalt based alloy as bond coating.

In order to have a more quantitative interpretation of the data, all the plots have been fitted using the software FRA.

Figure 59, 60, 61, 62 show some example of the fitting realized for the different plot.

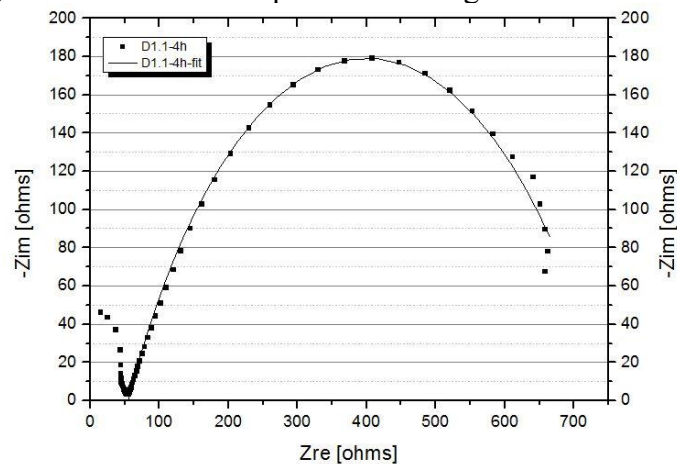


**Figure 59** – Fit for the Nyquist plot obtained from sample D1.1 (Hastelloy C-276 as bond coating) after 4 hours of immersion.

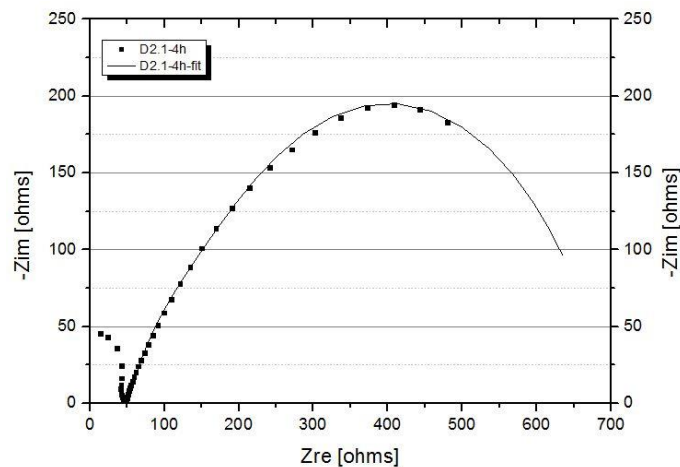


**Figure 60** – Fit for the Nyquist plot obtained from sample D2.1 (Ni-20Cr as bond coating) after 4 hours of immersion.

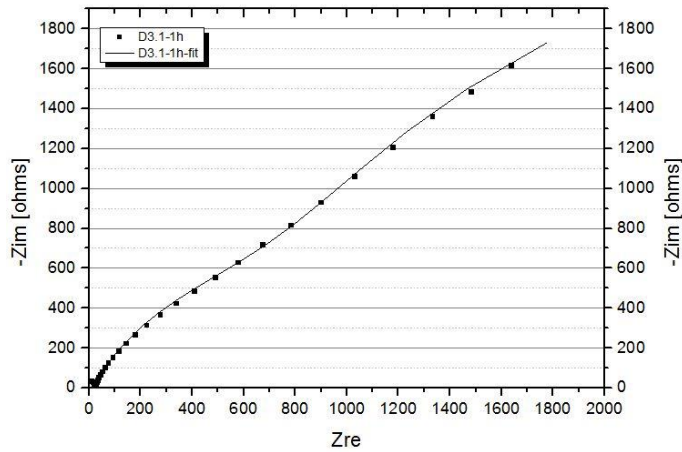


**Figure 61** – Fit for the Nyquist plot obtained from sample D3.1 (tantalum as bond coating) after 1 hour of immersion.

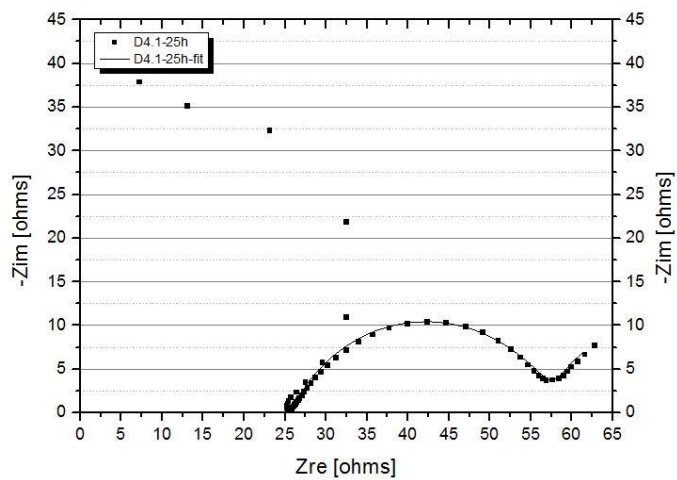


**Figure 62** – Fit for the Nyquist plot obtained from sample D4.1 (cobalt based alloy as bond coating) after 1 hour of immersion.

Tables 11, 12, 13, 14 show at different immersion time, the physical value of the elements used to compose the electrical equivalent circuit for each type of sample.

**Table 11** – Physical value of the elements that constitute the electrical equivalent circuit used to fit the different Nyquist plots after 1 hours of immersion.

Sample (bond coating)	Rs [ohms]	Rc [ohms]	Rct [ohms]	Y0c	n <sub>1</sub>	Y0dl	n <sub>2</sub>
D1.1 (Hastelloy C-276)	50	600	1250	4.6e <sup>-8</sup>	0.65	6e <sup>-8</sup>	0.40
D2.1 (Ni-20Cr)	55	300	470	9.6e <sup>-4</sup>	0.71	3e <sup>-3</sup>	0.8
D3.1 (tantalum)	18.66	1677	4650	3.17e <sup>-4</sup>	0.7762	2.79e <sup>-3</sup>	0.89
D4.1 (cobalt alloy)	20.5	65.7	65	1.89e <sup>-3</sup>	0.71	1.07	0.99

**Table 12** – Physical value of the elements that constitute the electrical equivalent circuit used to fit the different Nyquist plots after 4 hours of immersion.

<b>Sample (bond coatin)</b>	<b>Rs [ohms]</b>	<b>Rc [ohms]</b>	<b>Rct [ohms]</b>	<b>Y0c</b>	<b>n<sub>1</sub></b>	<b>Y0dl</b>	<b>n<sub>2</sub></b>
D1.1 (Hastelloy C-276)	55	450	240	3.5e <sup>-5</sup>	0.61	1e <sup>-7</sup>	0.89
D2.1 (Ni-20Cr)	50.7	300	350	1.45e <sup>-4</sup>	0.7	1e <sup>-3</sup>	0.81
D3.1 (tantalum)	18	930	4250	6e <sup>-4</sup>	0.8	5.5e <sup>-3</sup>	0.9
D4.1 (cobalt alloy)	22.66	51	30	5.98e <sup>-3</sup>	0.71	1.35	0.85

**Table 13** – Physical value of the elements that constitute the electrical equivalent circuit used to fit the different Nyquist plots after 7 hours of immersion.

<b>Sample (bond coating)</b>	<b>Rs [ohms]</b>	<b>Rc [ohms]</b>	<b>Rct [ohms]</b>	<b>Y0c</b>	<b>n<sub>1</sub></b>	<b>Y0dl</b>	<b>n<sub>2</sub></b>
D1.1 (Hastelloy C-276)	50	520	100	5e <sup>-5</sup>	0.64	3e <sup>-3</sup>	0.8
D2.1 (Ni-20Cr)	48	300	340	1.45e <sup>-4</sup>	0.7	1e <sup>-3</sup>	0.79
D3.1 (tantalum)	17.2	454	5410	4.35e <sup>-4</sup>	0.8	7.11e <sup>-4</sup>	0.73
D4.1 (cobalt alloy)	25	47.5	42	6.98e <sup>-4</sup>	0.71	1.99	0.9

**Table 14** – Physical value of the elements that constitute the electrical equivalent circuit used to fit the different Nyquist plots after 25 hours of immersion.

<b>Sample (bond coating)</b>	<b>Rs [ohms]</b>	<b>Rc [ohms]</b>	<b>Rct [ohms]</b>	<b>Y0c</b>	<b>n<sub>1</sub></b>	<b>Y0dl</b>	<b>n<sub>2</sub></b>
D1.1 (Hastelloy C-276)	52	405	28	5e <sup>-5</sup>	0.65	3e <sup>-3</sup>	0.35
D2.1 (Ni-20Cr)	44	230	440	1.45e <sup>-4</sup>	0.65	1e <sup>-3</sup>	0.71
D3.1 (tantalum)	17.29	467	7640	4.38e <sup>-4</sup>	0.8	2.82e <sup>-4</sup>	0.65
D4.1 (cobalt alloy)	25.7	32.9	21	9.98e <sup>-4</sup>	0.72	2.4	0.9



Before analyzing the data from the previous tables it must be said that to interpret the different plots the two ideal capacitor ( $C_c$  and  $C_{dl}$ ) have been substituted with two constant phase elements.

A time constant element is characterized by two index ( $Y_0$  and  $n$ ), when these element act as an ideal capacitor the value of  $Y_0$  is equal to the value of the capacitance  $C$  and  $n=1$  otherwise  $Y_0$  is different from  $C$  and  $n<1$ .

As a first approach to the problem, only the value of the different resistances will be analyzed even because they give a quicker interpretation of the corrosion phenomena.

From the results obtained with the fitting is possible to see that the resistance values for the case with tantalum as bond coating are higher at every immersion time (except the value for  $R_c$  after 7 hours of immersion which is smaller than the same value for sample D1.1, the difference is anyway not so relevant).

For the sample with the cobalt based alloy as bond coating is possible to observe that its value of resistance  $R_c$  and  $R_{ct}$  are always smaller than the other values from the others samples (except the value for  $R_{ct}$  after 25 hours of immersion which is higher than the same value for sample D1.1 anyway the difference is anyway not so relevant).

Moreover, except the pre-mentioned case, the values of resistance  $R_c$  and  $R_{ct}$  for this type of coating are one magnitude smaller than the others, the confirm the low corrosion resistance for this type of sample.

Concerning the values of resistances for the sample with Hastelloy C-276 and Ni-20Cr as bond coating, they are between the values obtained from the sample with tantalum and with the cobalt based alloy.

The value of resistance  $R_c$  for the sample with Hastelloy C-276 as bond coating is higher than the same value for the sample with Ni-20Cr as bond coating while the value of resistance  $R_{ct}$  for the sample with Ni-20Cr as bond coating is generally higher than the same value for the sample with Hastelloy C-276 as bond coating (except after 1 hour of immersion).

Another trend that is important to observe for each type of sample, is how the resistances value,  $R_c$  and  $R_{ct}$ , change with the time of immersion.

If  $R_c$  decrease with the time it means that the coating becomes more electrically conductive, this can be attributed to the formation of new crack and open porosity caused by the corrosion which allow an easily penetration of the electrolyte.

A decrease of resistance  $R_{ct}$  means that the corrosion phenomena is becoming more intense because at the interface between the solution and the metal surface a more quantitative of charge is transferred.

Sample D1.1 (Hastelloy C-276 as bond coating) presents a decreasing value of  $R_c$  and  $R_{ct}$  with the immersion time (except after 7 hours of immersion where the  $R_c$  increase).

For sample D2.1 (Ni-20Cr as bond coating) the resistance  $R_c$  is quite stable with the immersion time while the resistance  $R_{ct}$  decrease with the time until 7 hours of immersion and the increase at 25 hours of immersion.

Sample D3.1 (tantalum as bond coating) presents a decreasing value of  $R_c$  with the immersion time (except from 7 hours to 25 hours of immersion where this value increases slightly), the value of  $R_{ct}$  decreases from 1 hour to 4 hours of immersion but then increase considerably until 25 hours of immersion.

Concerning the sample D4.1 (cobalt alloy as bond coating) the value of  $R_c$  and  $R_{ct}$  decrease with the immersion time (except between 4 hours and 7 hours of immersion where  $R_{ct}$  increase).

In any case it's possible to say that except some minimal variation all the samples present a decreasing trend of the resistances values, this means that the corrosion is taking place, only the sample with tantalum as bond coat presents a considerable

increase of the resistance  $R_{ct}$  with the immersion time, this can be seen as an improve of the corrosion resistance.

Regarding the value of resistance  $R_s$  should be the same for each type of sample because it represents the solution resistance and this value should not change between the different samples because they are tested with the same solution.

Anyway is possible to see that this value changes for each type of sample, this trend can be explained by saying that some test condition can change from one test to another and therefore those change can influence some experimental data like the solution resistance.

### 4.3 Open circuit potential as a function of time

The open circuit potential values as a function of time are showed in Figure 63.

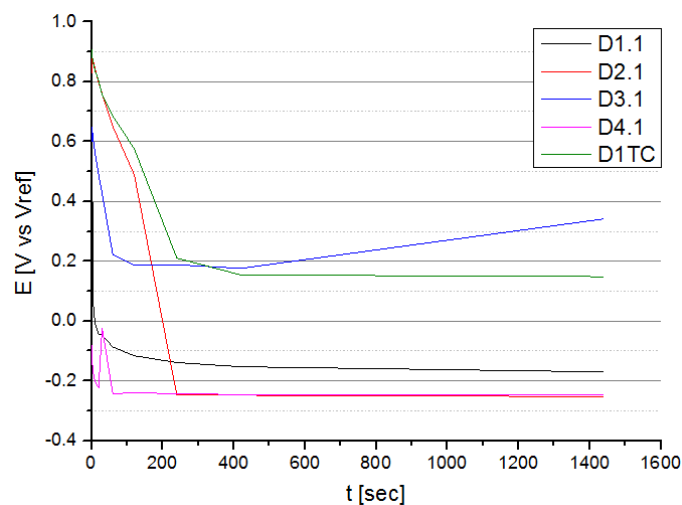


**Figure 63** – Electrochemical potential values measured along time with the OCP test.

The results obtained from the OCP test respects the trend showed also in the polarization test.

All the samples show a decrease of the electrochemical potential value along time which means that corrosion phenomena are taking place.

In any case very sample shows different trends for the electrochemical potential value.

The sample with only the top coat (D1TC) has the higher electrochemical potential value therefore is the more noble, the sample D2.1 (Ni-20Cr as bond coating) initially has a potential value similar to the one presented by D1TC but then it rapidly decreases with the time.

The potential value of the sample with tantalum as bond coating (D3.1) is a bit lower than the one of the sample with Ni-20Cr as bond coating (D2.1) but then it's more stable along time and it even increase at the end of the test.

The sample with Hastelloy C-276 as bond coating (D1.1) present initially a positive value of the potential which became negative along time while the sample with the cobalt based alloy (D4.1) presents the lowest value of the potential.

From the OCP test is possible to say that the best bond coating is represented by tantalum because it has an electrochemical potential value similar to the one presented by D1TC and it's quite stable along time while the worst bond coat is the one made by the cobalt based alloy.

The bond coating made by Ni-20Cr has initially an higher value of the electrochemical potential value but then it rapidly decrease due to corrosion attacks that are taking place,

the bond coating made by Hastelloy C-276 has a trend similar to the one presented by D4.1, in fact its electrochemical potential value is low and it decrease with time.

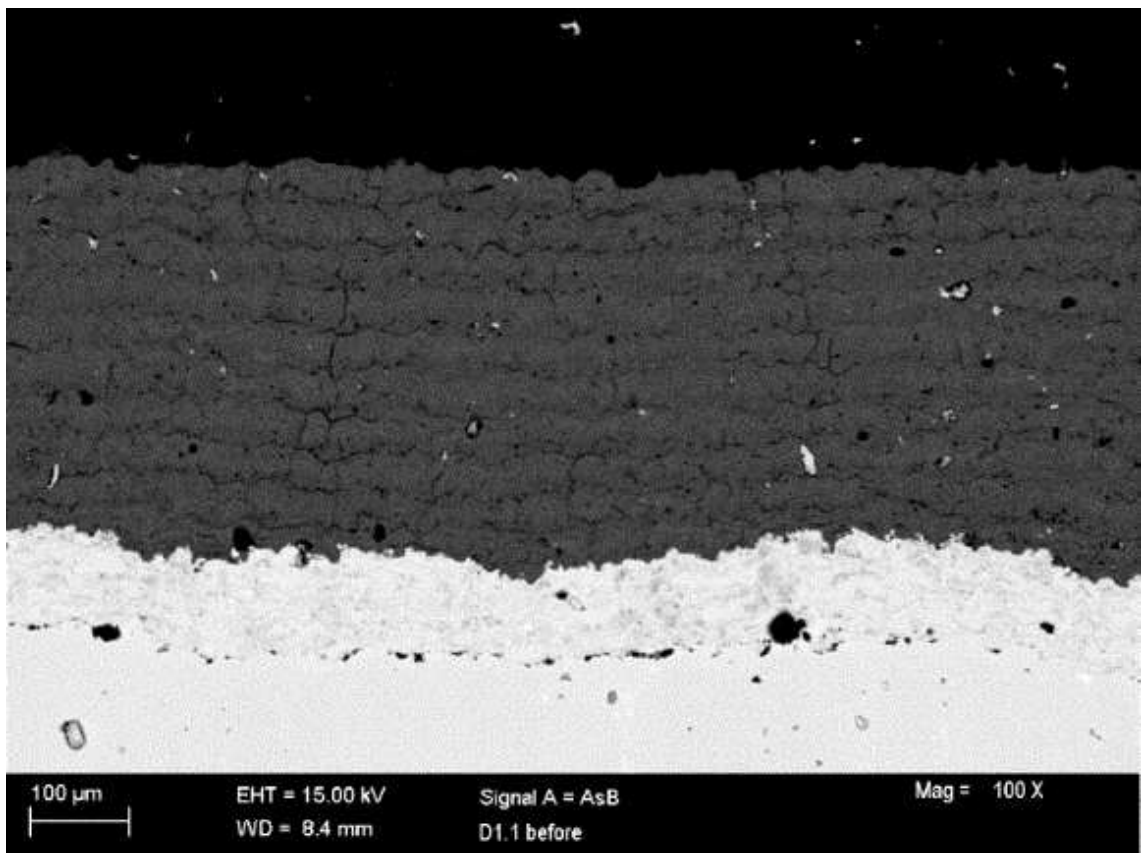
#### 4.4 Corrosion behavior in the immersion test

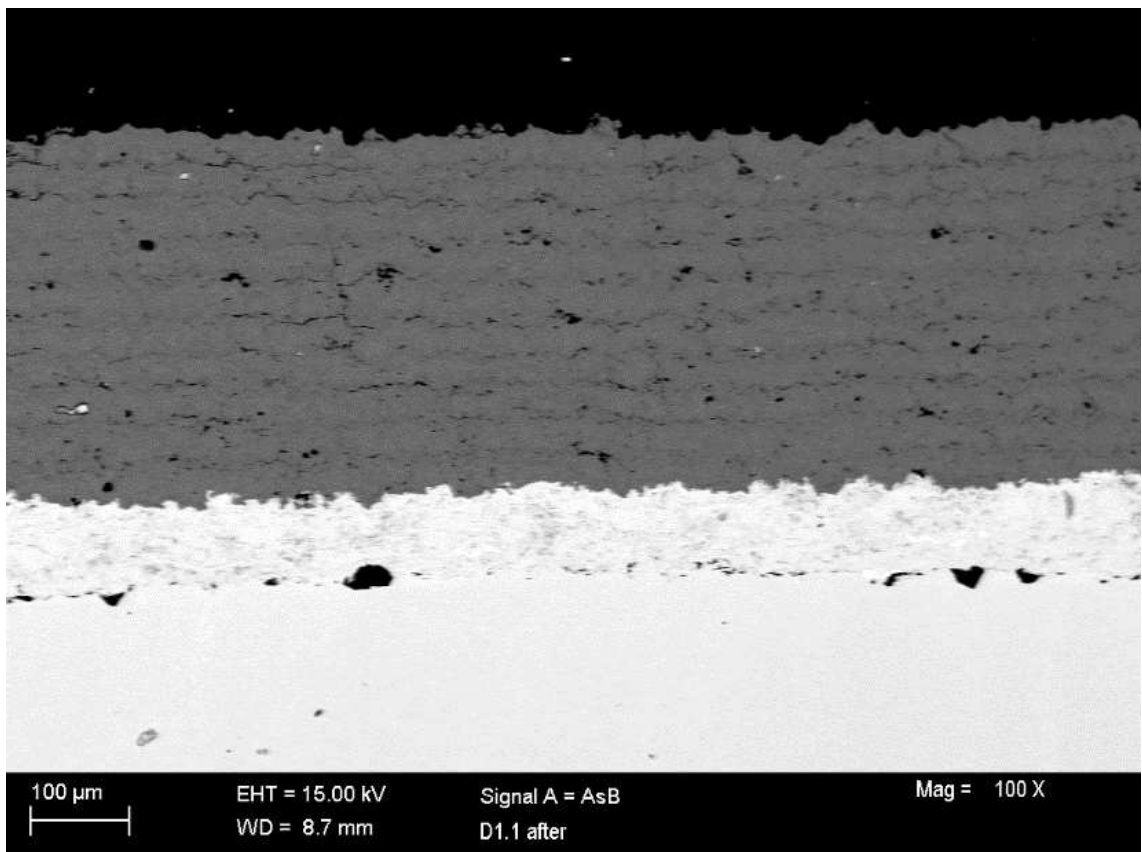
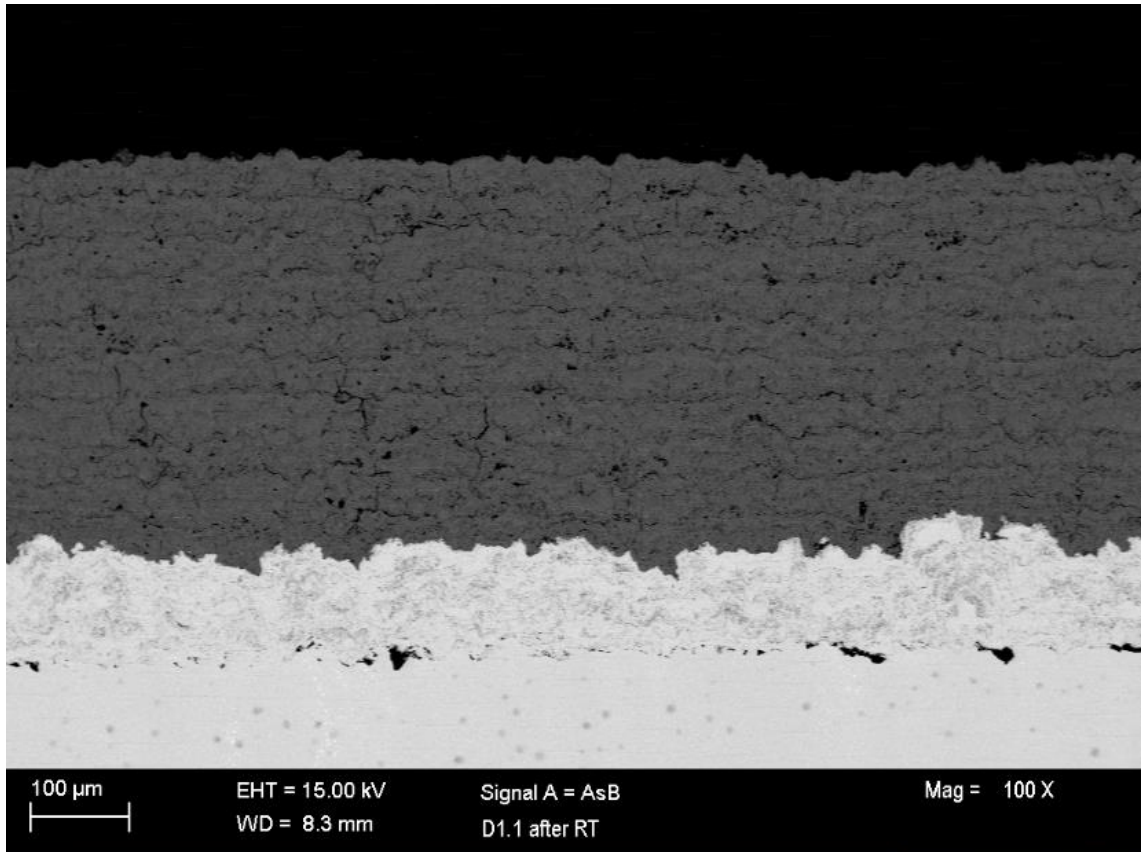
As mentioned in section 3.6 immersion test consisted on immersing the sample in a solution made by sulfuric acid at 1M using an acid vessel.

The immersion has been performed at two different temperatures (60°C and room temperature) for 120 hours.

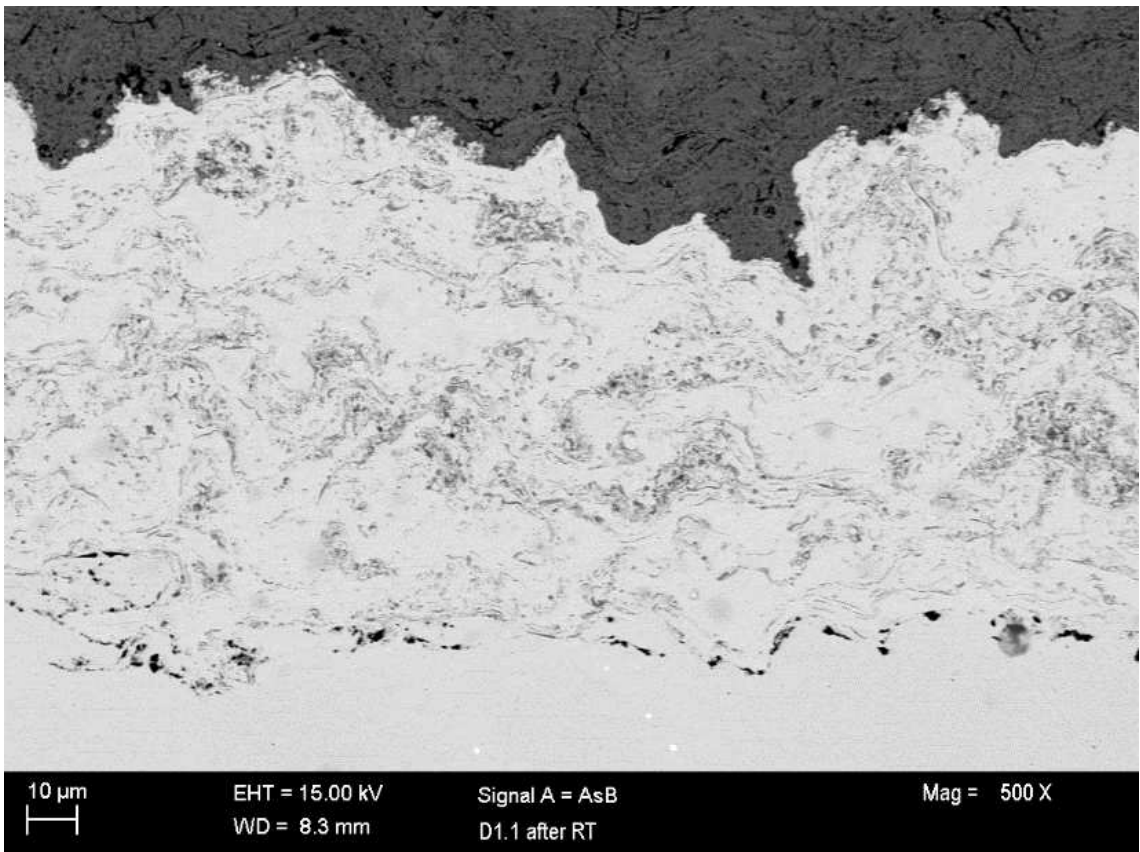
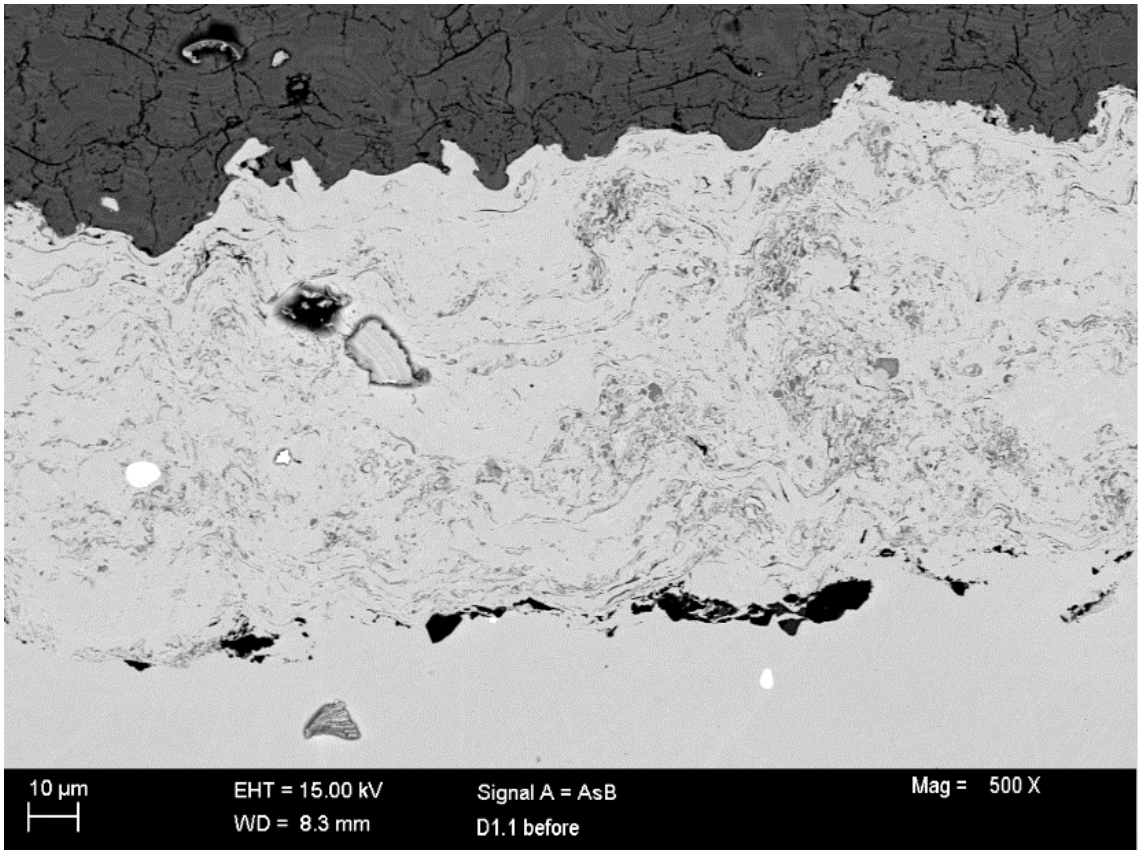
The corrosion phenomenon has been evaluated by observation of cross section with SEM before and after the test.

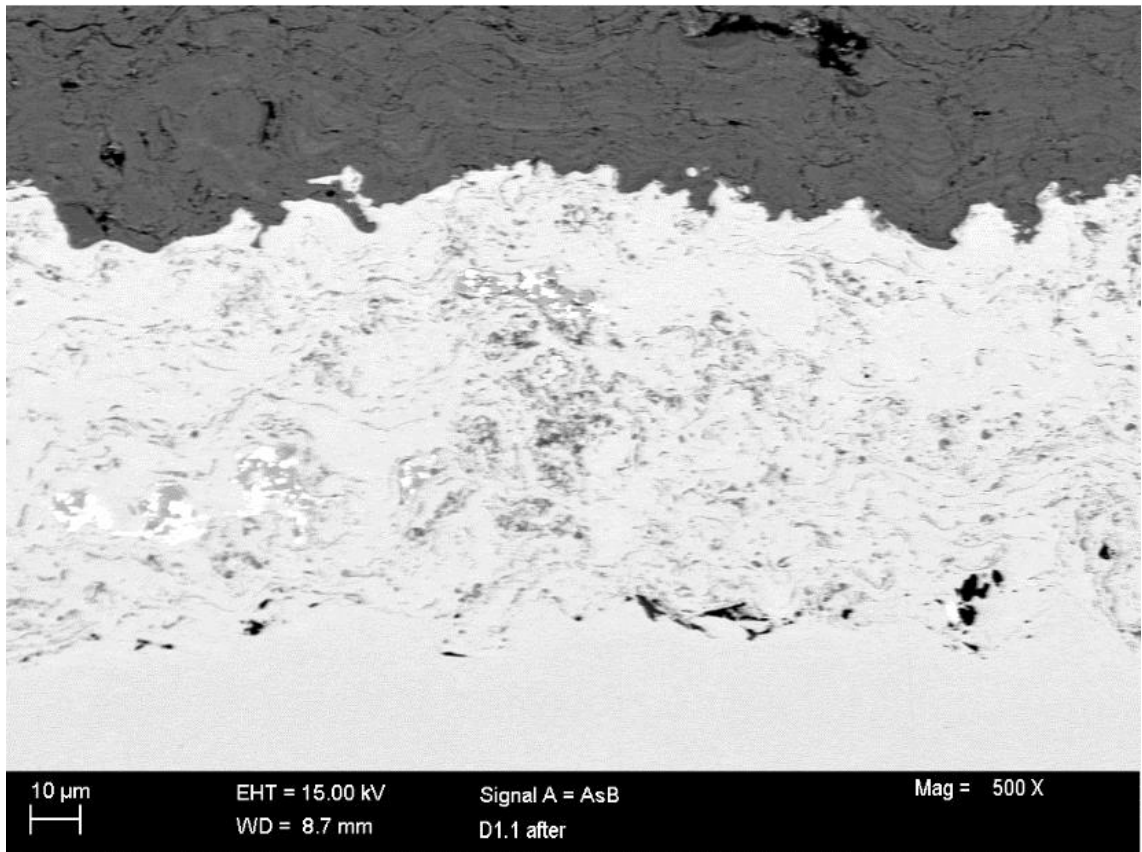
The following figures show the cross section before and after the test at the different temperatures.



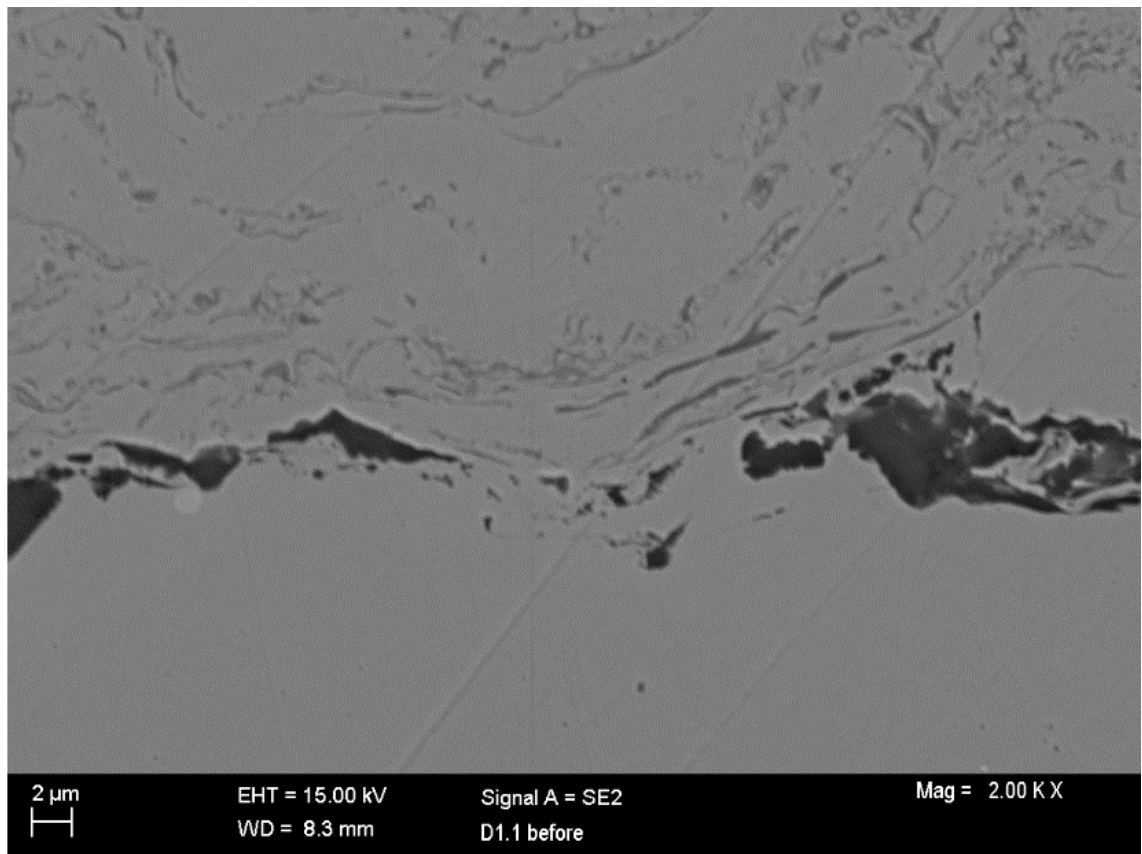


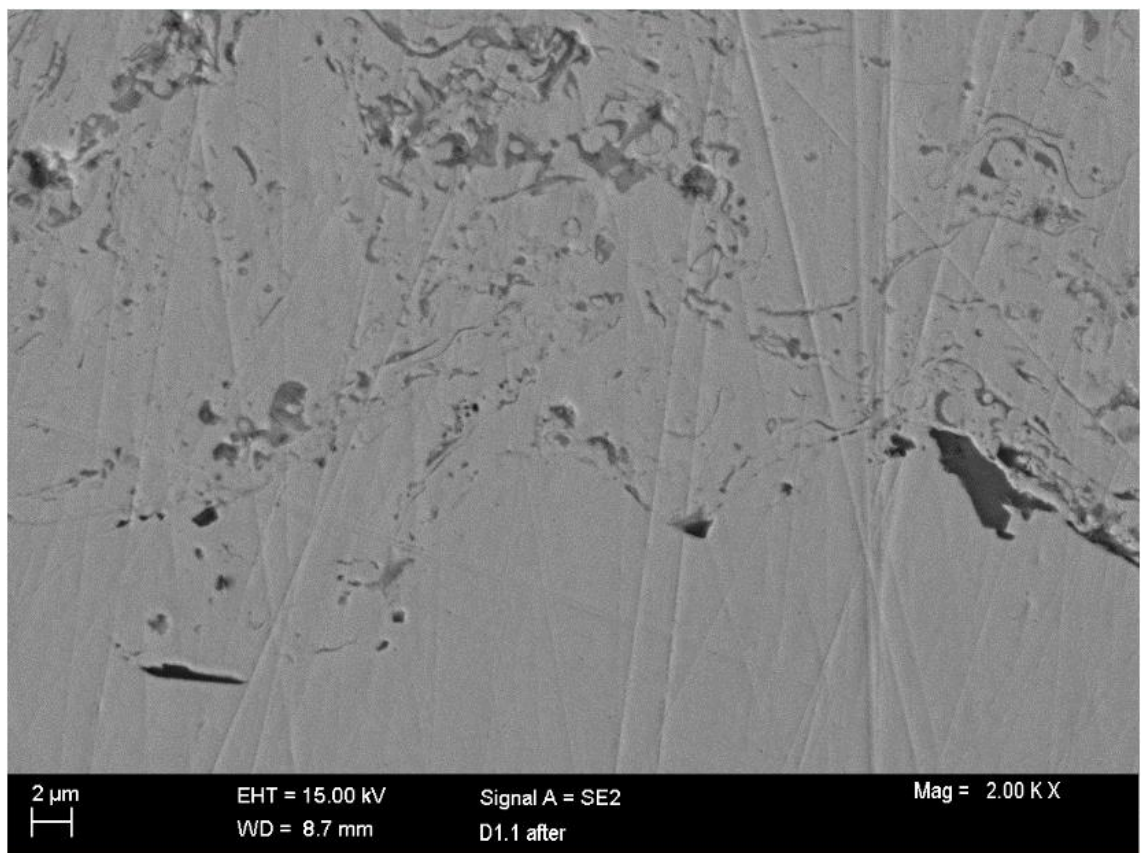
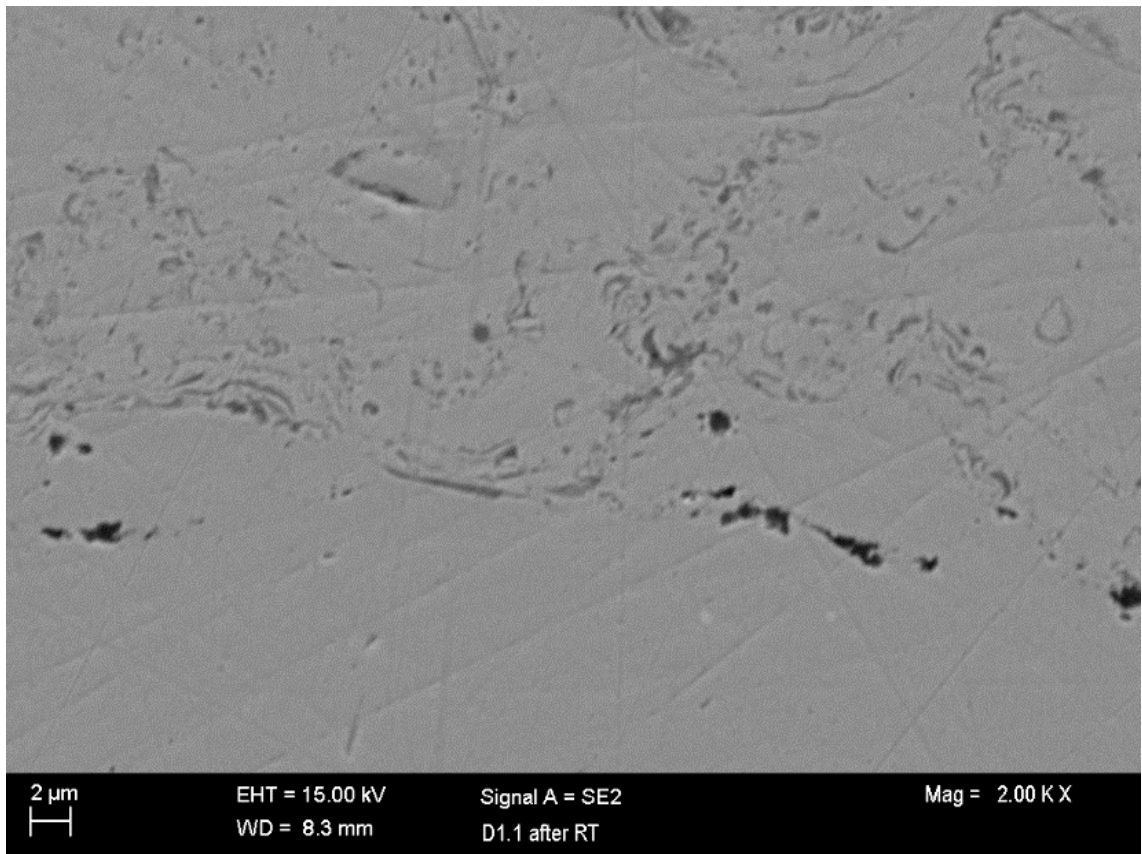
**Figure 64** – SEM cross section for sample D1.1 (Hastelloy C-276 as bond coating) at 100X before and after the immersion test at different temperature.





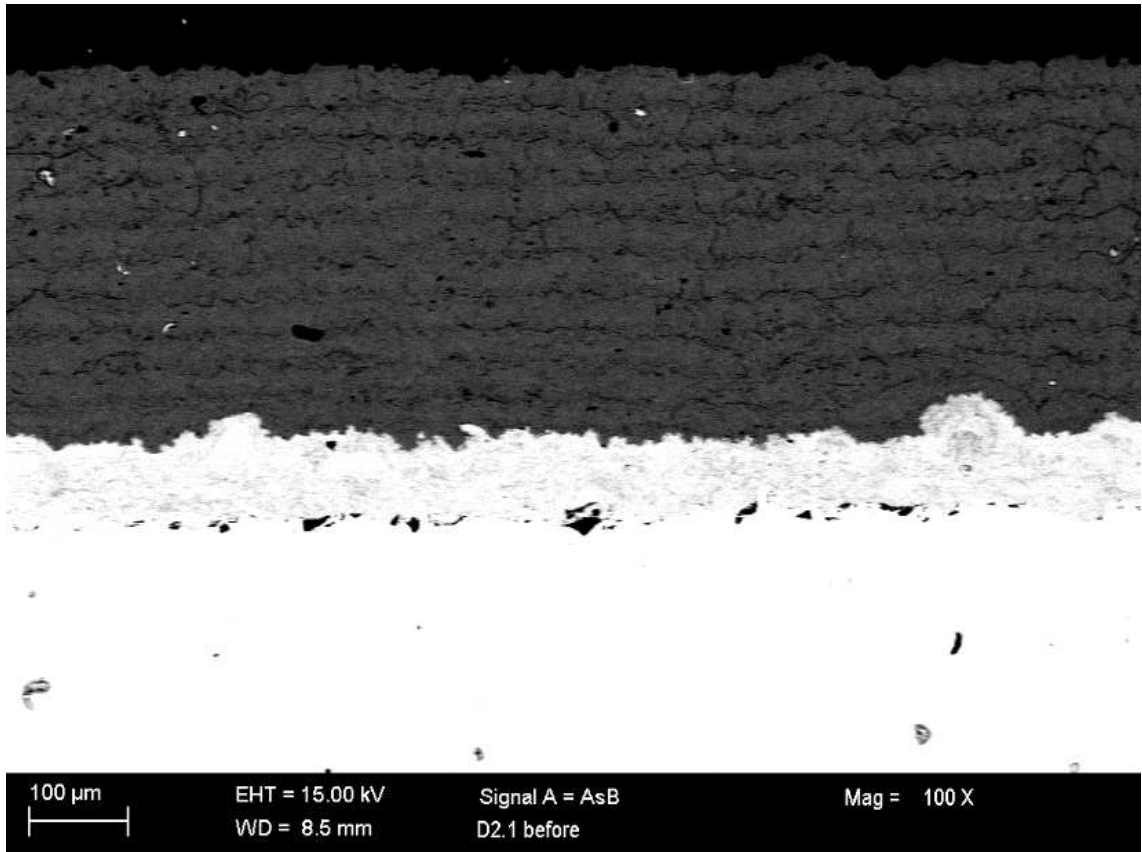
**Figure 65** – SEM cross section for sample D1.1 (Hastelloy C-276 as bond coating) at 500X before and after the immersion test at different temperature.



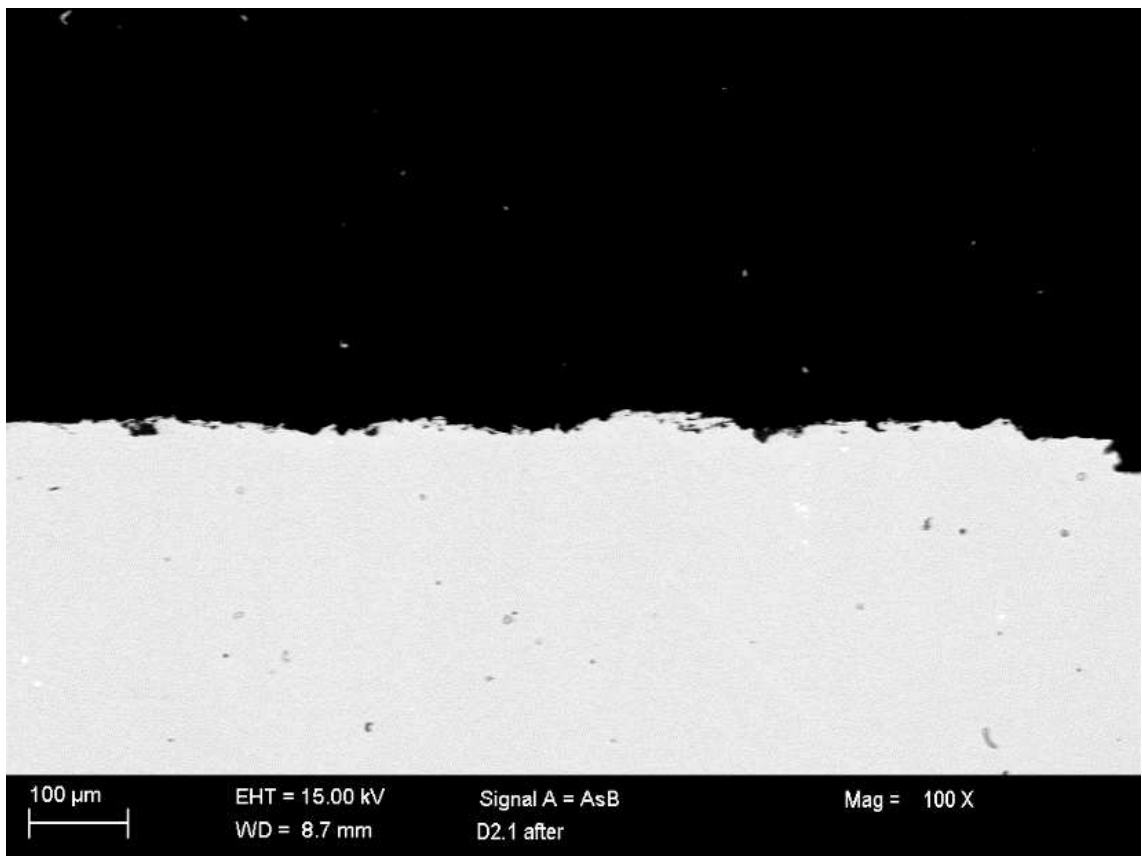
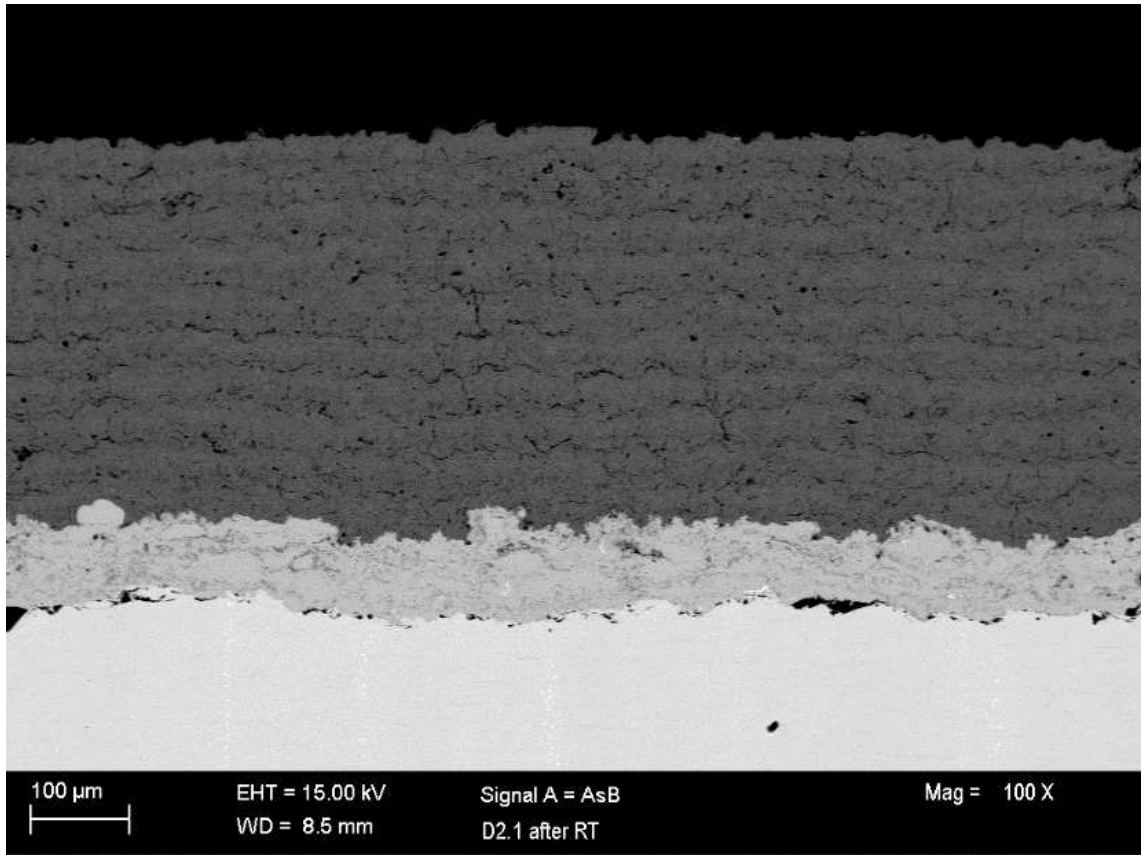


**Figure 66** – SEM cross section for sample D1.1 (Hastelloy C-276 as bond coating ) at 2000X before and after the immersion test at different temperature.

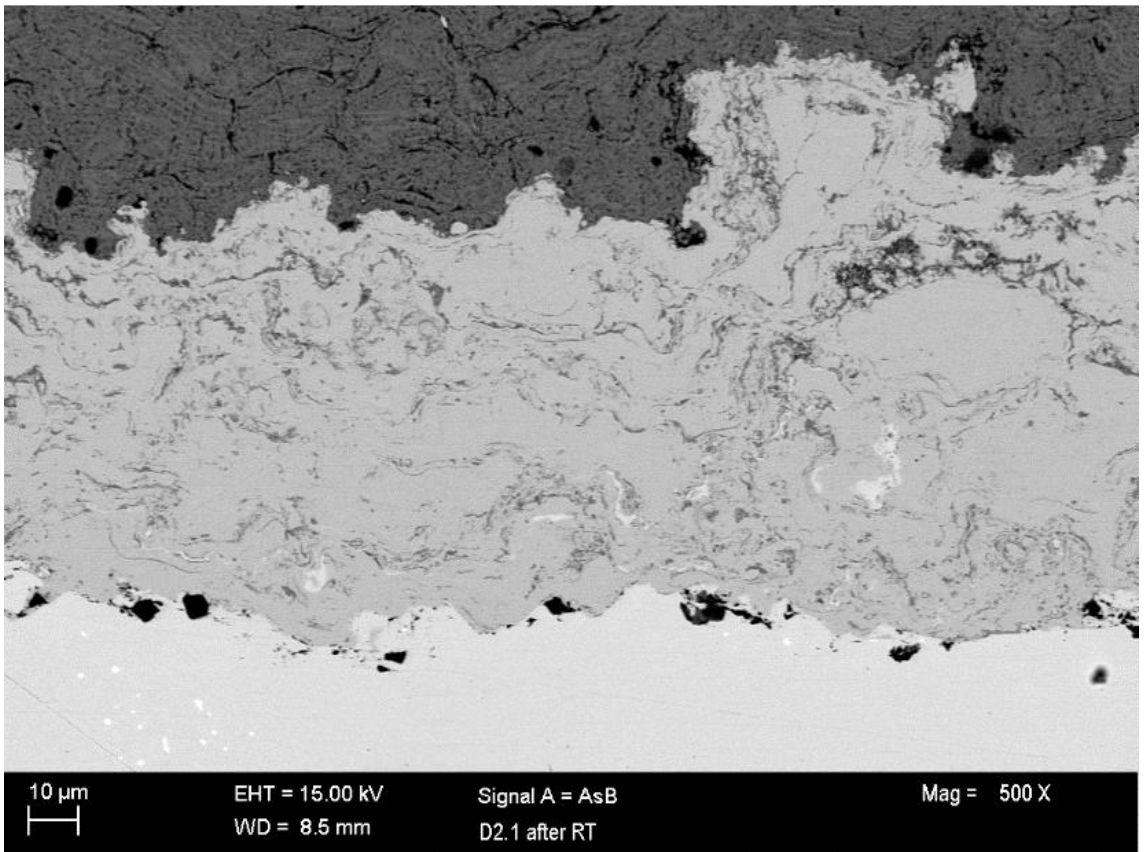
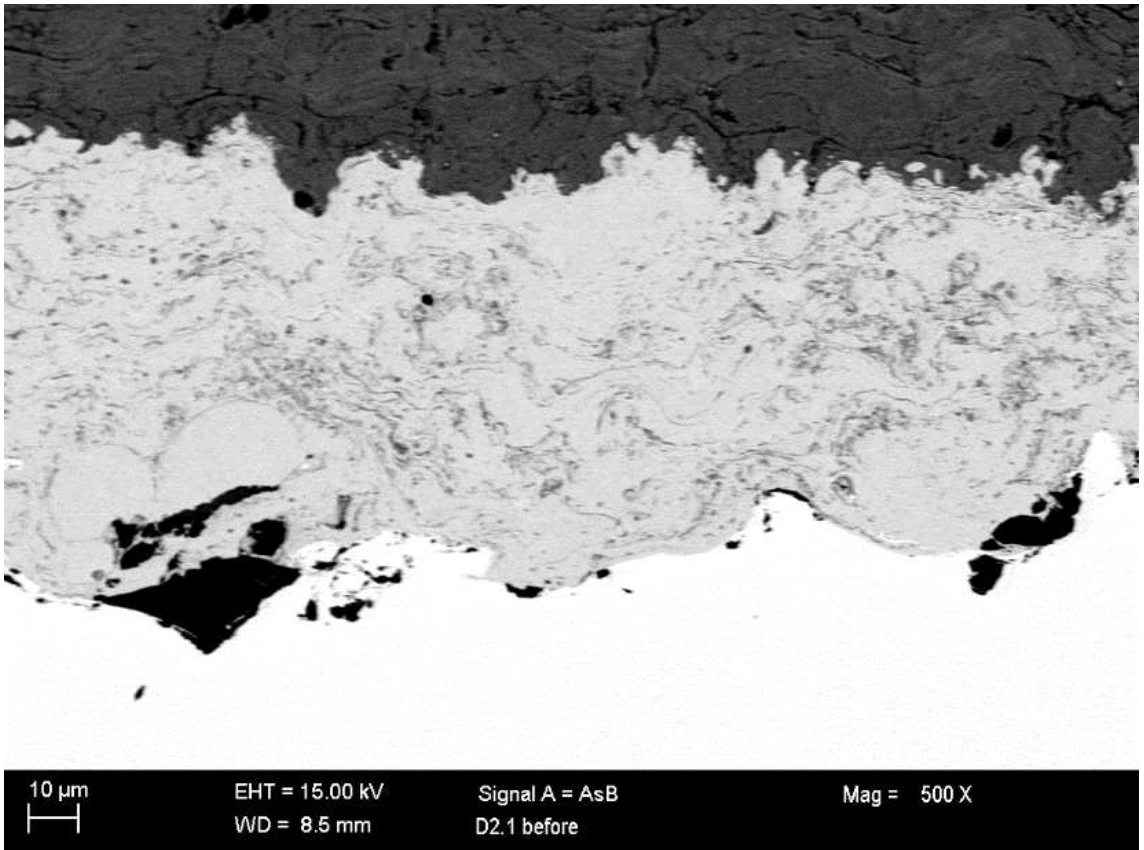
From the cross section reported in Figures 64, 65, 66 is possible to notice that regarding the as sprayed condition the top coating doesn't present a good quality, in fact it presents different cracks and a clear problem of overlaying; anyway this is not compromising for the test because it only means that the electrolyte will reach more easily the bond coat, fact that can be seen as a positive aspect because it increment the corrosion attack. The bond coating constituted by HVOF sprayed Hastelloy C-276 is quite dense and presents some oxides which come from the spray process. After the immersion either the bond coating and the top coating doesn't present evident corrosion phenomena, moreover the temperature has not a relevant role because the cross section for the test at room temperature and the test at 60°C are quite similar.

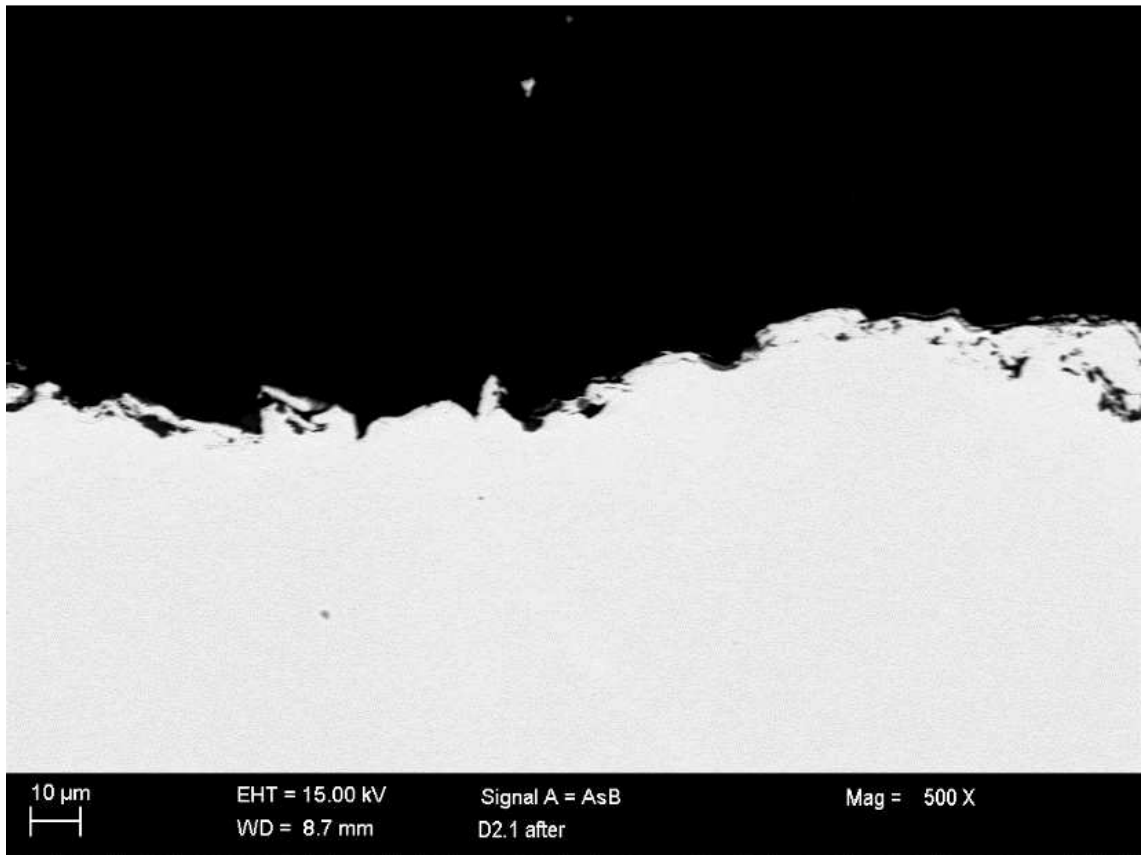




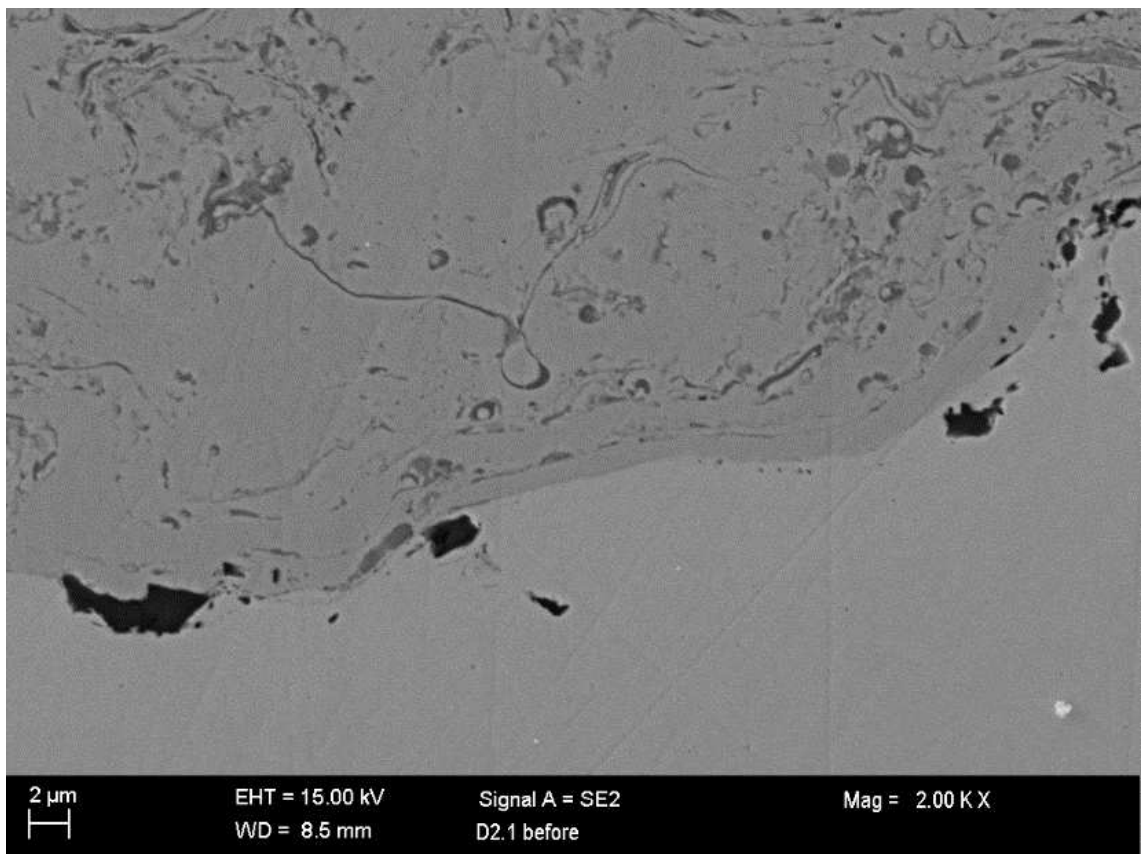


**Figure 67** – SEM cross section for sample D2.1 (Ni-20Cr as bond coating) at 100X before and after the immersion test at different temperature.





**Figure 68** – SEM cross section for sample D2.1 (Ni-20Cr as bond coating) at 500X before and after the immersion test at different temperature.



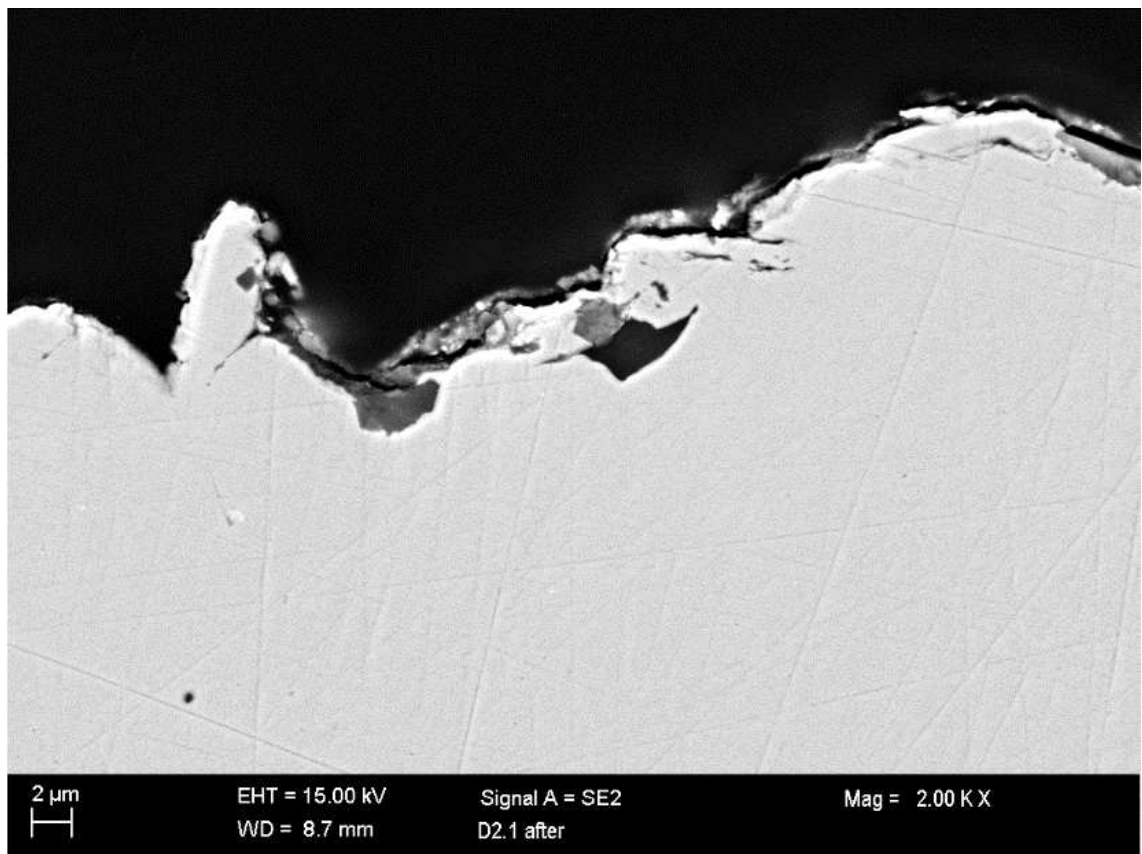
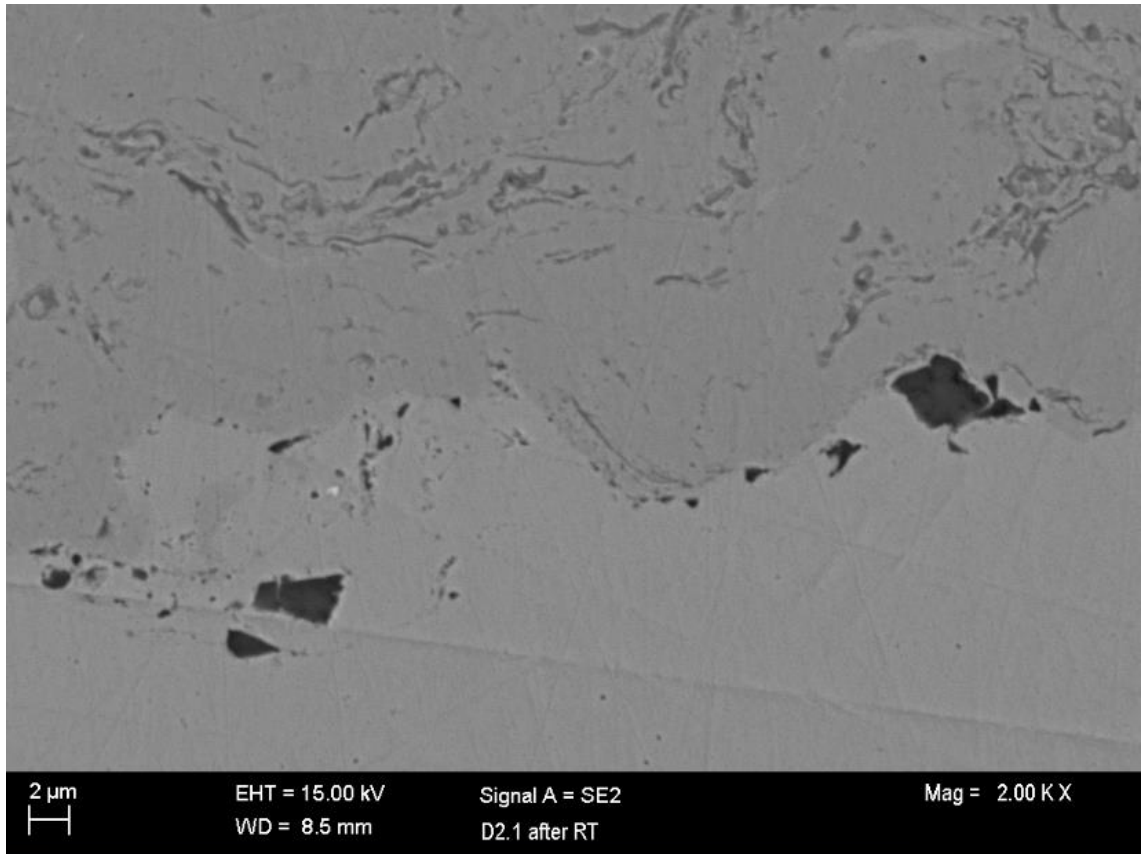
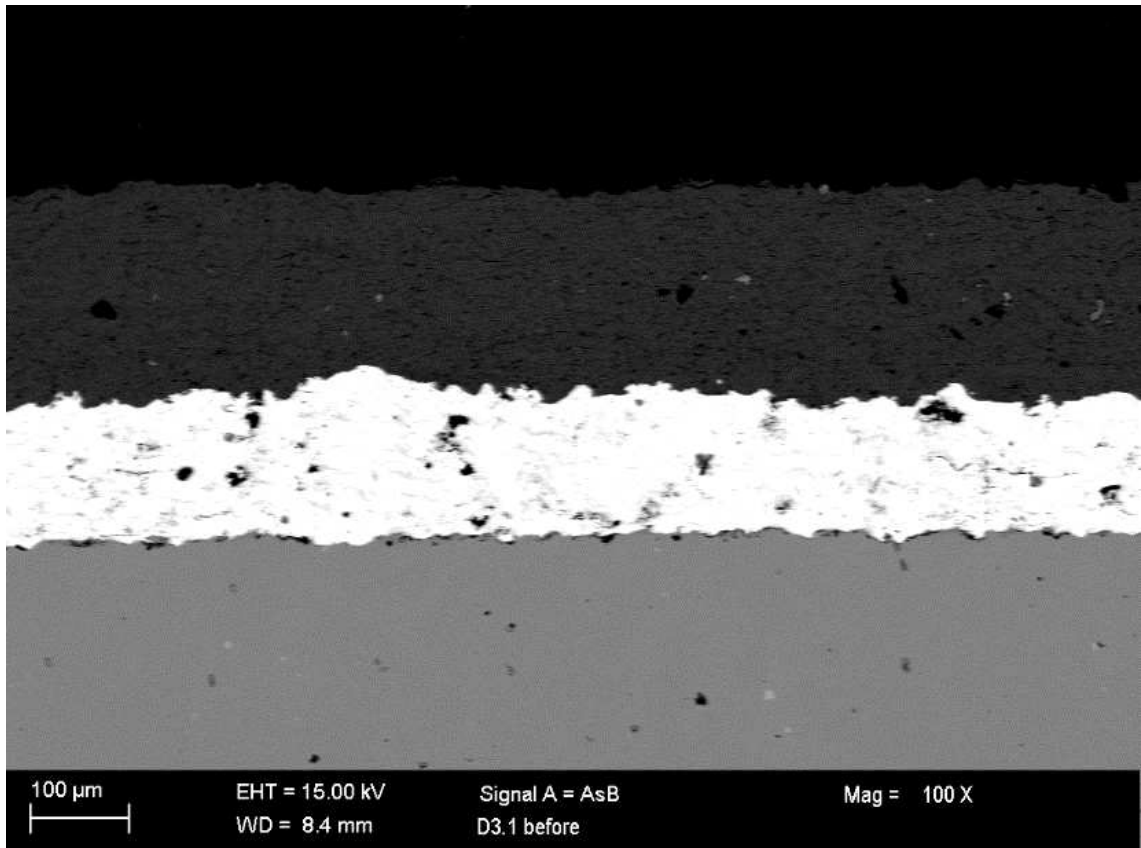


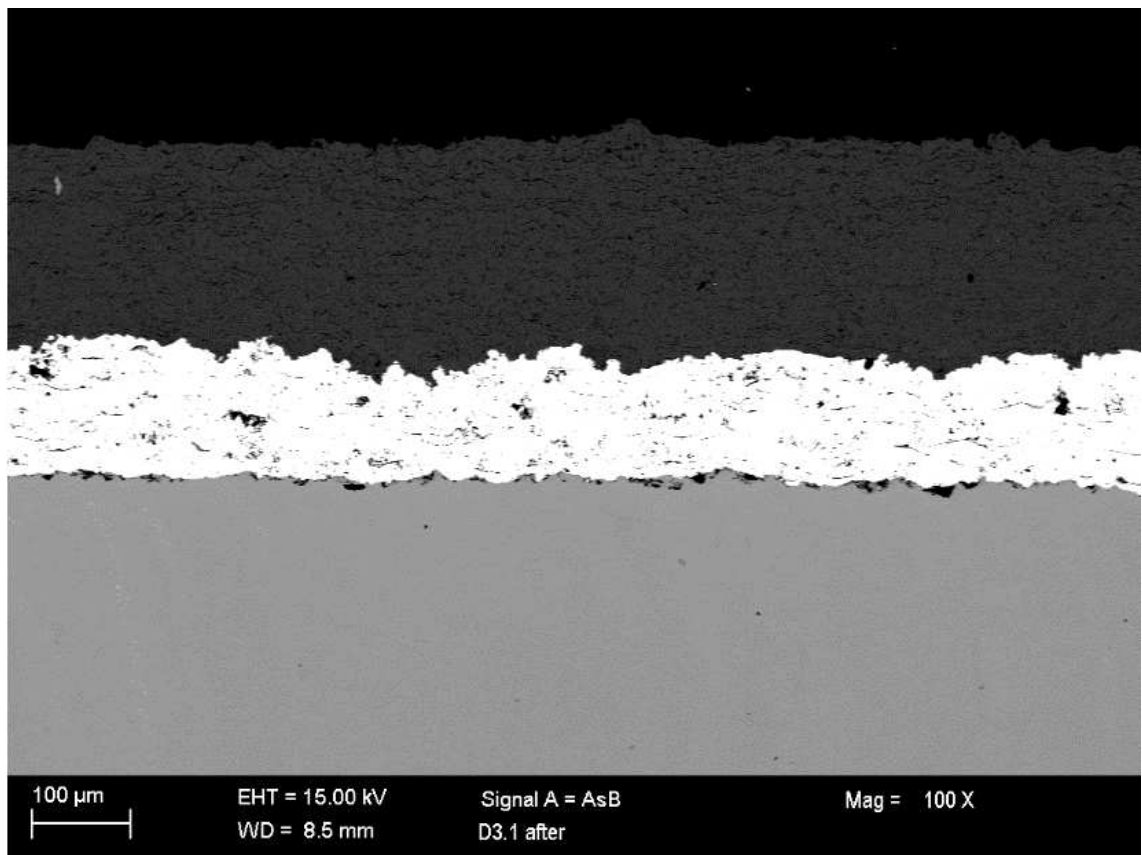
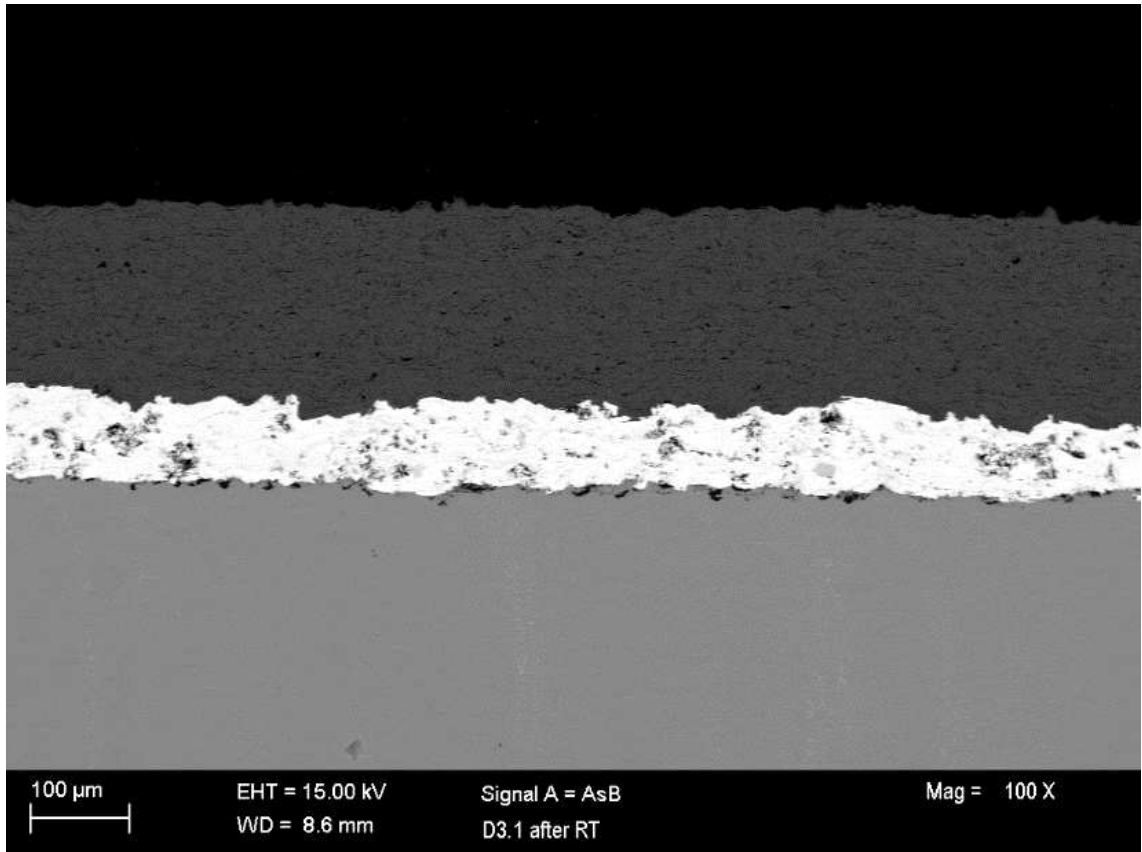
**Figure 69** – SEM cross section for sample D2.1 (Ni-20Cr as bond coating) at 2000X before and after the immersion test at different temperature

From the cross section reported in Figures 67, 68, 69 is possible to notice that even in this case the top presents different cracks and the problem of overlaying; this can be related to the fact that both top coating of the samples D1.1 and D2.1 have been sprayed together with the same spray parameters.

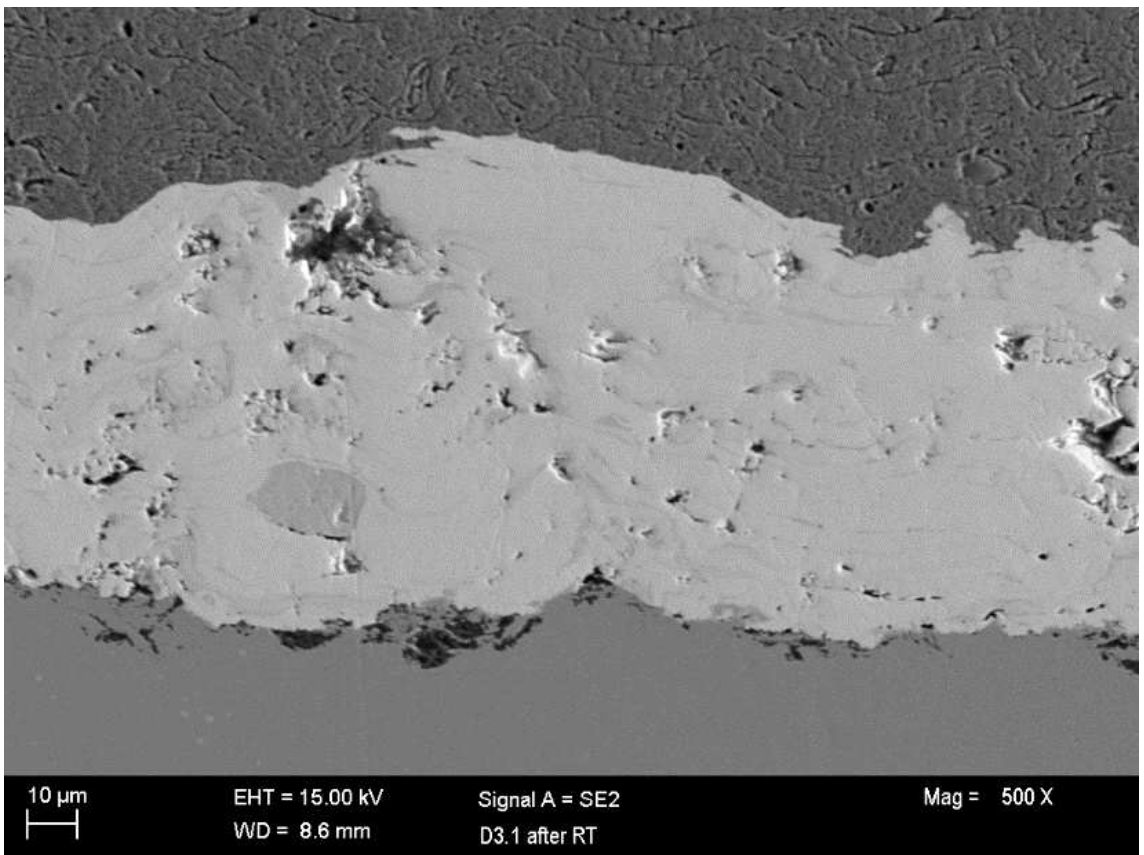
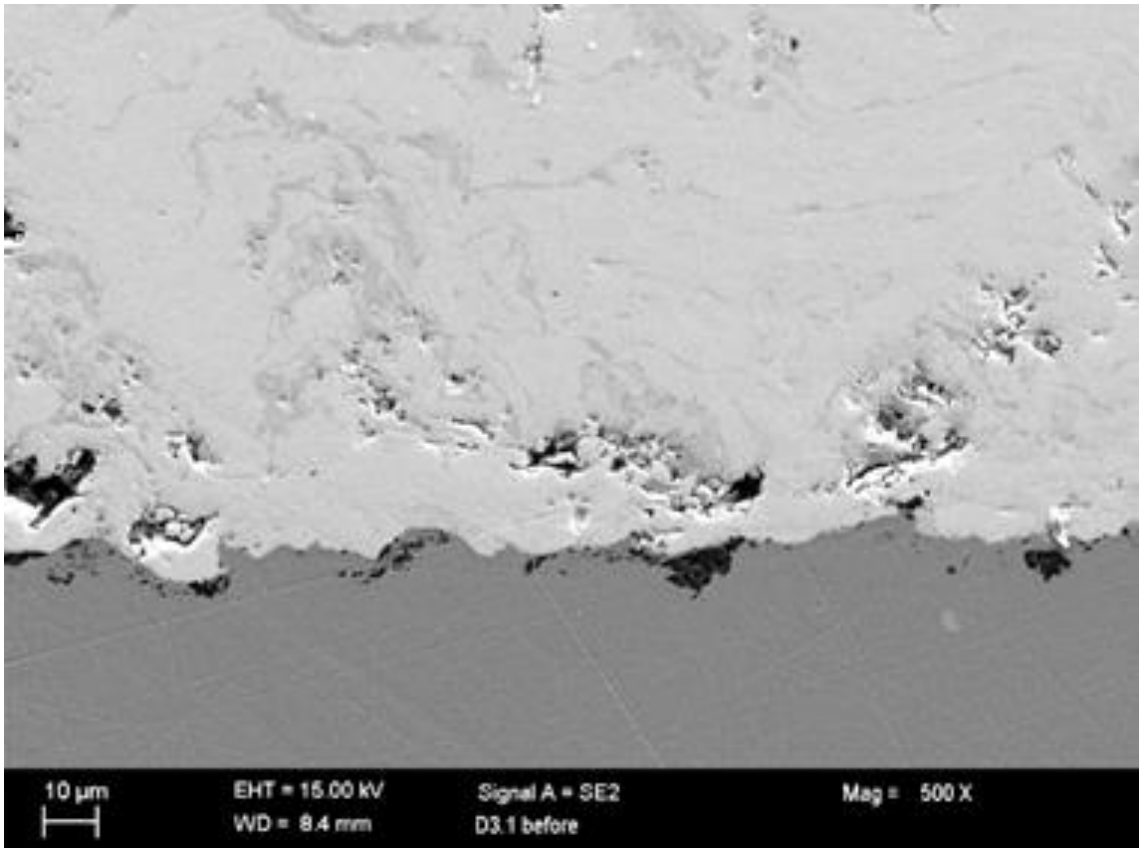
Also in this case the HVOF sprayed Ni-20Cr bond coating is quite dense with some oxide content.

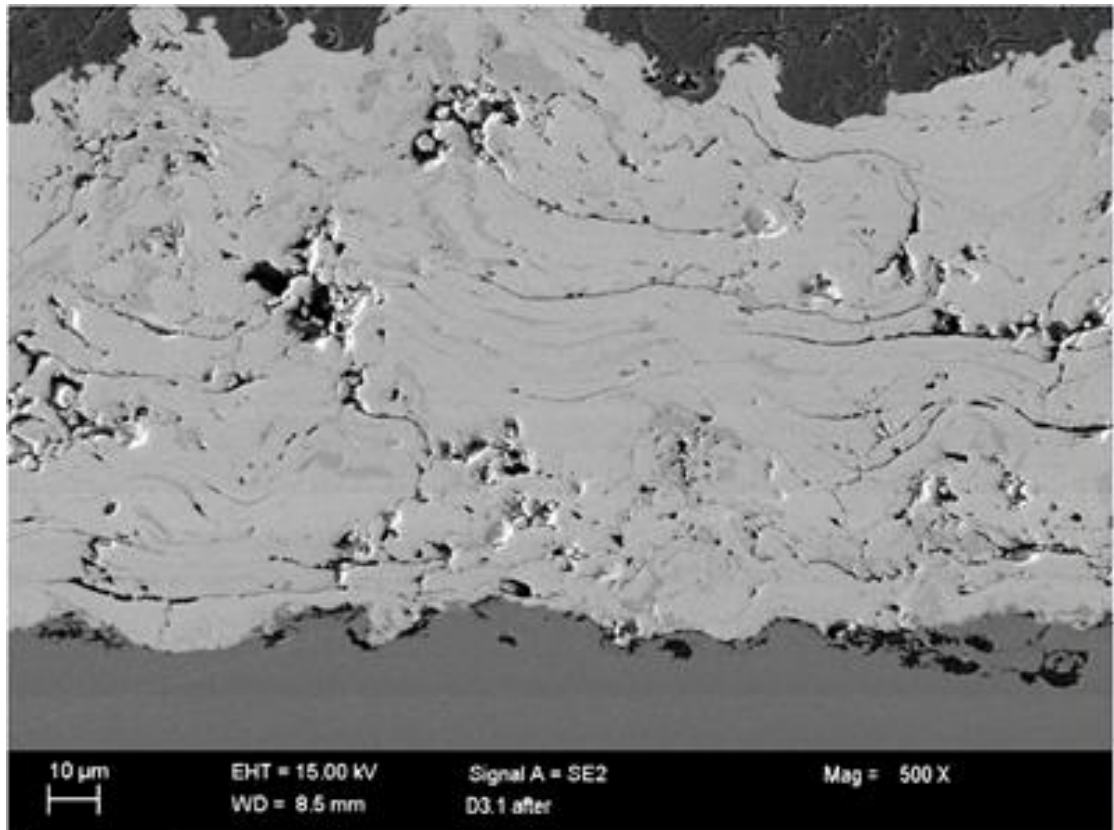
The results after the immersion test are clearly correlated to the test temperature. In fact, at room temperature, the bond coating doesn't present evident signs of corrosion and it is still attached to the substrate while at a temperature of 60°C the bond coating dissolves completely causing the separation of the top coating from the substrate (the top coating resisted to the test condition but was not attached anymore to the substrate).



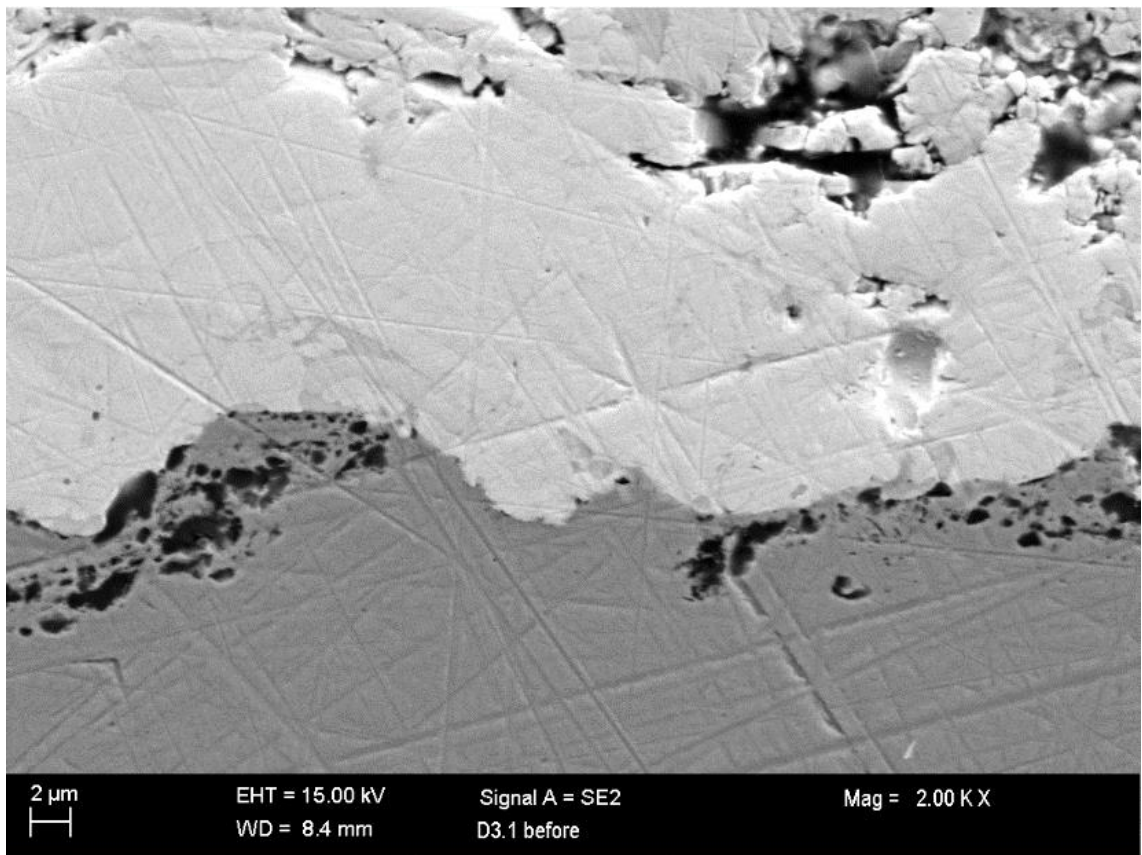


**Figure 70** – SEM cross section for sample D3.1 (tantalum as bond coating) at 100X before and after the immersion test at different temperature.





**Figure 71** – SEM cross section for sample D3.1 (tantalum as bond coating) at 500X before and after the immersion test at different temperature.





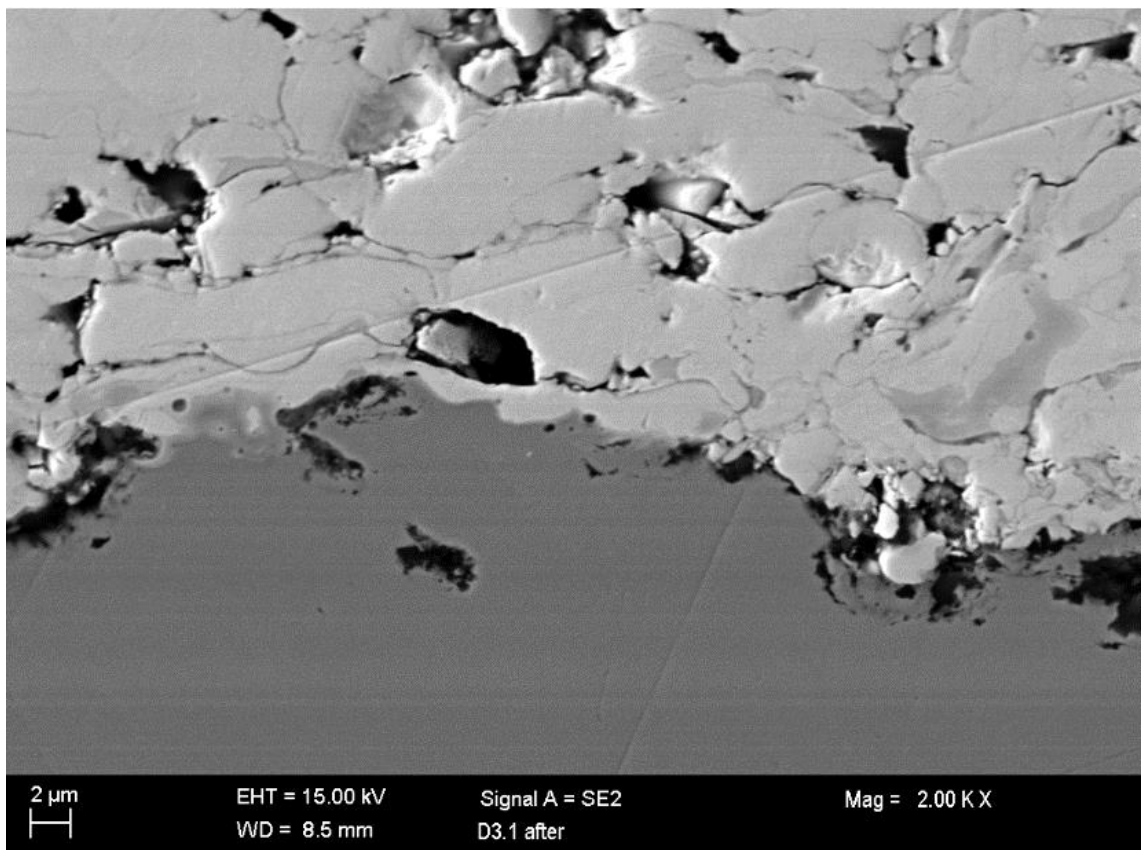
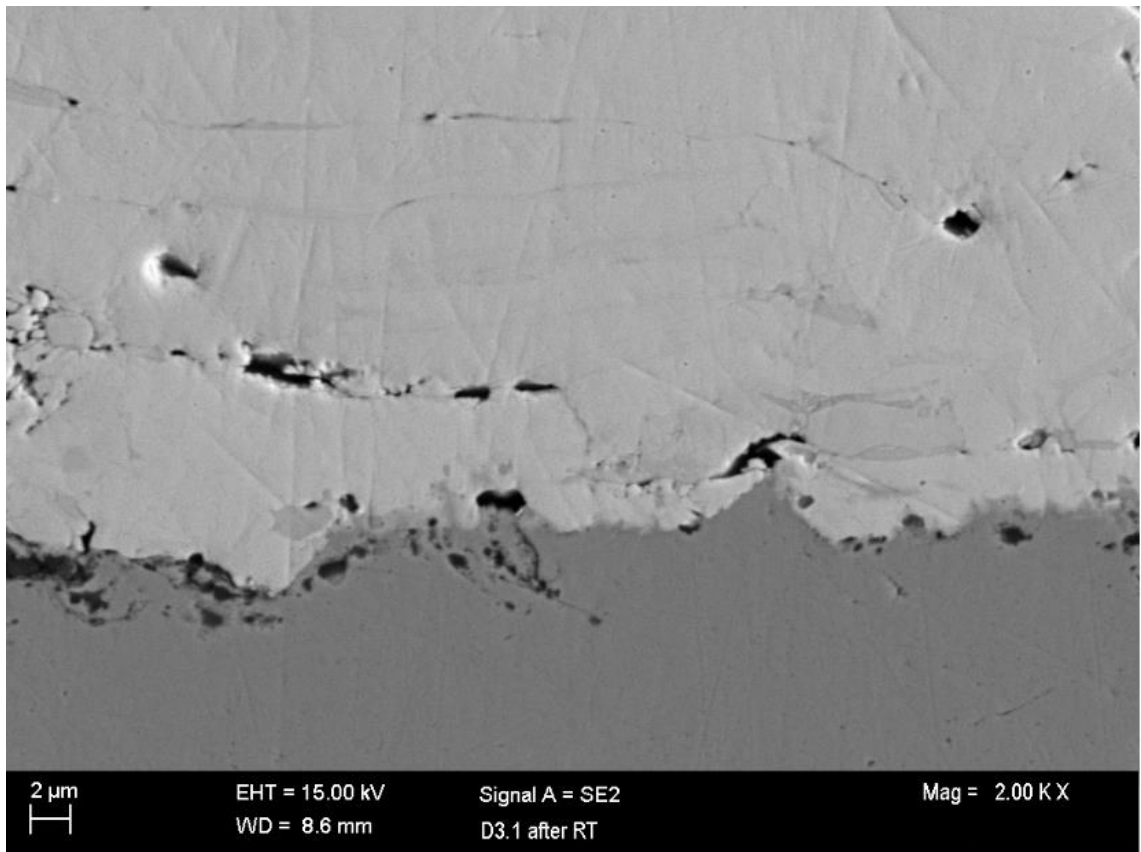


**Figure 72** – SEM cross section for sample D3.1 (tantalum as bond coating) at 2000X before and after the immersion test at different temperature.

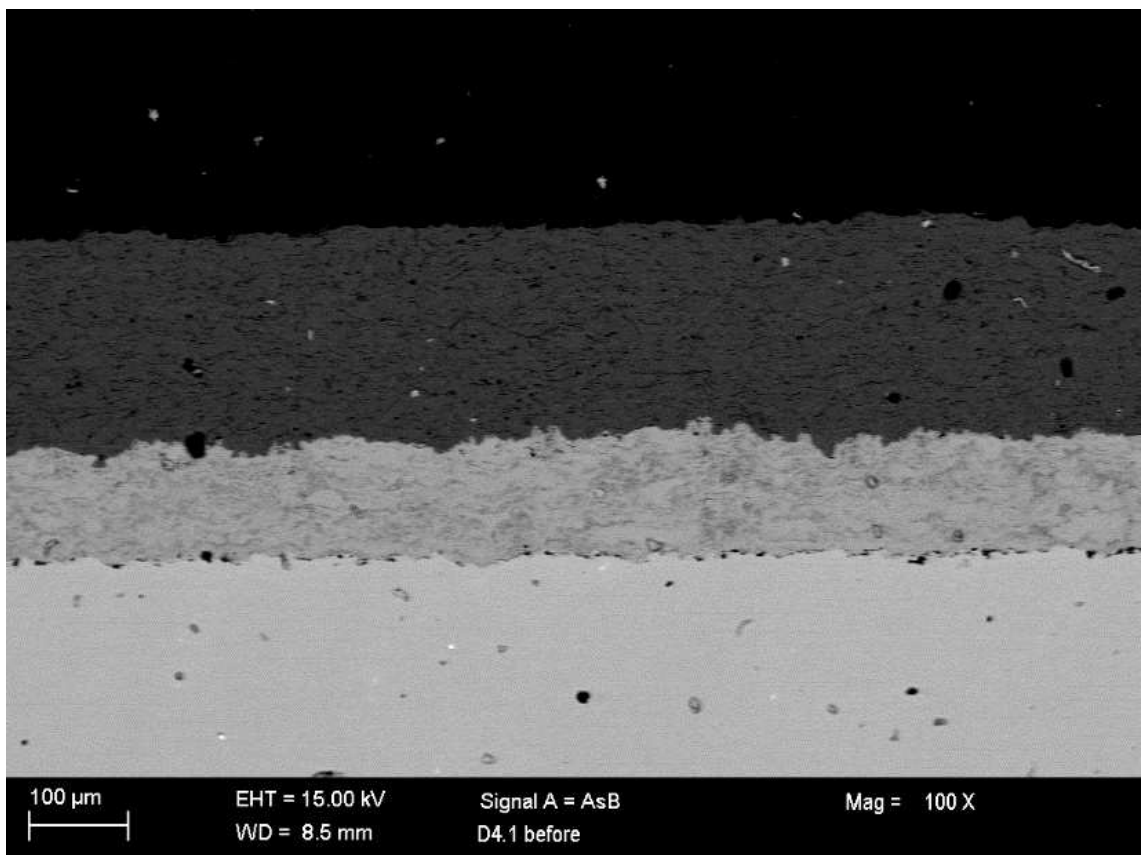
From the cross section reported in Figures 70, 71, 72 is possible to notice that the top coating presents a good quality, in fact it's denser with a lower content of microcracks and without the problem of overlaying.

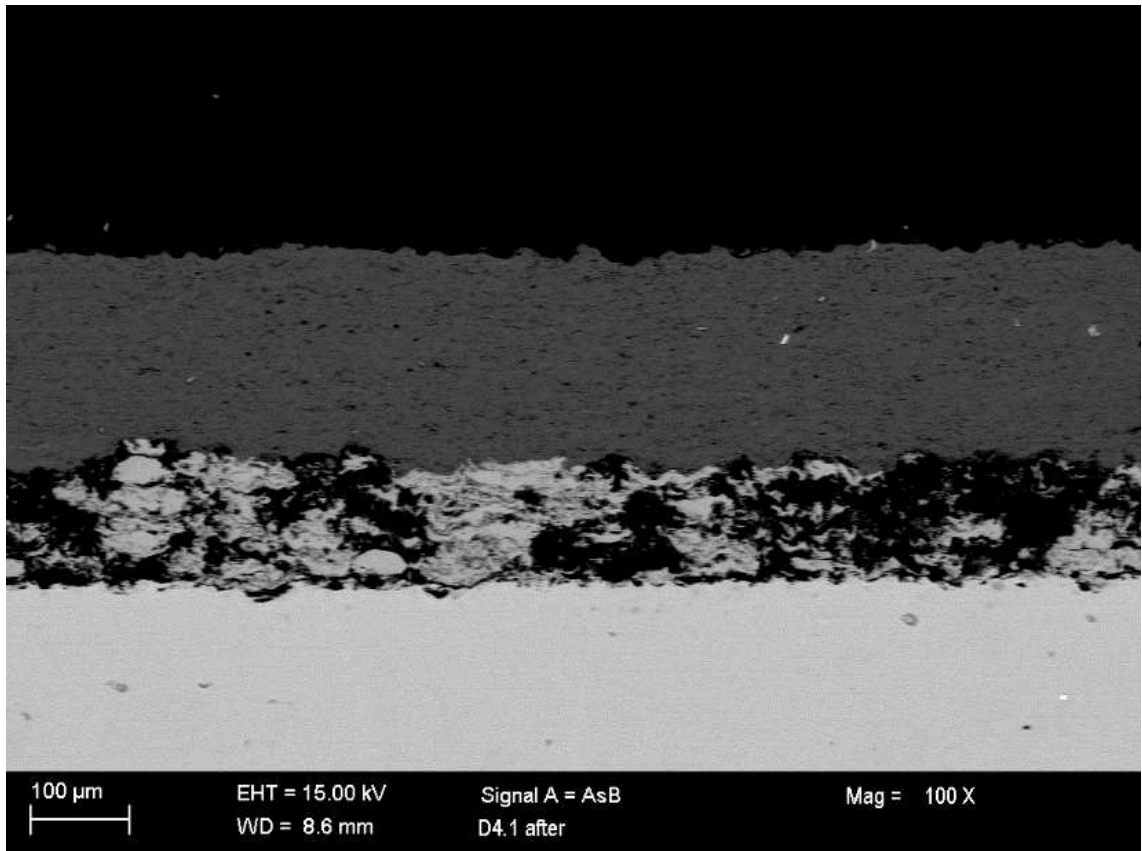
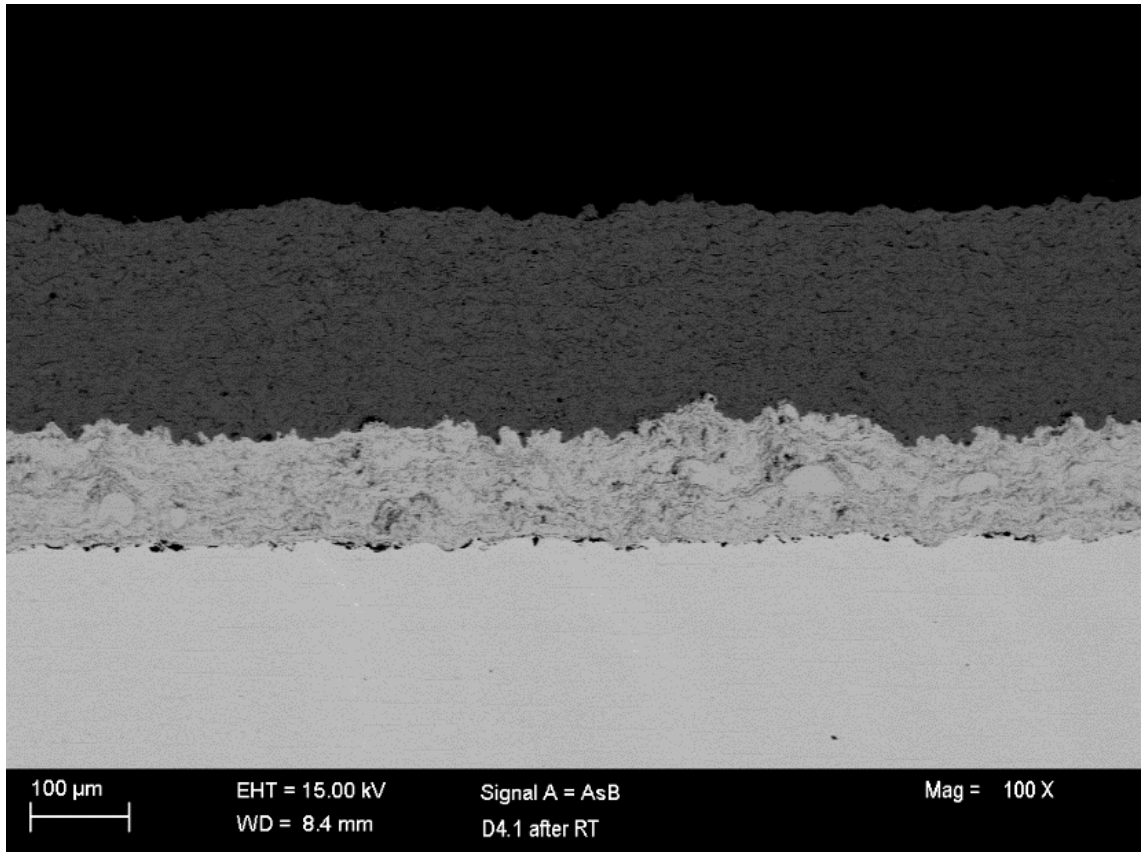
This quality has been reached by changing some parameters, the robot speed and the number of passes have been increased while the hydrogen flow and the carrier gas flow have been reduced.

Also the tantalum bond coat sprayed with APS seems to have a good quality, in fact it's dense with a low content of oxide.

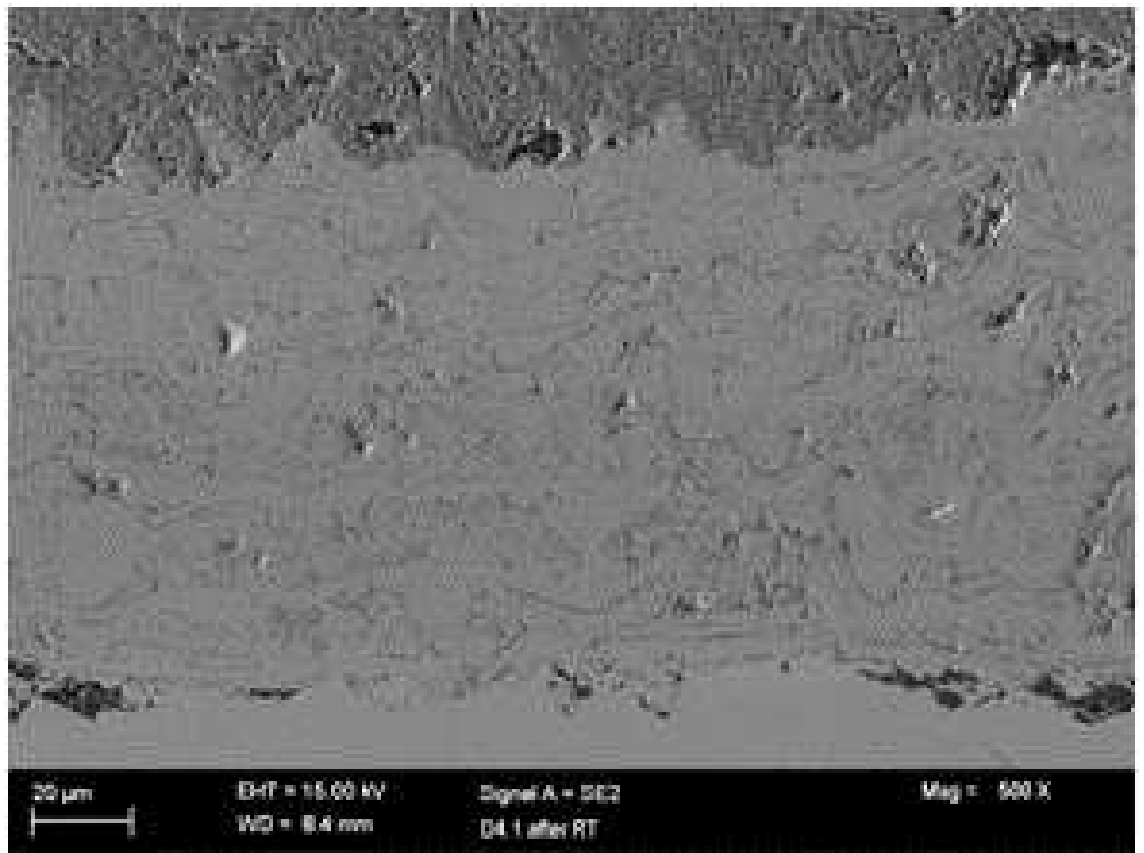
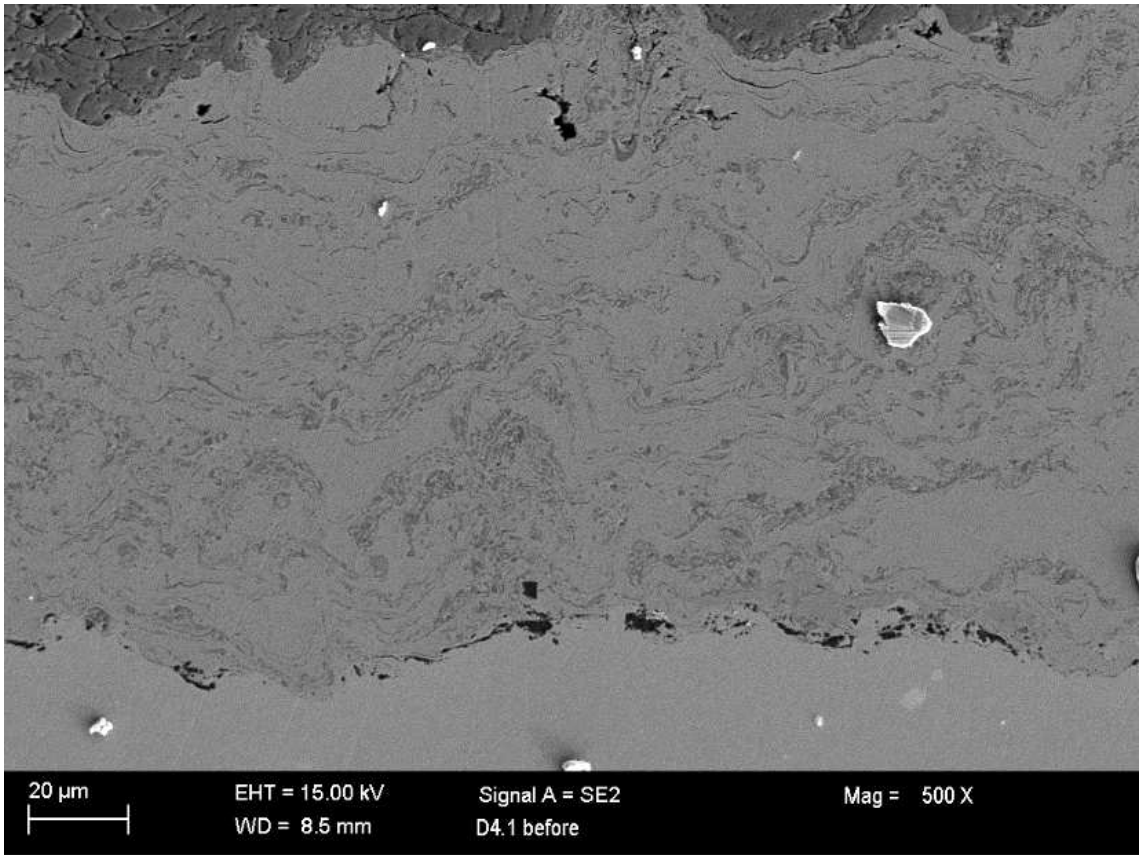
After the immersion the bond coating doesn't present evident damage of corrosion in both temperature conditions.

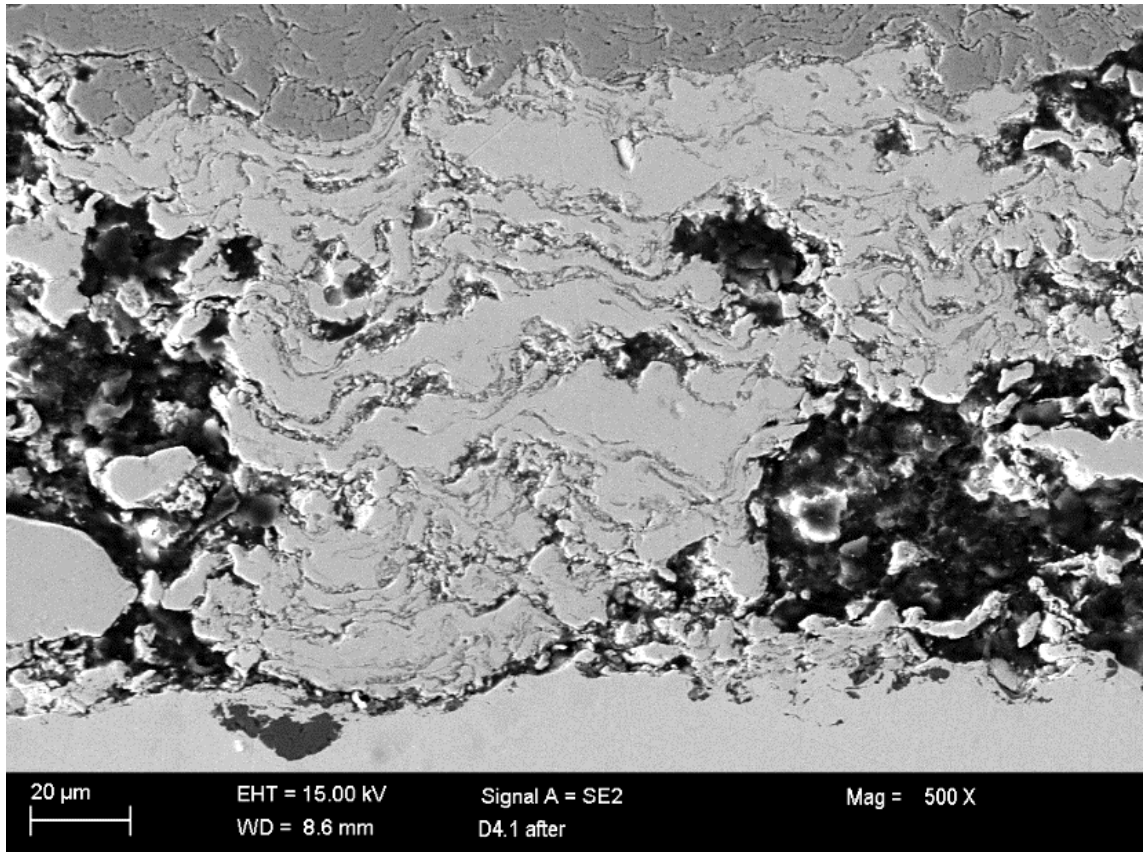
At  $T=60^{\circ}\text{C}$  the bond coating seems to have a higher content of microcracks but it's not possible to relate those cracks with a corrosion phenomenon, in fact they can also be formed due to the thermal stress induced with the heating and the cooling.



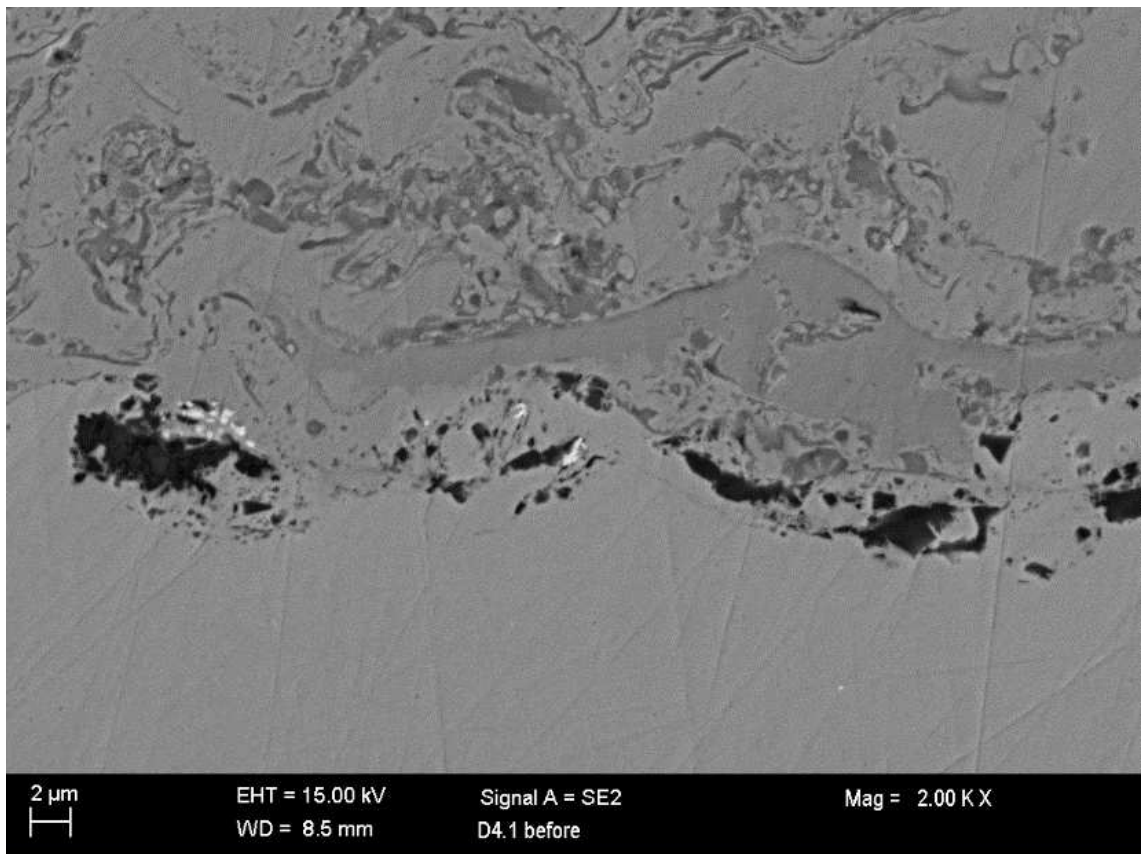


**Figure 73** – SEM cross section for sample D4.1 (cobalt based alloy as bond coating) at 100X before and after the immersion test at different temperature.





**Figure 74** – SEM cross section for sample D4.1 (cobalt based alloy as bond coating) at 500X before and after the immersion test at different temperature.



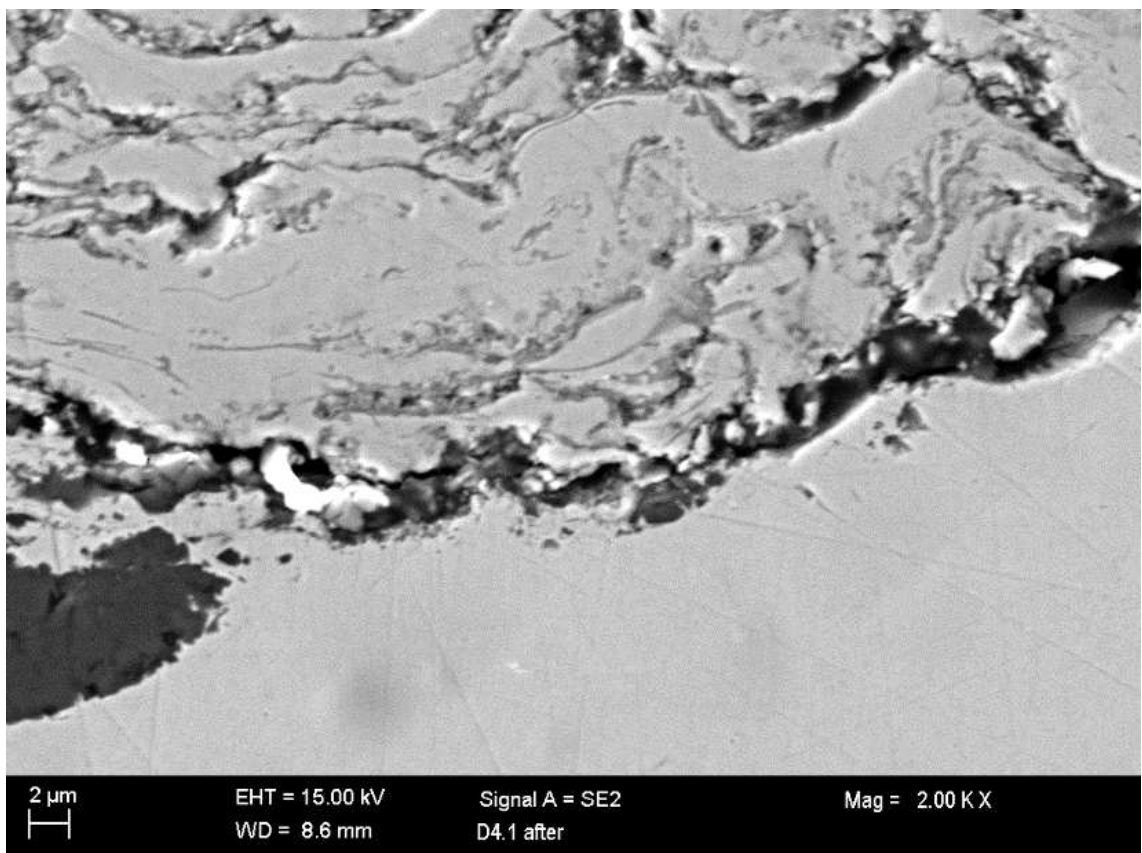
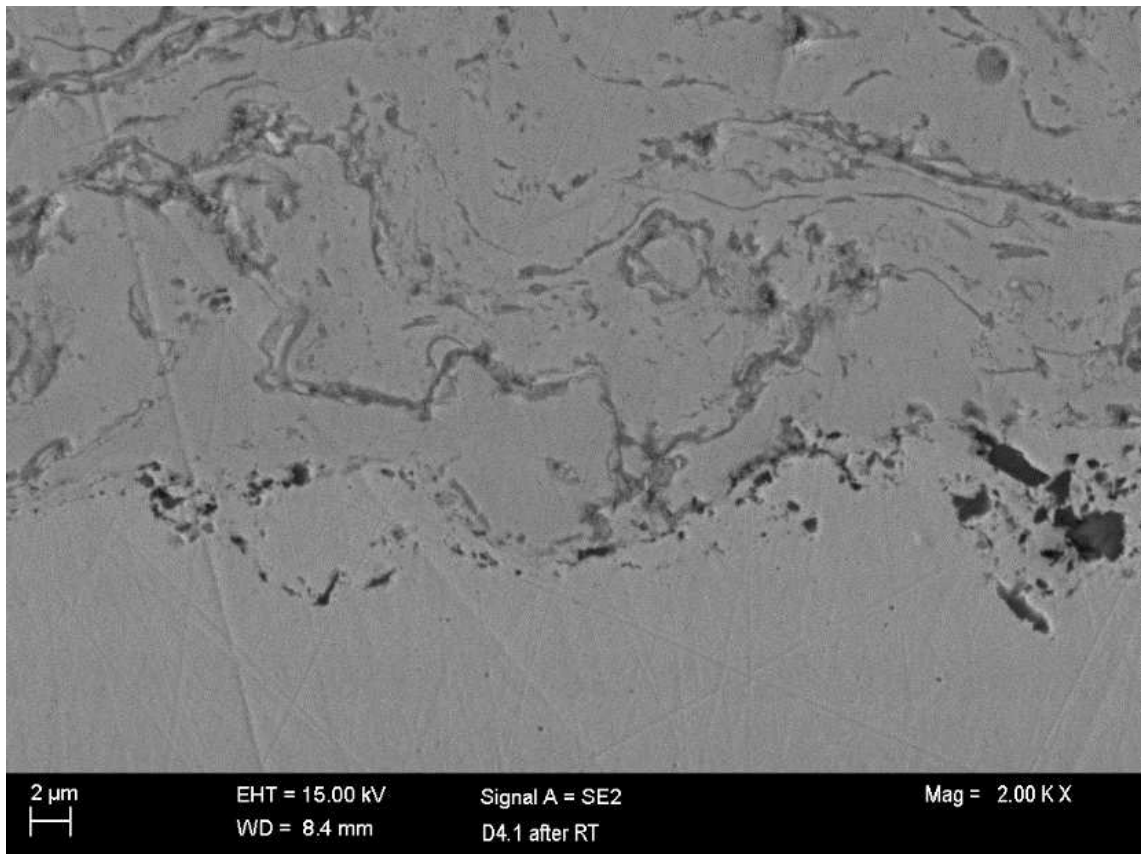


**Figure 75** – SEM cross section for sample D4.1 (cobalt based alloy as bond coating) at 2000X before and after the immersion test at different temperature.

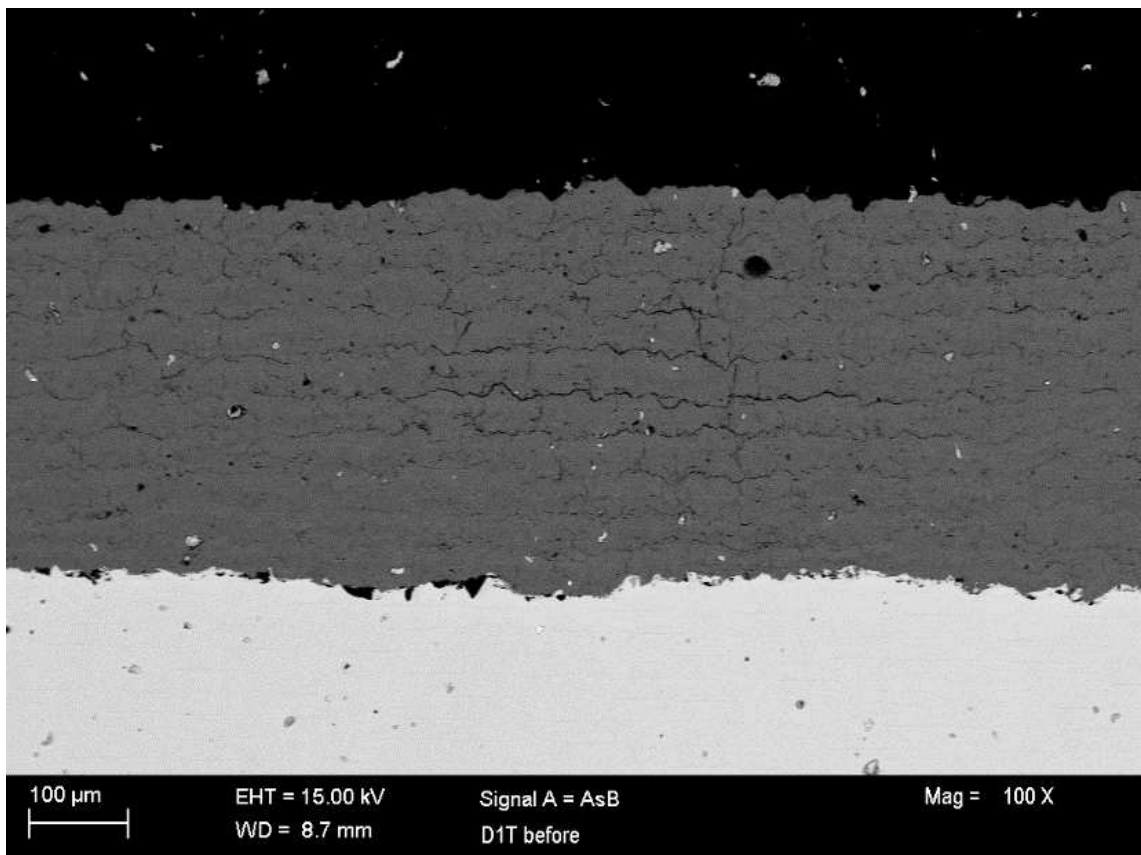
From the cross section reported in Figures 73, 74, 75 is possible to notice that even in this case the top coat presents a good quality, in fact the top coating for the samples D3.1 and D4.1 have been realized together, with the same parameters.

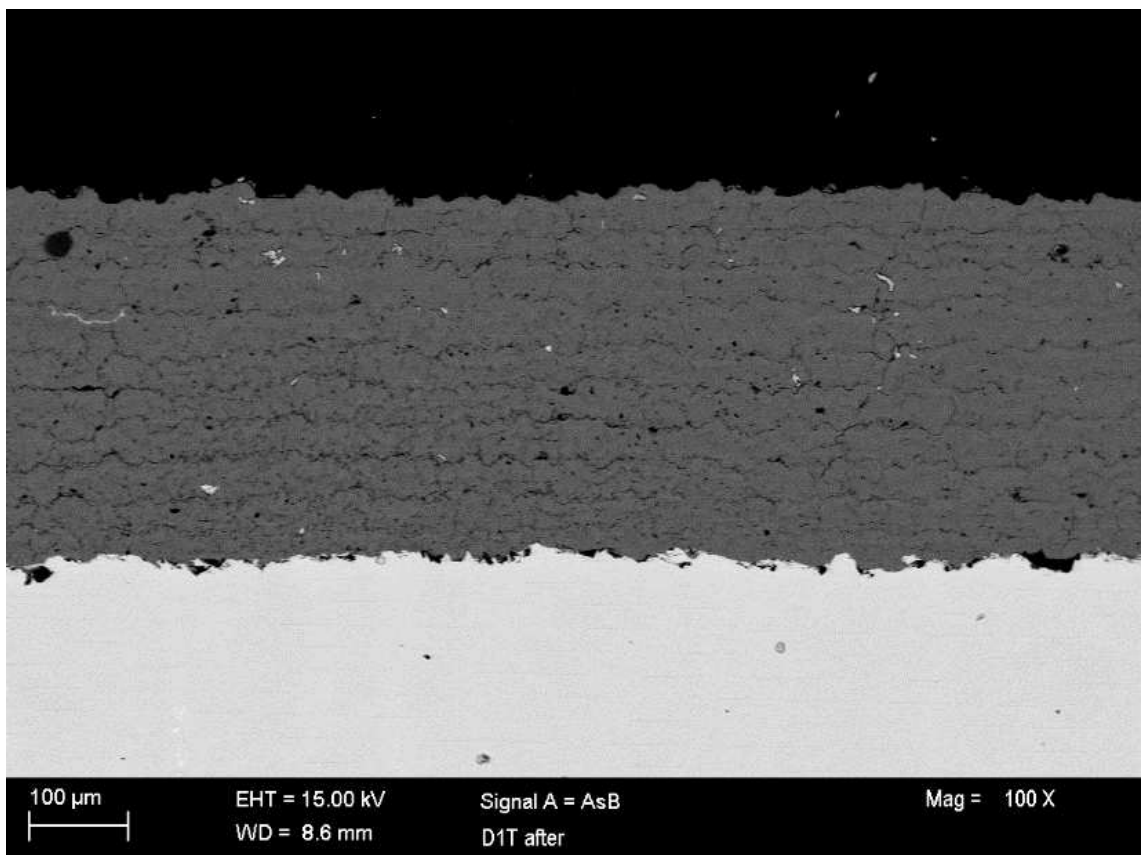
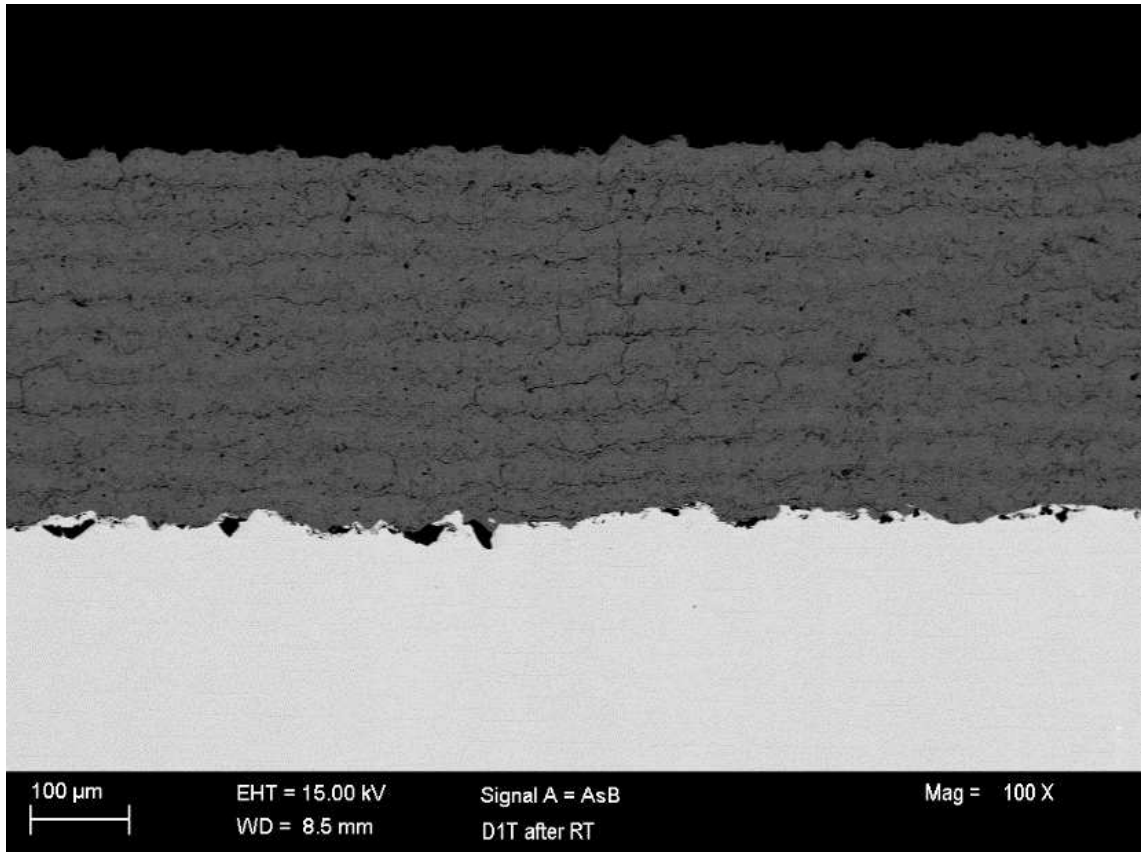
The HVOF sprayed cobalt based alloy as bond coating seems to have a good quality, in fact it's dense with a low content of oxide.

After the immersion test the bond coating presents different conditions depending from the test's temperature.

At room temperature the bond coating doesn't present evident signal of corrosion but at the temperature of 60°C the bond coating seems quite damaged, it's possible to see that the corrosion attacked the bond coating on the splats' boundary which leads to their isolation from the rest of the bond coating.

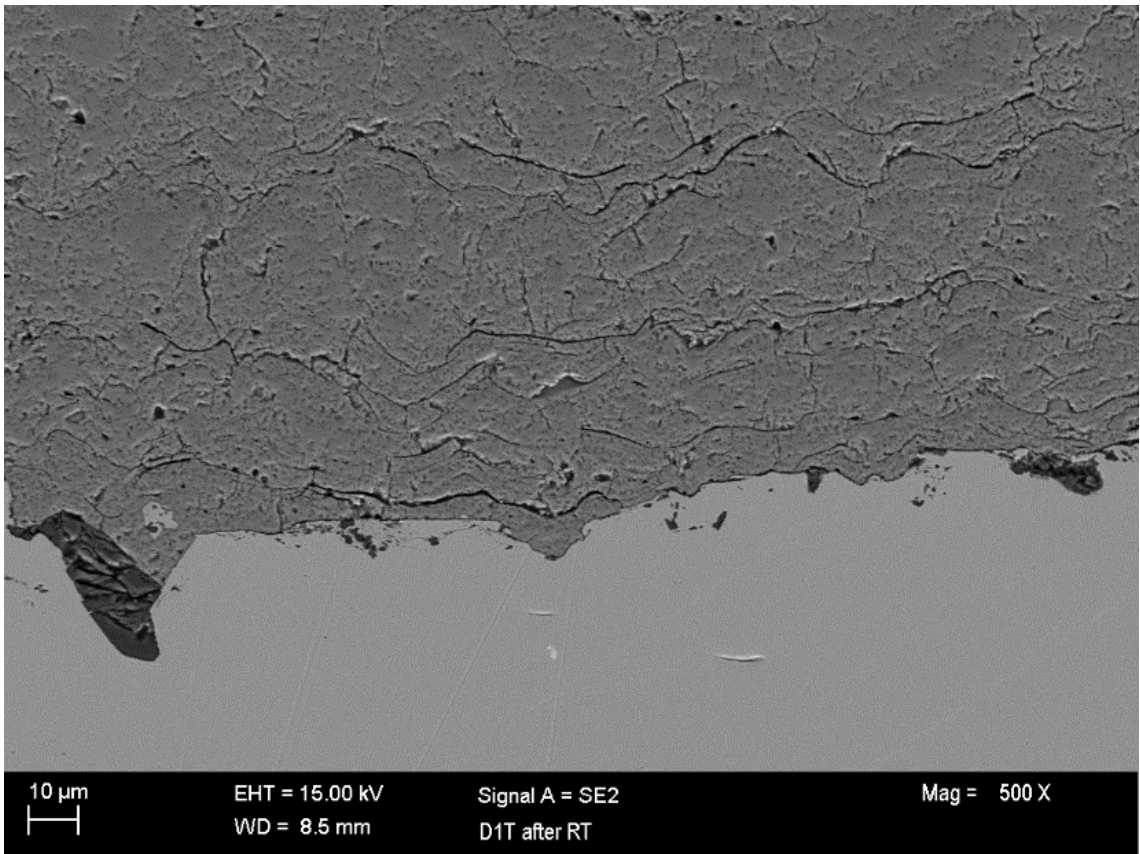
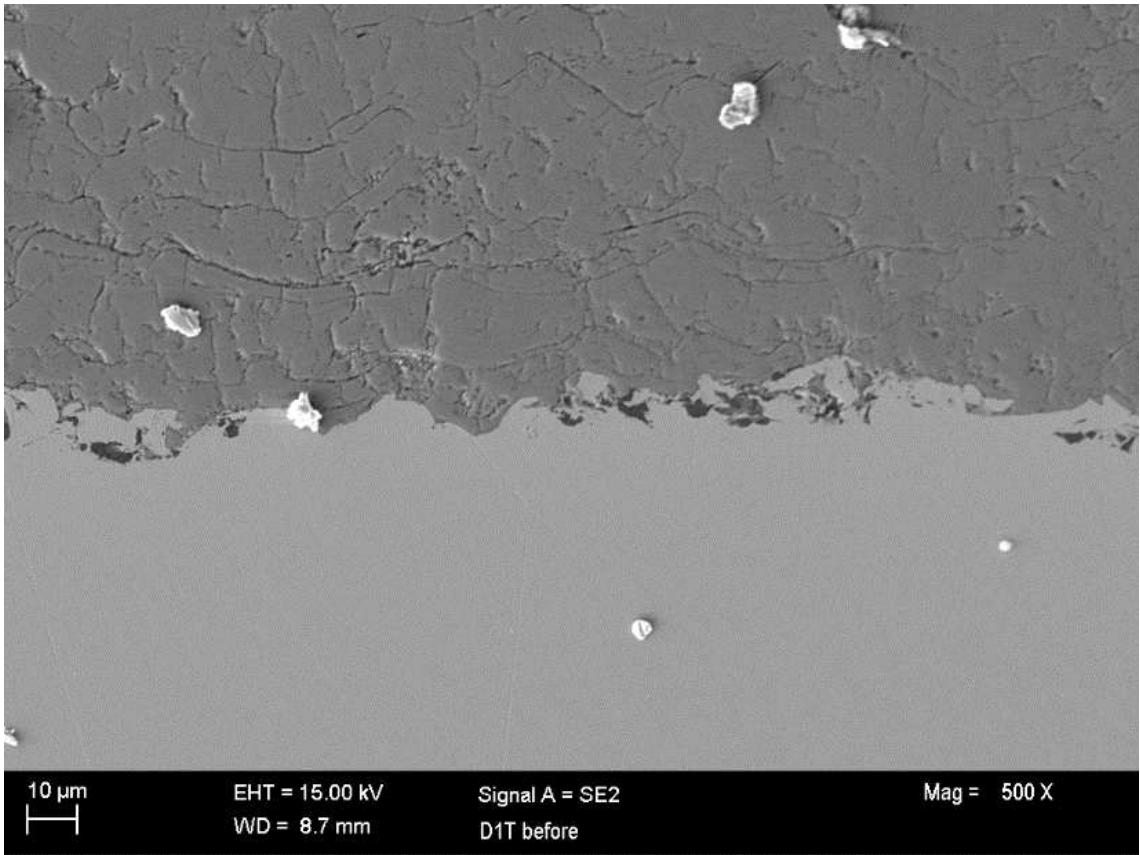
The black area that are possible to observe in the picture can be related to the penetration of carbon from the epoxy resin or to the penetration of others elements during the polishing of the samples.

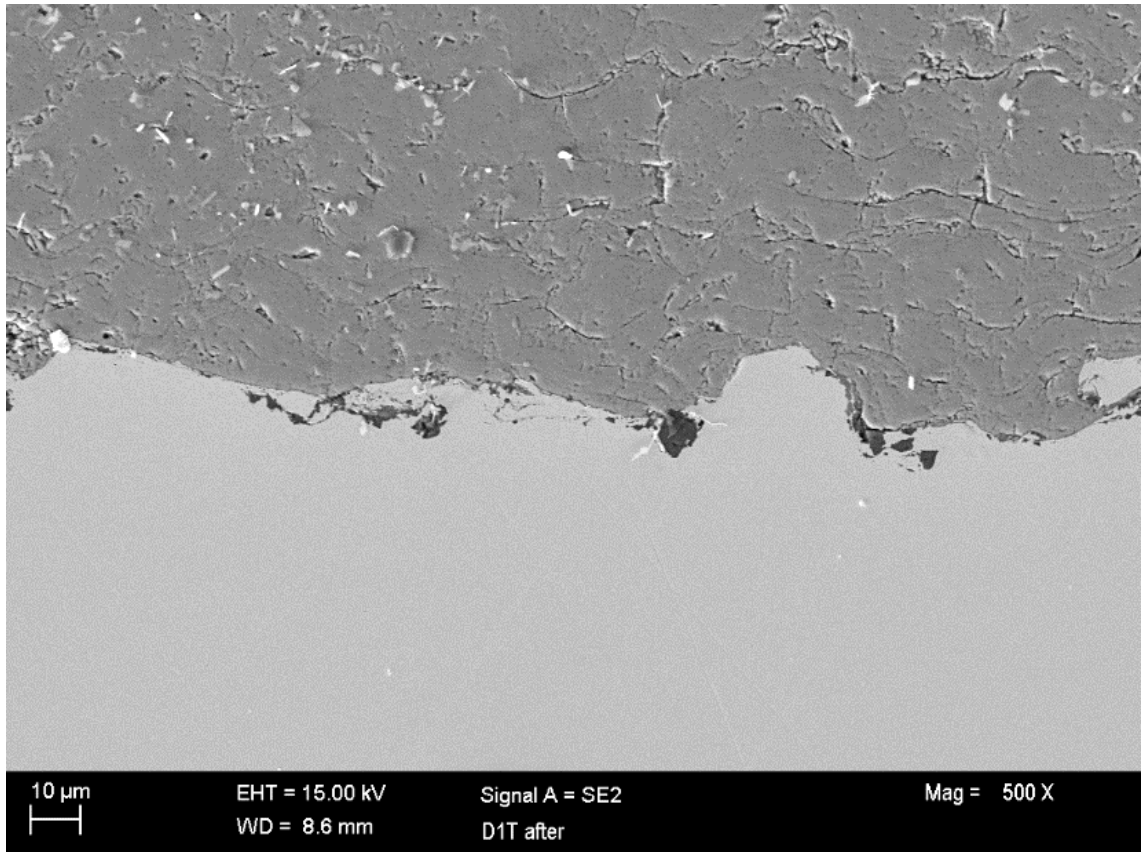




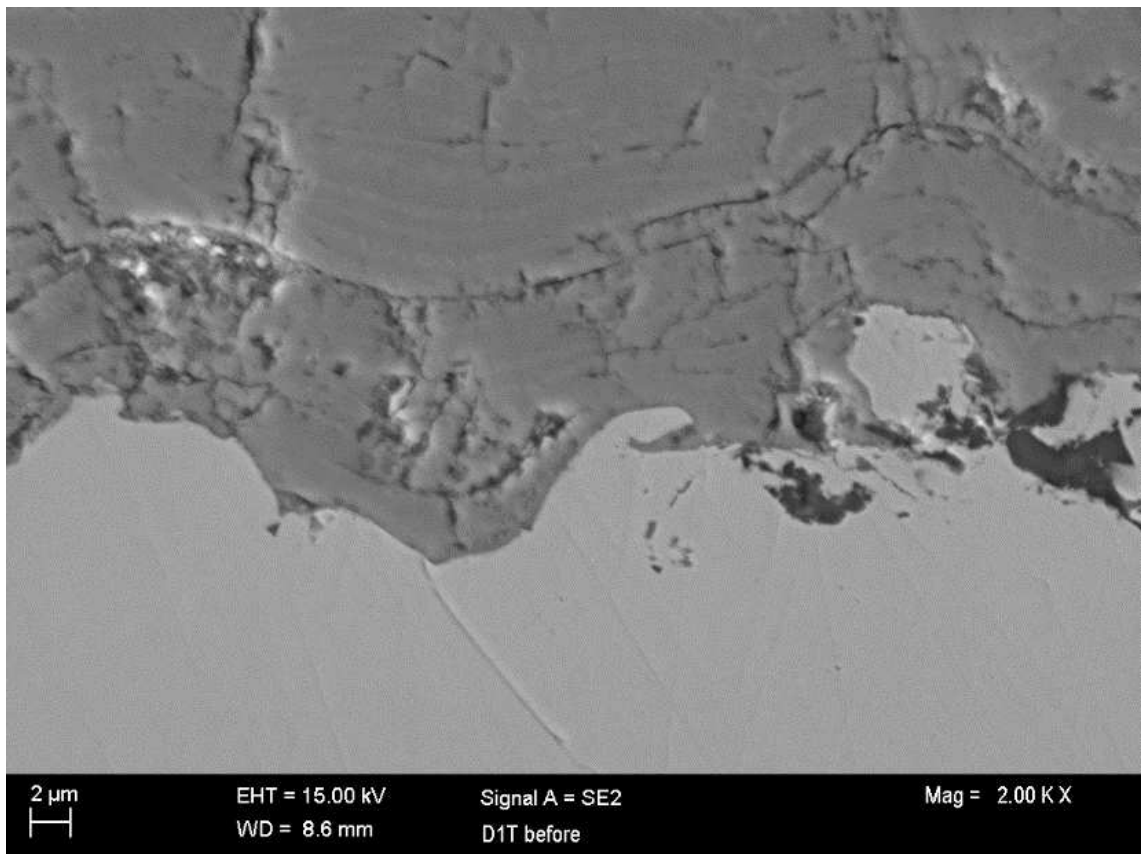
**Figure 76** – SEM cross section for sample D1TC (no bond coating) at 100X before and after the immersion test at different temperature.







**Figure 77** – SEM cross section for sample D1TC (no bond coating) at 500X before and after the immersion test at different temperature.



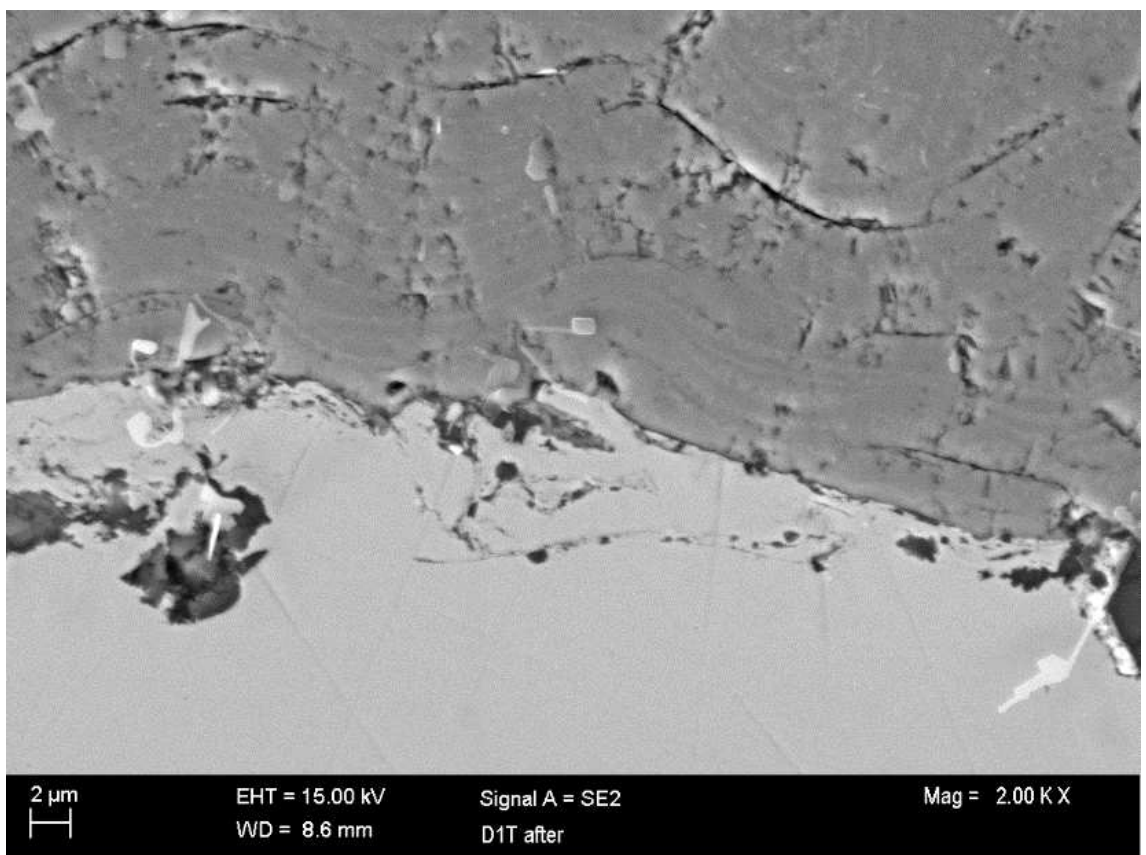
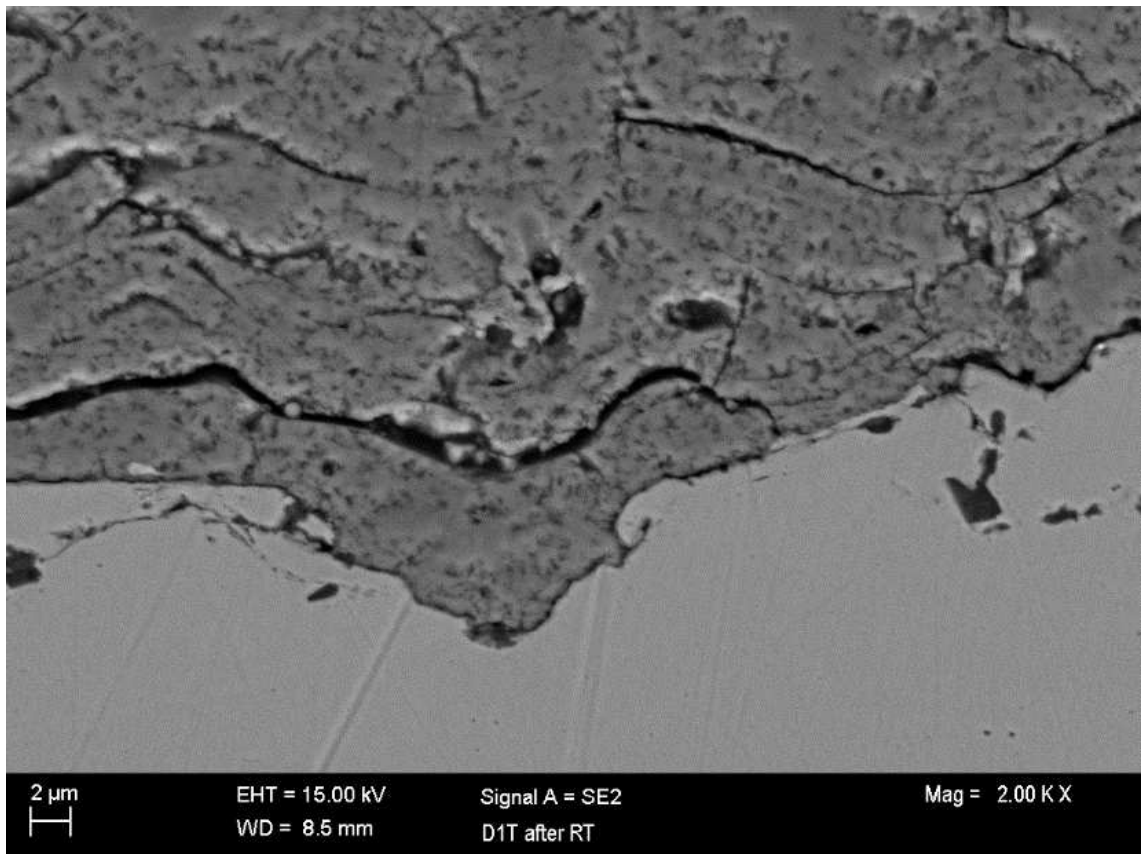


**Figure 78** – SEM cross section for sample D1TC (no bond coating) at 2000X before and after the immersion test at different temperature.

From the cross section reported in Figures 76, 77, 78 is possible to notice that the top coating doesn't have a good quality because it has been sprayed with the same parameters of samples D1.1 and D2.1.

In any case the top coating doesn't present evident signs of corrosion at both test's temperature, this means that it can resist to the test's conditions

Moreover, even if the top coating presents a lot of cracks which facilitate the penetration of the electrolyte, the substrate is not interested by corrosion.

This fact can be related to the choice of adopting an alloy with a high corrosion resistance.

The immersion test, even if it's only a qualitative test, allows to obtain important information about the corrosion behavior of the different bond coats. In fact, it's possible to say all the bond coatings can resist to the immersion test at room temperature but at high temperature  $T=60^{\circ}\text{C}$  they have different responds.

HVOF sprayed Hastelloy C-276 and plasma sprayed tantalum can resist even at high temperature but HVOF sprayed Ni-20Cr and HVOF sprayed cobalt based alloy are not resistance at this temperature, the first one dissolves completely in the electrolyte while the second one presents evident signs of corrosion.

## 5. Conclusion

According to the consideration and the results presented in the previous sections, the following conclusions can be drawn.

At room temperature only the electrochemical tests are useful to describe the corrosion resistance because with the immersion test there are not so much changes to identify correctly the corrosion phenomenon in every sample.

Regarding the room temperature, the configuration with plasma sprayed tantalum as bond coating (D3.1) presents the best corrosion resistance.

In fact, it presents the best response to the electrochemical tests due to the fact that it is characterized by the lower corrosion current in polarization test and by the higher resistances in the EIS test. Moreover, it presents also the highest potential value during the OCP test, this value is also quite stable with the time this confirms the nobility of this bond coating.

It can be said that the corrosion properties of this configuration are comparable with the one presented by the sample with only the  $\text{Cr}_2\text{O}_3$  top coating (D1TC).

The worst configuration at room temperature is the one with the HVOF sprayed cobalt based alloy as bond coating (D4.1) because either the corrosion current and the resistances values are less valuable than the one presented by the others samples. This difference is also quite considerable because they are more or less one magnitude higher for corrosion current and one magnitude lower for the electrical resistances values.

Even the OCP value is the lower compared to the one presented by the others sample, this confirms the low corrosion resistance of this configuration.

Concerning the coatings with HVOF sprayed Hastelloy C-276 (D1.1) and with HVOF sprayed Ni-20Cr as bond coating (D2.1) it can be said that they have an intermediate corrosion behavior between the one presented by the Tantalum and the one presented by the Cobalt alloy bond coat.

Anyway, according to the results obtained from the different tests, it can be said that the corrosion resistance of these two configurations is quite good because the responses obtained are comparable, at least for magnitude, to the one presented by the tantalum.

Also the OCP values for these two samples are between the one presented by the sample D3.1 and the sample D4.1.

Regarding the immersion test of  $60^\circ\text{C}$  it must be said that some samples changed their corrosion resistance.

In fact, while the sample with plasma sprayed tantalum and HVOF sprayed Hastelloy C-276 as bond coatings resisted even in these corrosion conditions, the sample with HVOF sprayed Ni-20Cr and with HVOF sprayed cobalt based alloy as bond coatings changed completely their response with respect to the immersion test at room temperature.

The bond coating constituted by Ni-20Cr was completely dissolved by the solution while the bond coating constituted by the cobalt based alloy was attacked consistently.

This fact confirms that even the temperature has a key role on the corrosion resistance of the thermal sprayed coatings.

## References

- [1] E. Celik, I. Ozdemir, E. Avcı, Y. Tsunekawa, *Corrosion behaviour of plasma sprayed coatings*, 2004.
- [2] Zhe Liu, Zhenhua Chu, Yanchun Dong, Yong Yang, Xueguang Chen, Xiangjiao Kong, Dianran Yan, *The effect of metallic bonding layer on the corrosion behavior of plasma sprayed Al<sub>2</sub>O<sub>3</sub> ceramic coatings in simulated seawater*, 2004.
- [3] The International Nickel Company, *The Corrosion Resistance of Nickel-Containing Alloys in Sulfuric Acid and Related Compounds*.
- [4] P. Fauchais, J. Heberlein and M. Boulos, *Thermal Spray Fundamentals – From powder to Part*, Springer, 2014.
- [5] L. Lusvarghi, *Educational material for the course "Surface and Coating Engineering"*, 2017.
- [6] ASM International, *ASM Handbook - Thermal Spray Technology*, vol. 5, Robert C. Tucker, Jr., 2013.
- [7] Jo Ann Gan, Christopher C. Berndt, *Thermal spray forming of Titanium and its alloy*, 2015.
- [8] ASM International, *ASM Handbook – Corrosion: Fundamentals, Testing and Protection*, vol. 13A, Stephen D. Cramer and Bernard S. Covino, Jr., 2003.
- [9] R. Winston Revie, *Uhlig's corrosion handbook*, Third edition, 2011.
- [10] ASM International, *Surface engineering for corrosion and wear application*, J. R. Devis, 2001.
- [11] R. Giovanarsi, *Educational material for the course "Corrosion and protection of metallic materials"*, 2017.
- [12] Jing Ning, Yougui Zheng, Bruce Brown, David Young, Srdjan Nešić, *A Thermodynamic Model for the Prediction of Mild Steel Corrosion Products in an Aqueous Hydrogen Sulfide Environment*, 2015.
- [13] Parr Instrument Company, *Acid Digestion Vessels, Operating Instruction Manual*.
- [14] J. Tuominen, P. Vuoristo, T. Mäntylä, S. Ahmaniemi, J. Vihinen, P. H. Andersson, *Corrosion behavior of HVOF-sprayed and Nd-YAG laser-remelted high-chromium, nickel-chromium coatings*, 2002.

- [15] Senol Yılmaz, Mediha Ipek, Gozde F. Celebi, Cuma Bindal, *The effect of bond coat on mechanical properties of plasma-sprayed Al<sub>2</sub>O<sub>3</sub> and Al<sub>2</sub>O<sub>3</sub>–13 wt% TiO<sub>2</sub> coatings on AISI 316L stainless steel*, 2004.
- [16] E.Sadeghimeresht, N. Markocsan, P.Nylén, *Microstructural and electrochemical characterization of Ni-based bi-layer coatings produced by the HVOF process*, 2016.
- [17] Alireza Jam, Seyed Mohammad Reza Derakhshansdeh, Hosein Rajaei, Amir Hossein Pakseresht, *Evaluation of microstructure and electrochemical behavior of dual-layer NiCrAlY/mullite plasma sprayed coating on high silicon cast iron alloy*, 2017.
- [18] David Loveday, Pete Peterson, and Bob Rodgers, *Evaluation of Organic Coatings with Electrochemical Impedance Spectroscopy, part 1: Fundamentals of Electrochemical Impedance Spectroscopy*, 2004.
- [19] R. A. Cottis, “Electrochemicals Methods”, *Comprehensive corrosion*, pp. 1358-1360, 2010.
- [20] David Loveday, Pete Peterson, and Bob Rodgers, *Evaluation of Organic Coatings with Electrochemical Impedance Spectroscopy, part 2: Application of EIS to coatings*, 2004.
- [21] Ivan Stojanovic , Vinko Šimunovic , Vesna Alar and Frankica Kapor, *Experimental Evaluation of Polyester and Epoxy– Polyester Powder Coatings in Aggressive Media*, 2018.